



# WPI

## **Diffusional Limitations During Solid Phase Peptide Synthesis**

A Major Qualifying Project  
Submitted to the Faculty of  
Worcester Polytechnic Institute  
In partial fulfilment of the requirements  
For the degree in Bachelor's of Science

In

Chemical Engineering

By

Sydney Gagne  
Meng Lian  
Alyssa Whitley

Date: April 28, 2022

Project Advisor: Professor Andrew Teixeira (CHE)

*This report represents the work of WPI undergraduate students submitted to the faculty as evidence of a degree requirement. WPI routinely publishes these reports on its website without editorial or peer review. For more information about the projects program at WPI, see <http://www.wpi.edu/Academics/Projects>.*

## **Acknowledgements**

We would like to thank WPI and the Office of Undergraduate Research for this opportunity. We would also like to thank Dr. Dale Thomas, Liam Kelly, and Abigail Campbell from Mytide Therapeutics for working with us on this project and for providing our team with experimental data. Finally, we would like to thank Muyun He for her support on data extraction.

## Abstract

Peptide therapeutics have immense potential for a variety of molecular targets. Their low toxicity makes them very desirable for oncology and other areas including personalized medicine.<sup>49</sup> However, large-scale peptide manufacturing is expensive with large waste e-factors. Long coupling, deprotection, washout times, and potential diffusional limitations hinder solid phase peptide synthesis (SPPS), generating tremendous solvent and reagent waste. This report aims to identify the cause of these problems, determine how to decrease these inefficiencies, and minimize the time needed per coupling. Residence time distribution experiments were run to understand the time it takes for an amino acid to flow through the reactor as well as the dispersion present during synthesis. A zero-length chromatography (ZLC) column was used to characterize diffusion limitations in which the uptake and release of a tracer amino acid through resin was measured and then analyzed. Ultimately, it was found that hydrodynamic oscillations lower the residence time and reducing headspace lowers the dispersion in the reactor. The system was found to be diffusion limited 4-5 minutes after initial release of the tracer amino acid. By reducing the headspace, retaining the oscillation, and controlling the flow rate after the initial washout period, SPPS processes are optimized with less waste and less cost, making the process more sustainable.

# Table of Contents

<b>ACKNOWLEDGEMENTS</b> .....	<b>II</b>
<b>ABSTRACT</b> .....	<b>III</b>
<b>LIST OF FIGURES</b> .....	<b>1</b>
<b>LIST OF TABLES</b> .....	<b>2</b>
<b>CHAPTER 1 INTRODUCTION</b> .....	<b>3</b>
<b>CHAPTER 2 TECHNICAL BACKGROUND</b> .....	<b>6</b>
2.1 SOLID PHASE PEPTIDE SYNTHESIS (SPPS).....	6
2.1.1 Resin .....	9
2.1.2 Mixing Challenges, Diffusional Limitations, and Potential Resolutions.....	11
2.2 FLOW IN PACKED COLUMNS.....	13
2.2.1 Height of the Theoretical Plates (HETP).....	15
2.3 DIFFUSION IN POROUS MEDIA .....	17
2.3.1 Zero-Length Chromatography (ZLC).....	18
2.3.2 ZLC Mathematical Model.....	19
2.4 MODELING PACKED BED REACTORS .....	20
2.4.1 Pressure Drop: Ergun Equation.....	21
2.4.2 Residence Time Distribution .....	22
<b>CHAPTER 3 MATERIALS AND METHODS</b> .....	<b>27</b>
3.1 ZERO LENGTH CHROMATOGRAPHY EXPERIMENTS .....	27
3.1.1 HPLC Configuration .....	27
3.1.2 Amino Acid Diffusivity in Resin .....	29
3.1.3 Safety.....	31
3.2 RESIDENCE TIME DISTRIBUTION EXPERIMENTS .....	33
3.2.1 RTD of Current Peptide Synthesis Method .....	33
3.2.2 RTD Experiments .....	35
<b>CHAPTER 4 RESULTS</b> .....	<b>37</b>
4.1 ZLC RESULTS .....	37
4.1.1 Amino Acids under Different Flow Rates.....	37
4.1.2 Amino Acids under Different Bed Schematics.....	38
4.1.2 Diffusivity under Different Flow Rates and Bed.....	39
4.2 RESIDENCE TIME DISTRIBUTION RESULTS .....	40
4.2.1 Residence Time and Dispersion of Amino Acids in Peptide Synthesis .....	40
4.2.2 Residence Time and Dispersion in RTD Experiments .....	43
<b>CHAPTER 5 DISCUSSION</b> .....	<b>53</b>
5.1 ZLC.....	53
5.2 RESIDENCE TIME .....	54
<b>CHAPTER 6 CONCLUSIONS &amp; RECOMMENDATIONS</b> .....	<b>56</b>
<b>REFERENCES</b> .....	<b>58</b>
<b>APPENDICES</b> .....	<b>62</b>

APPENDIX A: CODES .....	62
<i>Appendix A.1: MATLAB Code for ZLC analysis</i> .....	62
<i>Appendix A.2. Python Code for data extraction</i> .....	63
<i>Appendix A.3. MATLAB Code for RTD analysis</i> .....	64
APPENDIX B: ZLC DIFFUSION FITS .....	64
APPENDIX C: ZLC RELEASE PROFILES .....	69
APPENDIX D: RESIDENCE TIME GRAPHS FOR PEPTIDE DEPROTECTION PEAKS.....	84
APPENDIX E: DIMENSIONLESS DISPERSION GRAPHS FOR PEPTIDE DEPROTECTION PEAKS .....	86
APPENDIX F: RESIDENCE TIME EXPERIMENT GRAPHS .....	89
<i>Appendix F.1: Flowrate Graph</i> .....	89
<i>Appendix F.2: Oscillation Graphs</i> .....	89
<i>Appendix F.3: Headspace Graphs</i> .....	93
<i>Appendix F.4: Growing Peptide Graphs</i> .....	94

## List of Figures

FIGURE 1. SCHEMATIC OF PEPTIDE BOND FORMATION <sup>41</sup> .....	6
FIGURE 2. SCHEMATIC OF SOLID PHASE PEPTIDE SYNTHESIS <sup>43</sup> .....	8
FIGURE 3. CHEMMATRIX® RESIN. LEFT: MOLECULAR STRUCTURE OF CHEMMATRIX® RESIN BUILT ON COMPLETELY STABLE POLYETHER BONDS. RIGHT: MICROSCOPY ON CHEMMATRIX® RESIN BEAD (150 ±10 μm SWELLED IN DIFFERENT SOLUTIONS). <sup>12 30</sup> .....	11
FIGURE 4: HPLC FLOW SCHEMATIC AND MAIN PARTS <sup>28</sup> .....	13
FIGURE 5. SOLID PHASE PEPTIDE SYNTHESIS (SPPS). A) FLOW SCHEMATIC OF Fmoc SPPS B) REACTION VESSEL <sup>42</sup> .....	14
FIGURE 6. GAUSSIAN CHROMATOGRAPHIC PLOT OF RELATIVE PEAK HEIGHT V. TIME, WITH KEY PARAMETERS INDICATED ON THE CURVE <sup>5</sup> .....	16
FIGURE 7. FLOW PATHS IN A PACKED BED REACTOR <sup>11</sup> .....	23
FIGURE 8. CONCENTRATION VERSUS TIME GRAPHS FOR PULSE INJECTION <sup>11</sup> .....	24
FIGURE 9. CONCENTRATION VERSUS TIME CURVES FOR THE STEP INPUT EXPERIMENT <sup>11</sup> .....	25
FIGURE 10. ILLUSTRATION OF THE DIFFERENCES IN RTD CURVES FOR CONVOLUTED, BYPASS, AND EMPTY CONVOLUTED PROCESS SCHEMATIC .....	26
FIGURE 11. HPLC AND ZLC SET UP.....	28
FIGURE 12. SCHEMATIC OF 6-PORT VALVE CONFIGURATION .....	29
FIGURE 13 ZLC COLUMN.....	30
FIGURE 14 SAMPLE RESIDENCE TIME DISTRIBUTION CURVE OBTAINED FROM MATLAB.....	34
FIGURE 15. ZLC NORMALIZED ABSORPTION V. TIME RELEASE PROFILE FOR (A) FRESH RESIN, (B) EMPTY, (C) PEPTIDE BOUND RESIN, AND (D) GLASS BEAD FILLED COLUMNS UNDER DIFFERENT FLOWRATES .....	37
FIGURE 16. ZLC RELEASE PROFILE FOR DIFFERENT BED SCHEMATICS AT 2 mL/MIN FLOW RATE.....	38
FIGURE 17. RESIDENCE TIMES VERSUS AMINO ACID COUPLE NUMBER FOR FOUR SAMPLE PEPTIDES ....	41
FIGURE 18. DISPERSION NUMBER VERSUS COUPLE NUMBER FOR FOUR SAMPLE PEPTIDES.....	42
FIGURE 19. DISPERSION NUMBER VERSUS RESIDENCE TIME FOR FOUR SAMPLE PEPTIDES .....	43
FIGURE 20. RESIDENCE TIME DISTRIBUTIONS OF THE FIVE FLOWRATES USED .....	44
FIGURE 21. BOX AND WHISKER PLOT SHOWING AVERAGE RESIDENCE TIMES AND DISTRIBUTION OF RESIDENCE TIMES FOR EMPTY, GLASS BEAD, AND RESIN FILLED COLUMN .....	45
FIGURE 22. AVERAGE RESIDENCE TIMES FOR A GLASS BEAD FILLED REACTOR WITH AND WITHOUT OSCILLATIONS .....	46
FIGURE 23. AVERAGE RESIDENCE TIMES FOR A RESIN FILLED REACTOR WITH AND WITHOUT OSCILLATIONS .....	47
FIGURE 24. DIMENSIONLESS DISPERSION NUMBER WITH RESPECT TO HEADSPACE FOR A GLASS BEAD FILLED REACTOR .....	48
FIGURE 25. RESIDENCE TIME DISTRIBUTIONS EXTRACTED FROM MATLAB FOR A FULL GLASS BEAD REACTOR, A 100 MG GLASS BEAD REACTOR, AND A 60 MG GLASS BEAD REACTOR.....	49
FIGURE 26. EFFECT OF GROWING PEPTIDE ON RESIN WITH NO OSCILLATION .....	50
FIGURE 27. AVERAGE RESIDENCE TIMES WHEN THERE ARE 0, 5, 10, 15, AND 20 AMINO ACIDS COUPLED TO THE RESIN WITH RESPECT TO OSCILLATION .....	51
FIGURE 28. BOX AND WHISKER PLOT SHOWING AVERAGE RESIDENCE TIMES AND DISTRIBUTION OF RESIDENCE TIMES FOR A GROWING PEPTIDE AT FLOW D WITH RESPECT OT OSCILLATION.....	52
FIGURE 29. FRESH V. PEPTIDE BOUND RESIN POLYMER NETWORK.....	54

## List of Tables

TABLE 1. ZLC EXPERIMENTAL PLAN .....	30
TABLE 2. SUMMARY OF RESIDENCE TIME DISTRIBUTION EXPERIMENTS .....	35
TABLE 3. ZLC DIFFUSIVITY UNDER DIFFERENT FLOWRATES AND COLUMN BED SCHEMATICS .....	39
TABLE 4. SAMPLE PEPTIDES AND CORRESPONDING AMINO ACID SEQUENCE .....	40

## Chapter 1 Introduction

Since the 18<sup>th</sup> century, modern medicine has grown rapidly to what is observed today. There are many types of therapeutics available, including small molecules, biologics, protein-based, peptide-based, and more. While small molecule, biologics, and protein-based therapeutics are relatively explored in the 20<sup>th</sup> century, peptide therapeutics has swiftly developed over the last two decades.<sup>17</sup>

The use of peptides as therapeutics has been studied for years as they have immense potential for a variety of molecular targets including receptor proteins, extracellular proteins, and intracellular proteins. They also have low toxicity which makes them very desirable for oncology and other areas including personalized medicine.<sup>49</sup> Over the last two decades, 7000 naturally occurring peptides have been discovered; peptide-based pharmaceuticals have immense potential for the pharmaceutical industry, and they continue to gain popularity as therapeutic agents. As of 2018, there were over 60 FDA-approved peptide drugs on the market, as well as 140 in clinical trials, and 500-600 in preclinical development.<sup>37</sup> Peptides have been recognized as key biological mediators with remarkable potency, selectivity, and low toxicity.<sup>17</sup>

Particularly, personalized medicine, or precision medicine, has gained much interest as a potential market for pharmaceuticals. For instance, interference peptides can be used to block selective interactions between proteins that are not easily treated by small molecules or larger biologics with the ability to access intracellular or secreted proteins. This way, cancer cell protein-protein interactions can be selectively targeted and manipulated by personalized peptides, impairing cancer progression.<sup>50</sup> Other potential uses of peptide in personalized medicine include treating diabetes by acting as a biomarker and treating cancer with vaccine.<sup>23,35</sup>

While peptides demonstrated strong potential as a pharmaceutical drug, large-scale peptide manufacturing is expensive. Even with the discovery of solid-phase peptide synthesis (SPPS), peptide synthesis proves to be costly, requiring copious quantities of reactants, solvents, and sequence accuracy. Combined, current methods for peptide manufacturing generate a tremendous amount of waste, making peptides unsuitable for mass production and keeping the peptide therapeutics market small.<sup>17</sup>

Solid phase peptide synthesis (SPPS) is typically the most efficient method of peptide manufacturing. Nevertheless, SPPS still generated substantial amounts of waste due to challenges and limitations. The current method of synthesis is inefficient due to long coupling times and can be quite costly. In order to obtain a high yield of the desired product, efficient coupling of every amino acid is required.<sup>49</sup> However, to achieve this, excess amino acids, deprotecting agents, and solvents are needed which produces a lot of extra waste and makes the process very expensive. This waste can be quantified using the e-factor, or environmental factor, which is the ratio of mass of waste to mass of product. Typically for small molecule synthesis the ratio is hundreds of kilograms of waste to one kilogram of product. However, for peptide synthesis, e-factor ratios have been reported as high as thousands of kilograms of waste per kilogram of peptide product.<sup>13</sup> This value is extremely high and correspondingly very costly. The challenge here is that when reducing the amount of excess material and coupling times, there are unwanted consequences. There can be deletions, where coupling was not fully completed, double coupling due to poor washout, or the resin could get clogged due to lack of solvent in the reactor.

In summary, SPSS is the process where amino acids are added one-by-one to a solid polymer resin, growing a peptide chain that will be cleaved and purified as a therapeutic product. In this process, amino acids are injected into the system in a sharp pulse, diffuse through the resin

to the active chain end, react and then have the excess washed out in preparation for the next step. This report aims to identify the cause of many of the problems that come with SPSS, determine how to decrease these inefficiencies, and minimize the time needed per coupling. Residence time distributions (RTDs) in the actual reactor bed are used to measure how sharp the injection is and how fast the washout is. Different parameters were analyzed to determine how they affect washout time and it was hypothesized that there are significant diffusional limitations are present within the resin as the peptide grows within it. Zero length chromatography (ZLC) is used to measure the slow diffusion step inside the polymer and to quantify the diffusivity in both fresh and peptide-bound resins. Ultimately, the goal is to decrease coupling and washout times to make the process more efficient and to decrease unnecessary waste. This will lead to higher product yields, a greener process, and will significantly decrease manufacturing costs.

## Chapter 2 Technical Background

### 2.1 Solid Phase Peptide Synthesis (SPPS)

Peptides are small proteins of less than 50 amino acids, linked together by peptide bonds. Amino acids are made up of an amino group, a carboxyl group, and a side chain, or R-group. Figure 1 below shows these components and how two amino acids can be covalently linked together by a peptide bond, resulting in a dipeptide.<sup>41</sup>

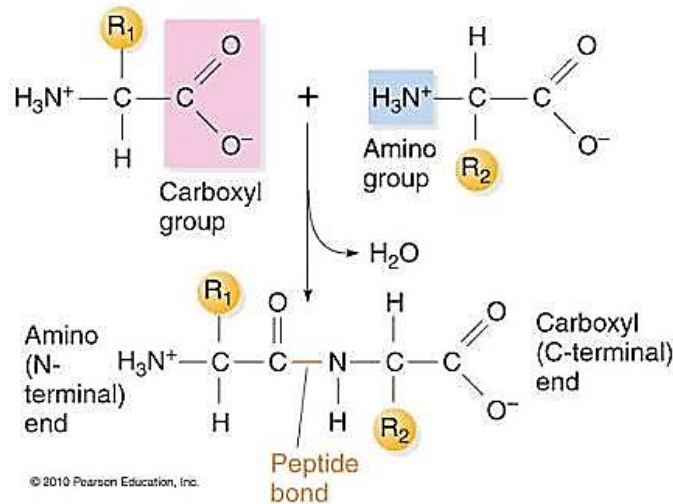


Figure 1. Schematic of Peptide Bond Formation <sup>41</sup>

Peptides occur naturally in the body and are produced in cells through transcription and translation. The instructions to build peptides are located in a person's DNA. However, DNA is just the storage of this information. To read the code, the DNA must first be transcribed into RNA using RNA polymerases. There are three different types of RNA, messenger RNA (mRNA), ribosomal RNA (rRNA), and transfer RNA (tRNA). mRNA contains the code to create proteins/peptides, rRNA molecules are a part of the ribosome where synthesis occurs, and tRNA is responsible for delivering amino acids to the ribosome throughout synthesis. After transcription,

the mRNA must be translated into a peptide. During translation, the ribosome reads the mRNA to string together amino acids. Each amino acid is represented by a three-nucleotide sequence called a codon, and there are start and stop codons to tell the ribosome when to begin and end translation. Once the ribosome hits the stop codon, synthesis ends, and the peptide is completed.<sup>31</sup>

Peptides can also be synthesized synthetically for use in the pharmaceutical field. During synthetic peptide synthesis, the amino acids are linked together from the C-terminus side (carboxyl group) to the N-terminus side (amino group), which is the opposite of what is done within cells.<sup>37</sup> There are two main types of synthesis: fragmented assembly and stepwise synthesis. Fragmented assembly involves covalently linking pre-constructed peptide fragments, while stepwise synthesis links amino acids one at a time. This report will focus on stepwise synthesis, also known as “Solid Phase Peptide Synthesis,” which was developed by Bruce Merrifield. The development of SPPS revolutionized how synthetic peptides were made by increasing yield, avoiding loss, increasing solvation, decreasing aggregation, and enabling automation. Merrifield was awarded the Noble Prize in Chemistry in 1984 for his impressive work. The process involves growing a peptide chain on solid matrix (resin) that is insoluble. The amino acids are added on in a stepwise manner and stay anchored to the matrix. Since both the peptide and matrix are insoluble, any excess reactants or products formed at each step can be washed away before adding the next amino acid. This process has a variety of advantages including preventing product loss, speeding up coupling reactions, and most importantly, it is a simple procedure.<sup>20</sup>

A summary of the peptide synthesis process can be seen in Figure 2 below. To begin, the resin must be prepared. The Merrifield resin is made using polystyrene beads with divinylbenzene as the crosslinking agent.<sup>20</sup> To increase the volume and make the gel-like resin, the organic solvent dichloromethane (DCM) is mixed with the beads. Once swollen to the desired volume the excess

solvent is removed and dimethylformamide (DMF) is used to wash the resin and is then removed as well. Next is the deprotection/coupling cycle.<sup>8</sup> The C-terminus of the first amino acid is bound to the resin via a covalent bond, while the N-terminus is blocked by an Fmoc (or Boc) group. This protects the amino acid end, but this protection needs to be removed before it can couple to another amino acid. This Fmoc group can be removed using a strong acid and is neutralized after using a strong base. Once deprotected, that resin-bound amino acid is ready to couple with a second Fmoc-amino acid. However, to do so, the reaction must be activated. The most common way to activate the reaction is using dicyclohexylcarbodiimide. As seen in Figure 2, to continue growing the peptide, the deprotection and coupling steps must be repeated for each amino acid. Once the desired peptide length is achieved, the final amino acid is deprotected and cleaved using a strong acid such as hydrofluoric acid (HF).<sup>8, 20</sup>

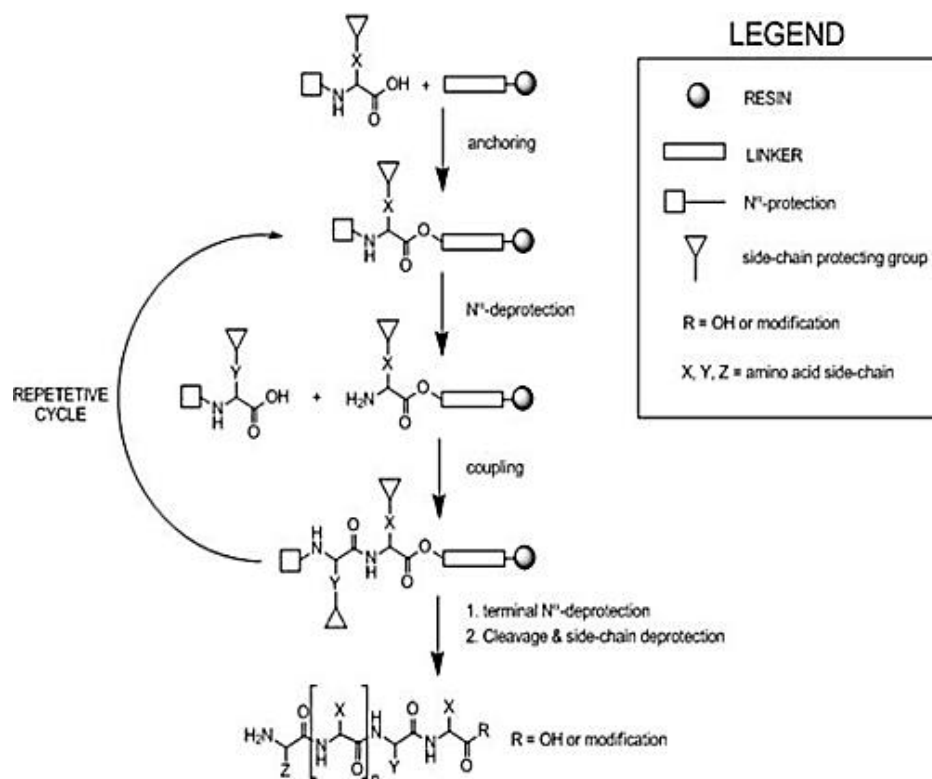


Figure 2. Schematic of Solid Phase Peptide Synthesis<sup>43</sup>

### 2.1.1 Resin

The choice of resin is integral in solid-phase peptide synthesis. Here, four types of resin are examined: polystyrene, Merrifield resin, Polyethylene glycol (PEG), and ChemMatrix®. Typically, resins used for SPPS are prepared and utilized as small, spherical beads. The resins are swelled before SPPS to minimize diffusion limitations by creating a porous environment for peptide synthesis. A larger swelling factor is usually desired for a higher diffusion rate, shorter reaction time, and more complete chemical conversion.<sup>30</sup> Loading, or the number of reactive sites per gram of resin, is also a crucial factor to consider. Having more loading sites will provide more active sites for peptides to react on. However, more loading sites also leads to an increased possibility for aggregation and side reactions. Resins also differ in how they behave in contact with acids or bases. This can be modified by adding permanent linkers that adjust the resin's acid-base properties.<sup>30</sup>

Polystyrene is a hydrophobic resin that is commonly used in SPPS, usually with 1% or 2% divinylbenzene (DVB) as a crosslinking agent since polystyrenes are insoluble in all common solvents.<sup>1</sup> Crosslinking involves joining at least two molecules through a covalent bond. Increasing the number of crosslinks in a material make it more rigid and less able to swell. Polystyrene resins are inexpensive, widely available, and inert to all reaction conditions seen in SPPS. Typically, 75- to-150-micron diameter beads are used to have faster reaction dynamics with consideration of filtration time; the smaller the bead, the faster the diffusion.<sup>1</sup> Filtration time is related to diffusion time by the following equation, where  $D_{AB}$  is the diffusion coefficient of substance A through B, and  $L_c$  the length of column:

$$\tau = \frac{L_c^2}{D_{AB}} \quad (1)$$

While polystyrene is routinely used for large-scale SPPS, it is not suitable for longer, larger, and more complicated peptide synthesis processes. Its hydrophobicity amplifies aggregational behavior. When synthesizing longer, larger peptides, secondary structures are more likely to form than other resins. As the elongated peptide starts to form these secondary structures, the possibility of aggregation increases. Aggregation occurs when the peptide folds in on itself to become a cluster. The effects of aggregation on a peptide can range from slightly slower reaction rates to a failure of both deprotection and acylation reactions.<sup>16</sup> Deletion and incomplete fragmentation of peptides are also likely.<sup>30</sup>

Merrifield resin, or chloromethylated polystyrene, is the most fundamental substituted polystyrene used for peptide synthesis. This gel is prepared by suspension copolymerization of styrene and 1% DVB as a crosslinking agent as well as nucleophilic displacement of chlorine. The resulting spherical beads are about 50 micrometers in diameter when dry. With dichloromethane as the solvent, Merrifield resin can swell up to 5 to 6 times its original volume. Generally, it is stable for most of the reaction conditions in solid-phase synthesis and requires a strong acid for cleavage.<sup>1</sup>

Polyethylene glycol (PEG) is another resin that is commonly used for solid-phase peptide synthesis. It is polar, with nearly constant swelling during the course of synthesis using the continuous flow method. Compared to polystyrene resins, PEG offers enhanced purity for crude peptides by having a higher polarity and improved swelling properties in polar and nonpolar solvents. It is more suitable for use when synthesizing larger, longer peptides in terms of purity and yield compared to polystyrene resins.<sup>1</sup> However, PEG grafted resins only allow small loadings and are less chemically stable under SPPS conditions. The instability could lead to leaching during the cleavage step of SPPS.<sup>30</sup>

ChemMatrix® resin, seen in Figure 3, is a 100% PEG-based, polar resin that is constructed exclusively with primary ether bonds, making it chemically stable and less prone to leaching. It has high loading (0.4-0.7 mmol/g), excellent swelling properties (up to 8 times the original volume in dimethylformamide), and great solvent compatibility.<sup>12,30</sup> Compared to using polystyrene resins, ChemMatrix® resin is more suitable for long, complex, or hydrophobic peptides.<sup>19</sup> ChemMatrix® resin is considered to be a breakthrough resin used in SPPS, providing the conditions to synthesize and obtain difficult peptides through simple synthesis.

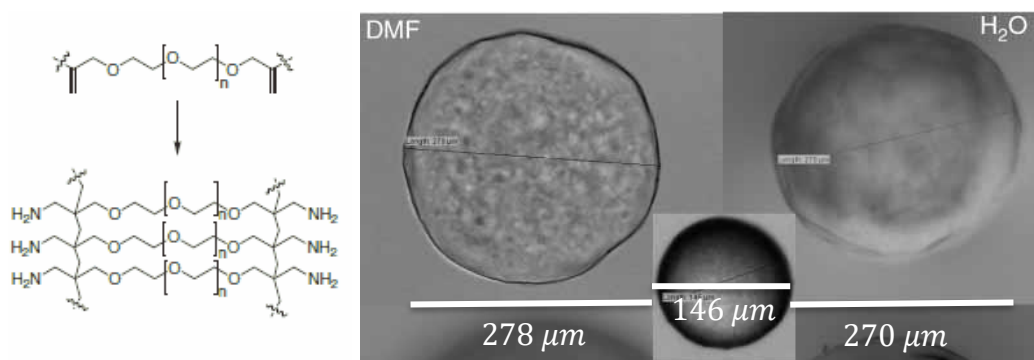


Figure 3. ChemMatrix® Resin. Left: molecular structure of ChemMatrix® Resin built on completely stable polyether bonds. Right: Microscopy on ChemMatrix® Resin bead ( $150 \pm 10 \mu\text{m}$  swelled in different solutions).<sup>12,30</sup>

### 2.1.2 Mixing Challenges, Diffusional Limitations, and Potential Resolutions

While SPPS is convenient for generating a large quantity of peptides through a continuous flow process, there are many limitations to this process. Previous research found that the time required to assemble polypeptides is a major limitation for flow based, continuous SPPS methods. Standard Fmoc SPPS methods require 60 to 100 minutes to incorporate each amino acid residue, leading to slow washes.<sup>42</sup> Multiple washes are also necessary to effectively wash out the solute, requiring up to hours of time. While increasing the flow rate helps to increase the pressure and drive SPPS, the increase in flow rate may collapse the solid support and increase the backpressure too rapidly. Additionally, the SPPS systems recirculate low concentration reagents rather than

continuously replenishing high concentration reagents. While doing so conserves activated amino acids, it results in slower amide bond formation.<sup>42</sup> Furthermore, increasing the flow rate demands leads to more waste. For instance, if the flow rate of a particular wash step is 40 mL/min and flushing out all remnants of the previous step requires 2 hours, 120min, 4.8 L of solvent are consumed for this single step in SPPS. Now, consider synthesizing a peptide with 15 amino acids – there will be more than 30 steps required, each of which requires liters of solvent. A large amount of waste is highly undesirable.

Other limitations include the clogging of the packed bed, or resin, during SPPS. Peptides that formed during the process may not be removed between washes and this aggregates the resin-packed bed. SPPS is driven by pressure – with clogging of the packed bed, more pressure, or more flow is necessary to push fluid through it. Mixing problems also occur where molecules are trapped in one place and do not react when needed. There are two distinct zones within SPPS where mixing is critical; a zone within the resin beads through solid phase diffusion, and another within the fluid through reactor-scale mixing and dispersion. This type of mixing problem can be monitored with spectrometers such as UV-Vis. Increasing the temperature of the reaction process may help with activation, thus reducing the likelihood of trapped molecules within the packed bed. Clogging of the packed bed and mixing problems usually result in slow washing as well as double coupling or deletions during SPPS. Double coupling or deletions can also result from a fast wash that did not wash out cells very well or a fast-deprotecting process that did not deprotect all amino acids. To improve the quality of the crude yield and eliminate the number of double coupling or deletion occurrences, different resin, solvent, and protecting groups can be considered for the process. The reaction time and the temperature at which SPPS is operating can also be increased to reduce double coupling and deletions during synthesis.<sup>43</sup>

## 2.2 Flow in Packed Columns

Flow in packed column reactor is similar to a high-performance liquid chromatography column (HPLC) due to chromatographic hold ups as well as similar flow schematic.<sup>28</sup> HPLC is one of the most common techniques used in chemical and pharmaceutical analysis. It is an analytical technique in which the components of a mixture can be separated and purified.<sup>55</sup> The separated components can then be analyzed individually in the detector to prevent the interference of other components. Under appropriate conditions, HPLC has a high level of reproducibility and a level of sensitivity even while there is a low sample consumption. HPLC also allows for samples to be dissolved in the solvent without the need to be vaporized, making this method much more widely used in the pharmaceutical field than gas chromatography.<sup>40</sup> As seen in Figure 4 the solvent and the sample are pumped at a specified flow rate to the injection valve which then sends them to the column. The mobile phase, which is the moving liquid, passes through the stationary phase, which for HPLC is typically a packed column. After going through the column, the components pass through a UV detector to be analyzed. HPLC is a relatively simple technique to use due to the automation of the sample trays and valve changes.<sup>40</sup>

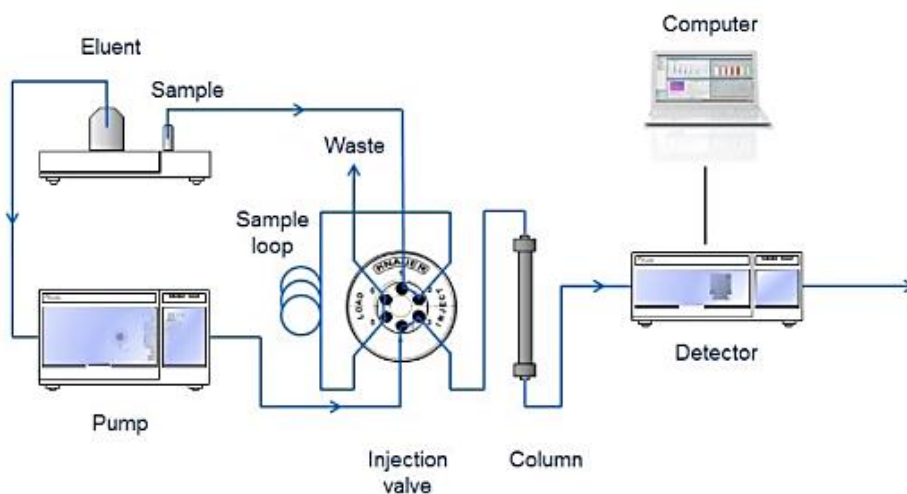


Figure 4: HPLC Flow Schematic and Main Parts<sup>28</sup>

Figure 5 illustrates a SPPS process that utilizes the advantages of an HPLC stack. Here, the affluent and the amino acid are pumped, and the coupling solution is pumped into the system separately. The two streams then enter a reactor in a warm bath where peptide synthesis occurs. The SPPS flow schematic is very similar to the HPLC flow schematic. In fact, it is an alteration of the HPLC schematic, with reactor replacing the column and additional inlet streams.

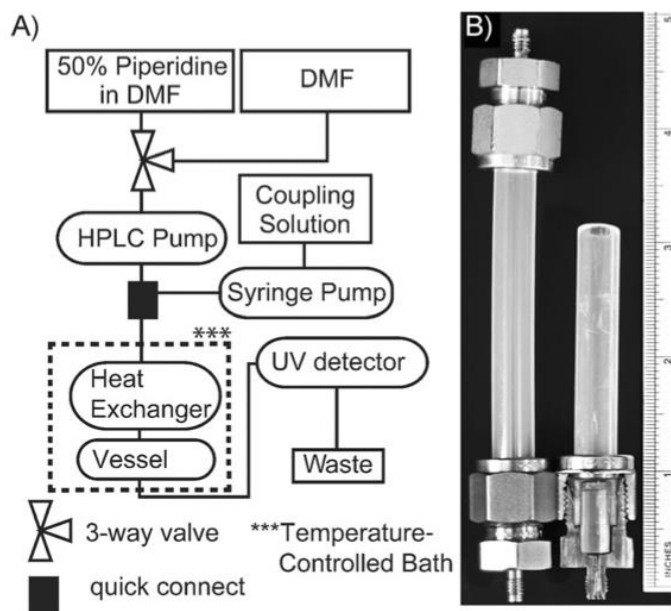


Figure 5. Solid Phase Peptide Synthesis (SPPS). A) Flow Schematic of Fmoc SPPS B) Reaction Vessel<sup>42</sup>

Due to the similarity to the flow in a packed bed reactor, the HPLC platform will be used to experimentally find the diffusion coefficient of various amino acids in different resins. To do so the reactor vessel will be replaced with a zero-length column (ZLC). For our method, UV-vis is able to be used as the detector since the amino acids being used are Fmoc protected. Fmoc has an aromatic ring that absorbs well in the UV range.

### 2.2.1 Height of the Theoretical Plates (HETP)

The height of the theoretical plate (HETP) can be used to analyze the chromatography column efficiency, as well as chromatographic hold up which is the time that the amino acids remain stuck within the column. HETP is a measure of zone broadening that is based on the theory that the chromatographic column contains many separate layers, or theoretical plates, with separative equilibria.<sup>47</sup> Each plate represents an equilibrated partition of the solute. Generally, the larger the number of plates or the smaller the number of HETP, the greater the efficiency of the chromatographic column, and the narrower the absorption peaks are for chromatography. HETP and the number of theoretical plates is useful when optimizing the injection column, sample concentration, flow rate, and column temperature of the SPPS.<sup>3</sup>

Several assumptions are made universal for chromatography techniques. First, the separation is assumed to be uniform throughout a chromatographic column. Theoretically, a column can be equally divided into a number of lengths, segments, or stages. It is also assumed that there is sufficient time to reach equilibrium, partitioning the solute into mobile and stationary phases within each stage of the column. Additionally, each stage approximately equals one theoretical plate for liquid chromatography, which is the case for HPLC as well as ZLC, which is another chromatography method that will be discussed in the following section. After equilibrium is reached, the solute is transferred to the next stage by the mobile phase until the solute reaches the end of the column, where the characteristic retention time and peak widths can be recorded. The number of theoretical plates can be then calculated with Gaussian distribution. When the curve is skewed, the non-Gaussian peaks give underestimated plate counts.<sup>3</sup>

For the HETP, the Gaussian distribution method that can be used to determine the number of theoretical plates through derivation:

$$N = 16 \frac{t_r^2}{w_t^2} \quad (2)$$

Here,  $N$  is the number of theoretical plates,  $t_r$  is the retention time, and  $w_t$  is the peak width in units of time. These variables can be obtained by observing the Gaussian chromatographic plot of relative peak height v. time as shown in Figure 6.<sup>3</sup> The variable values can then be used to interpret residence time distribution profiles.

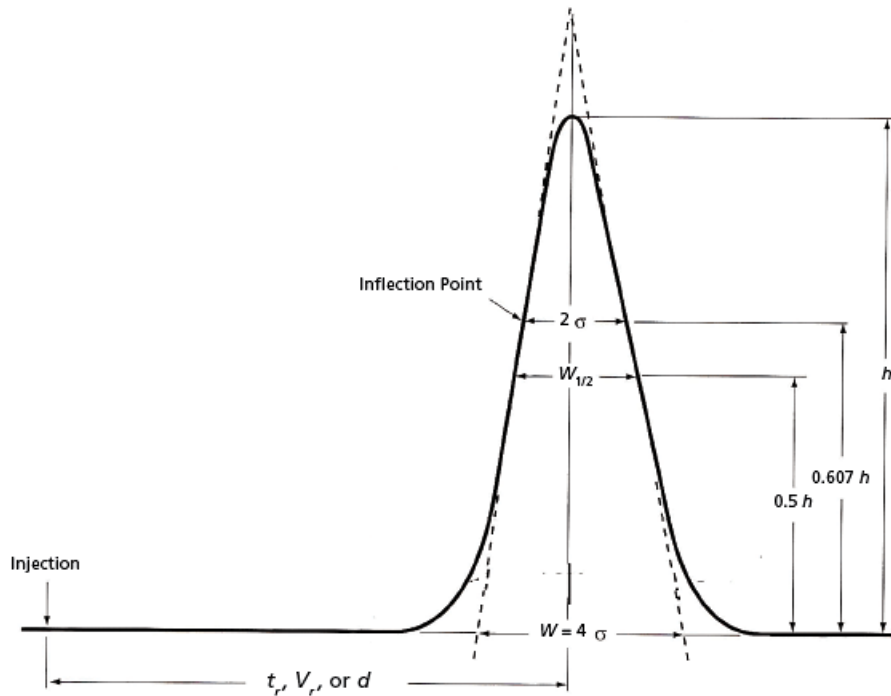


Figure 6. Gaussian Chromatographic Plot of Relative Peak Height v. Time, with key parameters indicated on the curve<sup>5</sup>

HETP is also related to the intraparticle diffusion. Using moment equations for a single solute pulse within a packed chromatography column that is also valid for liquid chromatography in a packed column, the effect of superficial fluid velocity ( $U$ ) on HETP equation relate HETP to is given by:

$$HETP = 2 \frac{D_L}{U} + 2U \frac{\epsilon}{1 - \epsilon} \left( \frac{R_p}{3k_f} + \frac{R_p^2(K - \epsilon_p)}{15K^2 D_e} \right) \left( 1 + \frac{\epsilon}{(1 - \epsilon)K} \right)^{-2} \quad (3)$$

Here,  $\epsilon$  is the void fraction of the packed column,  $K$  is the absorption constant for the solute on the catalyst assuming linear adsorption isotherm,  $D_e$  is the effective diffusivity of the solute within the catalyst micro- or meso- pores ( $\text{cm}^2/\text{s}$ ),  $D_L$  is the axial dispersion coefficient ( $\text{cm}^2/\text{s}$ ),  $k_f$  is the convective mass transfer coefficient of solute for flow of solvent around the catalyst particle, and  $\epsilon_p$  is the void fraction occupied by catalyst pores.<sup>33</sup>

In Equation 3 above, the axial dispersion ( $D_L$ ), convective mass transfer resistance, and the effective diffusion resistance terms are linearly additive. This means that with Reynolds numbers  $0.0015 < \text{Re}_p < 55$ , for  $\text{Re}_p$  based on diameter of particle  $d_p$ , the value of  $k_f$  can be estimated using the mass-transfer velocity since the intraparticle mass-transfer resistance is usually match greater than the convective mass-transfer resistance at such small Reynolds numbers.<sup>33</sup>

HETP is also related to the binding affinity ( $K$ ), or the binding interaction between an immobilized ligand and its binding partner in a chromatography column in Equation 3.  $K$  can be obtained using the slope of  $\mu$  v.  $1/U$  data from the following equation:

$$\mu = \frac{L}{U} \left( 1 + \frac{1 - \epsilon}{\epsilon} K \right) \quad (4)$$

As the surface diffusion coefficient for solute diffusion in liquid-filled pores decrease logarithmically, the absorption constant  $K$  increases. Solute-adsorbent interaction led differences in surface diffusion coefficients may be integral in determining the overall effective diffusivity.<sup>33</sup>

### 2.3 Diffusion in Porous Media

Diffusivity is a term that describes the movement of one material through another. It is the relationship between the concentration flux ( $J$ ) and the gradient of chemical potential.<sup>29</sup> The diffusion coefficient is a measure of the rate at which a material moves.<sup>14</sup> This coefficient changes as the parameters of a system change. The diffusion coefficient  $D$  can often be solved by using

Fick's law of diffusion and a mass balance around a transient sphere with no reaction or advection which consists of the following two equations:<sup>10</sup>

$$\text{Fick's Law of Diffusion} \quad \frac{\partial q}{\partial t} = \frac{D}{r^2} \frac{\partial}{\partial r} \left( r^2 \frac{\partial q}{\partial r} \right) \quad (5)$$

$$\text{Reactor Mass Balance} \quad \frac{\partial q}{\partial t} = D \left( \frac{\partial^2 q}{\partial r^2} + \frac{2}{r} \frac{\partial q}{\partial r} \right) \quad (6)$$

Using Equation 5, the diffusion coefficient can be fit by integrating the equation over time and comparing the changing concentration  $q(t)$  with the experimentally measured concentration that is absorbed or released from a polymer bead. Equation 5 can be applied to systems that are not steady.<sup>10</sup> Here Fick's law is shown in radial coordinates.<sup>27</sup> Typical diffusion coefficients for a molecule in the gas phase are from  $10^{-6}$  to  $10^{-5}$  m<sup>2</sup>/s while diffusion for molecules in the liquid phase is typically much slower from  $10^{-10}$  to  $10^{-9}$  m<sup>2</sup>/s.<sup>9</sup> Fick's law of diffusion can be used to calculate the diffusion coefficient of a molecule when using zero-length chromatography by using the mathematical model that will be further discussed in section 2.3.2. In this case, the diffusion coefficient is the movement of an analyte (an amino acid) through the polymer resin. In an ideal situation, the diffusion will be the same in both pure liquids and through the resin. However, this is not typically accurate in experimental circumstances. Typically, as pores fill up further or you have higher cross-linking or higher loading the analyte will move through the system more slowly. It is expected that the diffusion coefficient will decrease by many orders of magnitude when in resin compared to in a pure liquid.

### 2.3.1 Zero-Length Chromatography (ZLC)

Zero-length chromatography is an experimental method that is typically used to measure adsorption equilibrium and kinetics.<sup>5</sup> One advantage of this method is that the mathematical

modeling of the desorption curves of the ZLC system with liquid takes into account the time constant for diffusion between the sorbent and washout time for the desorption of the sorbent. This method retains the features of conventional fixed-bed chromatographic techniques and eliminates any effects of axial dispersion.<sup>48</sup>

### 2.3.2 ZLC Mathematical Model

The following mathematical model can be used to analyze ZLC experimental data:<sup>6</sup>

$$\text{Fluid-Phase Mass Balance} \quad V_s \frac{d\bar{q}}{dt} + V_f \frac{dc}{dt} + F_c = 0 \quad (7)$$

$$\text{Solid-Phase Mass Balance} \quad \frac{\partial q}{\partial t} = D \left( \frac{\partial^2 q}{\partial r^2} + \frac{2}{r} \frac{\partial q}{\partial r} \right) \quad (8)$$

$$\text{Initial Condition} \quad q(r, 0) = q_0 K c_0 \quad c(0) = c_0 \quad (9)$$

$$\text{Boundary Conditions} \quad \left( \frac{\partial q}{\partial r} \right)_{r=0} = 0 \quad q(R, t) = K c(t) \quad (10)$$

One characteristic that makes the ZLC particularly useful is that the mass balance can be reduced to that of a perfectly mixed cell since the limit of the length of the column goes to zero. Equation 7 describes the mass balance for the fluid phase. In Equation 7,  $\bar{q}$  is the average adsorbed phase concentration,  $c$  is the fluid phase concentration,  $F_c$  is the volumetric flow rate,  $V_s$  is the volume of solid in the column, and  $V_f$  is the volume of the fluid in the column. Taking an integral of this equation will allow you to calculate the concentration of the adsorbed phase at any time.<sup>5</sup> Equation 8 describes the mass balance in the solid phase. This is Fick's second law of diffusion, where  $q$  is the adsorbed phase concentration,  $r$  is the components radial coordinate and  $D$  is the diffusivity. Equations 9 and 10 are the initial and boundary conditions for this system of equations, where  $K$  is the equilibrium constant.<sup>6</sup> By experimentally saturating the solid phase with the analyte

then instantly switching to pure solvent at  $t = 0$ , the desorption profile can be measured at the effluent. This profile ( $c(t)$  v. time) can then be fit using Equations 7 to 10 to solve for  $D$  and  $K$ .

For this project, a ZLC column was attached to an HPLC stack to measure the diffusion of a tracer amino acid through resin, and ultimately used to understand the diffusional limitations present during SPPS.

## **2.4 Modeling Packed Bed Reactors**

Packed-bed reactors are one of the most commonly used reactors due to their performance effectiveness and low operating and capital costs. They also can support both liquid and gas flow of reactants through the bed. With this both single-phase flow and two-phase flow are possible. However, in terms of peptide synthesis, single-phase flow is utilized as the reactants are all liquid. Also, in most packed-bed reactors, the packed bed is a catalyst that increases the reaction rate, whereas in peptide synthesis the packed bed is the resin and is a support system for the peptide to grow on. Despite these differences, both provide a porous system through which the reactants must flow. In processes in which there is liquid present, these pores become filled with the liquid which can lead to diffusional limitations in the bed due to low diffusivity in the liquid phase. This diffusivity can be adjusted by changing the size of the resin particles. More explicitly, the specific surface area of the bed, which is the ratio of the particle surface area to the particle volume, should be as high as possible. One way to achieve this is by decreasing the size of the particle. However, there is a limit to how small the resin particle can be based on the allowable pressure drop across the bed.<sup>32</sup> Typically, the resin particle size used for peptide synthesis is either 200-400 mesh, which is 35-75 microns in diameter, or 100-200 mesh, which is 75-150 microns in diameter.<sup>24</sup> It should also be noted that particle shape influences the degree of bed porosity which also affects the

pressure drop. Therefore, the resin being used is a particularly important factor in the effectiveness of peptide synthesis and should be properly analyzed to determine the best particle size.<sup>32</sup>

When working with packed bed reactors, there are many parameters that must be considered for the most efficient system. This section will discuss two methods for modeling the flow through packed-bed reactors and discuss how they can be used to design an ideal system.

### 2.4.1 Pressure Drop: Ergun Equation

Being able to model flow through porous media such as resin, has been a continued interest in the field of engineering.<sup>32</sup> For modeling and designing a packed-bed reactor, the pressure drop across the bed and the packing void fraction (porosity) are important variables.<sup>34</sup> However, considering both parameters can be complex, to simplify the model, it can be assumed that the porous bed is homogeneous. That is, the porosity does not vary much and there is a steady flow through the bed. Utilizing these assumptions, the pressure drop across the packed bed can be modeled using the Ergun equation as seen below.<sup>32</sup>

$$\Delta p = \frac{150\mu L (1 - \epsilon)^2}{D_p^2 \epsilon^3} v_s + \frac{1.75L\rho (1 - \epsilon)}{D_p \epsilon^3} v_s |v_s| \quad (11)$$

This equation models flow through a packed bed in which  $\Delta P$  is the pressure drop,  $L$  is the bed length,  $\mu$  is the fluid viscosity,  $v_s$  is the fluid velocity,  $D_p$  is the particle diameter, and  $\epsilon$  is the void space. This is useful to determine the pressure drop across the bed and indicates that the pressure drop is a function of the length of the bed, the packing size, and the fluid density and viscosity. Therefore, this equation can be utilized to understand how changing the parameters, including the size of the resin beads will affect the pressure drop in the system.<sup>52</sup>

## 2.4.2 Residence Time Distribution

Another way to measure mixing in a packed-bed reactor is by looking at the residence time distribution (RTD). RTDs are used constantly by chemical engineers to understand the mean residence time. That is, the distribution of time that a component, solid or fluid, remains in a system.<sup>25</sup> Another important aspect of residence time distributions is dispersion. Dispersion is based on two phenomena: diffusion and variation from ideal plug-flow behavior. In sum, dispersion is a measure of the degree of axial mixing in a reactor. If particle flow through a reactor follows ideal plug-flow and has no axial mixing, the dispersion coefficient is close to zero. Therefore, as the dispersion coefficient increases, so does the degree of mixing.<sup>36</sup> Finally, the RTD can also help engineers understand potential nonuniformities in the flow path. There may be channeling, where the particle tends to flow towards the wall, or the particle could get trapped in dead volume within the reactor. Both of which can increase the mean residence time. Overall, it is important to understand the flow profile of the target component to make a process more efficient. The information collected from a residence time distribution can then be compared to the time of the reaction or process as a whole, as characterizing the RTD is the first step to improving a process. By understanding the time distribution, engineers can then determine the problems in the reactor or system and then re-design and improve the process.<sup>25</sup>

During peptide synthesis, the peptide is grown on resin, and typically in a packed-bed reactor or column. Packed beds can make it difficult for the component of interest, in this case, amino acids, to flow through the system. There may be some parts where the amino acid can flow quickly thorough and other parts where it gets held up. This can be seen in Figure 7. This figure shows what may occur inside a packed bed reactor. There may be parts like Path 1 where there is little resistance to flow, and the particle or fluid can flow quickly through. On the other hand, there

are paths like Path 2 where there is a lot of resistance to flow causing the molecule to spend a longer time in the reactor. This is an example of an issue that can be investigated through characterizing the RTD.<sup>11</sup>

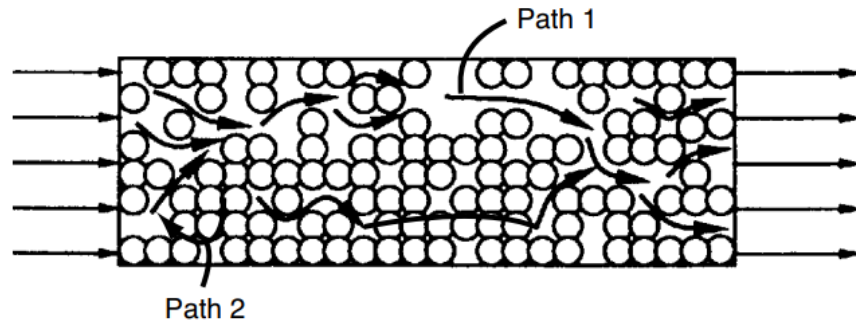


*Figure 7. Flow Paths in a Packed Bed Reactor<sup>11</sup>*

Residence time distribution can be determined experimentally using a tracer. This tracer can be an atom, an inert chemical, or a molecule, and is injected into the system or reactor at time  $t=0$ . Then the concentration of the tracer is measured in the exit stream as a function of time. When choosing the tracer, it is important to look at its properties, as it must imitate the actual component that will be flowing through the system. Consequently, for the tracer to be effective it must be a non-reactive species whose physical properties match that of the mixture. It also needs to be soluble in this mixture and a detectible molecule in order to measure the concentration. The most common methods to inject the tracer and perform an RTD experiment are pulse input and step input.<sup>11</sup>

In a pulse input experiment, a pre-determined amount of tracer is quickly injected into the feed all at once. The goal is to inject it in the shortest amount of time possible. Then the concentration leaving the system is measured as a function of time. The concentration versus time curves for this experiment are seen in Figure 8.<sup>11</sup>

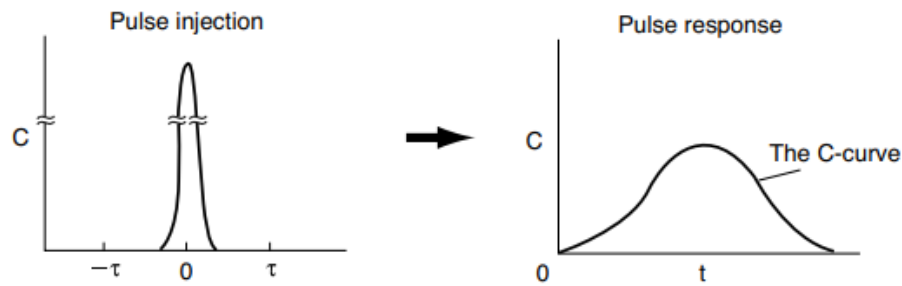


Figure 8. Concentration Versus Time Graphs for Pulse Injection<sup>11</sup>

The pulse injection curve should be a sharp peak, indicating the desired concentration of tracer ( $N_0$ ) was injected in a very short time as seen in Figure 8. The concentration-time curve of the effluent, or outlet stream, is known as the C-curve. In an ideal scenario, there is no dispersion, in which all the tracer comes out at once. However, in most scenarios, including that of a packed bed reactor, the data is non-ideal. When there is dispersion, not all the tracer leaves the system at once. This results in a C-curve, where there is a long tail on the right side of the graph. The goal is to shorten this tail and have a sharp peak instead.<sup>11</sup> From the C-curve the residence time distribution function,  $E(t)$ , can be obtained using Equation 12.

$$E(t) = \frac{C(t)}{\int_0^{\infty} C(t) dt} \quad (12)$$

If done right, the pulse injection experiment is a much easier and straightforward method of calculating the RTD. However, despite its simplicity, there are some drawbacks to this experiment. For one, it is extremely difficult to inject the tracer in such a short amount of time. Another issue is being able to fit the RTD function,  $E(t)$ , to a polynomial if the system is non-ideal, and has a long tail. When the C-curve has this shape, it can be difficult to integrate.<sup>11</sup>

The other common method to determine RTD is the step tracer experiment. Rather than injecting the tracer all at once a specific concentration ( $C_0$ ) of tracer is added at a constant

volumetric flow rate. This flow rate is kept constant until the concentration left in the effluent is equal to that of the feed. Once this is achieved the experiment can be stopped. The concentration versus time curves for the step injection and response is seen in Figure 9.<sup>11</sup>

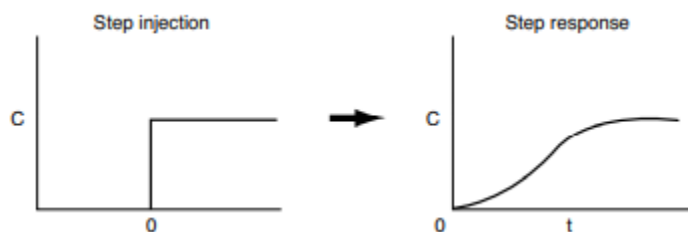


Figure 9. Concentration Versus Time Curves for the Step Input Experiment <sup>11</sup>

From these curves, the RTD function  $E(t)$  can be determined using Equation 13 below.

$$E(t) = \frac{d}{dt} \left[ \frac{C_{out}(t)}{C_o} \right]_{step} \quad (13)$$

This RTD method has some advantages over pulse input. For one, it is generally easier to run than the pulse input because the tracer does not need to be added all at once in a brief time period. Also, unlike the pulse experiment, the total tracer concentration throughout the feed over the time of the experiment does not need to be known. Although this may be true, the constant volumetric flow rate can lead to problems. Sometimes keeping a constant feed tracer concentration throughout the length of the test can be hard. Consequently, the constant inlet flowrate requires a substantial amount of tracer which can get expensive depending on the tracer being used. Finally, there is a large potential for error since the RTD function for this test requires the data to be differentiated.<sup>11</sup>

For this project, residence time distributions will be analyzed to study the flow of amino acids through the resin at different parameters. Currently, during peptide synthesis, the concentration versus time curves for each coupling step look similar to the non-ideal reactor C-

curve. That is, for each coupling step, the amino acid is added to the resin, the reaction occurs, and then the excess products are washed out. However, when washout occurs not everything leaves at the same time as some materials get stuck in the resin, leading to that long tail on the C-curve. Therefore, by running RTDs at different parameters, including changing flow rate, dead volume, or oscillations, the ideal parameters for fast coupling and washout can be determined.

It is also important to consider the difference between convoluted, empty-convoluted, and deconvoluted data. As shown in Figure 10, convoluted data, or data obtained without bypassing the reactor or the column, contains RTD data resulting from previous tubing and empty column. It is integral to deconvolute data obtained for more in-depth analysis of the RTD curves. Deconvolution can be done by subtracting the bypass data or the empty convoluted data from the convoluted RTD. This required running RTDs not only at different parameters, but also with different process schematics.

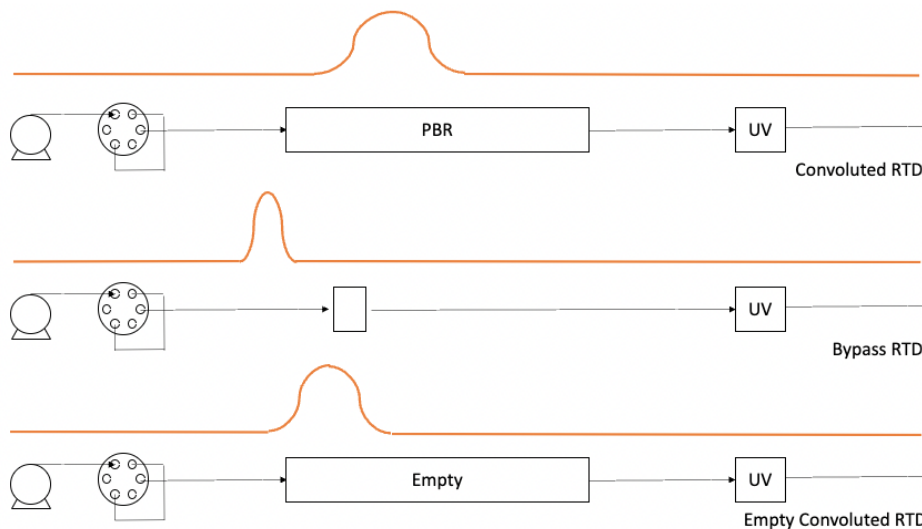


Figure 10. Illustration of the differences in RTD curves for Convoluted, Bypass, and Empty Convoluted Process Schematic

## **Chapter 3 Materials and Methods**

The goal of this project was to understand what leads to slow coupling and washout times to ultimately decrease them, making the process more efficient, and to decrease unnecessary waste.

To achieve this goal the following objectives were followed:

1. Measure the intrinsic diffusion of amino acids in fresh and peptide bound resins
2. Characterize mixing and propose changes to achieve near plug-flow operation
3. Minimize solvent waste and reduce coupling times

This chapter will discuss the experiments used to attain these objectives that in turn lead to recommendations for the future.

### **3.1 Zero Length Chromatography Experiments**

To begin, the intrinsic diffusion of glycine in fresh and peptide bound resins was measured using a zero-length column connected to an HPLC stack. This section will discuss the setup of the HPLC as well as the experimental plan that was followed.

#### **3.1.1 HPLC Configuration**

The HPLC system used was the Agilent 1100 series, as shown in Figure 11. On top of the stack were bottles with samples of amino acid and DMF. From top to bottom, the HPLC stack

contained a degasser, a binary pump, an autosampler, a column compartment, and a diode array detector. The degasser used was the Agilent G1379A. This is a micro vacuum degasser with 4 channels that contain structured membranes and a vacuum pump. When turned on a partial vacuum is generated, and the pressure is monitored by a pressure sensor. The binary pump used was the Agilent G1312A. This pump has dual pistons that allow for effective mixing and ensures a stable, pulse-free solvent flow. It should be noted that pump A was clogged so an external Sonntek P



*Figure 11. HPLC and ZLC Set Up*

4.1S pump was used instead. Pump B was used for the DMF sample while the external pump was used for the amino acid sample. Next is the G1313A autosampler and the G1316A column compartment. The column compartment contains a 6-port switching valve. The valve is configured with port 1 coming from the external pump, port 2 going to the zero-length chromatography column which then goes to the UV detector and finally is sent to waste port 3 coming from pump B, port 4 being recycled back to the DMF container, port 5 is blocked, and port 6 recycles back to the amino acid container. For this, valve position 1 is defined as flow from port 1 to 2 whereas position 2 flows from port 1 to 6. A schematic of this configuration can be seen below in Figure

12. The G1315B diode array detector can be used at wavelengths of 190 to 950 nm to verify separation quality.

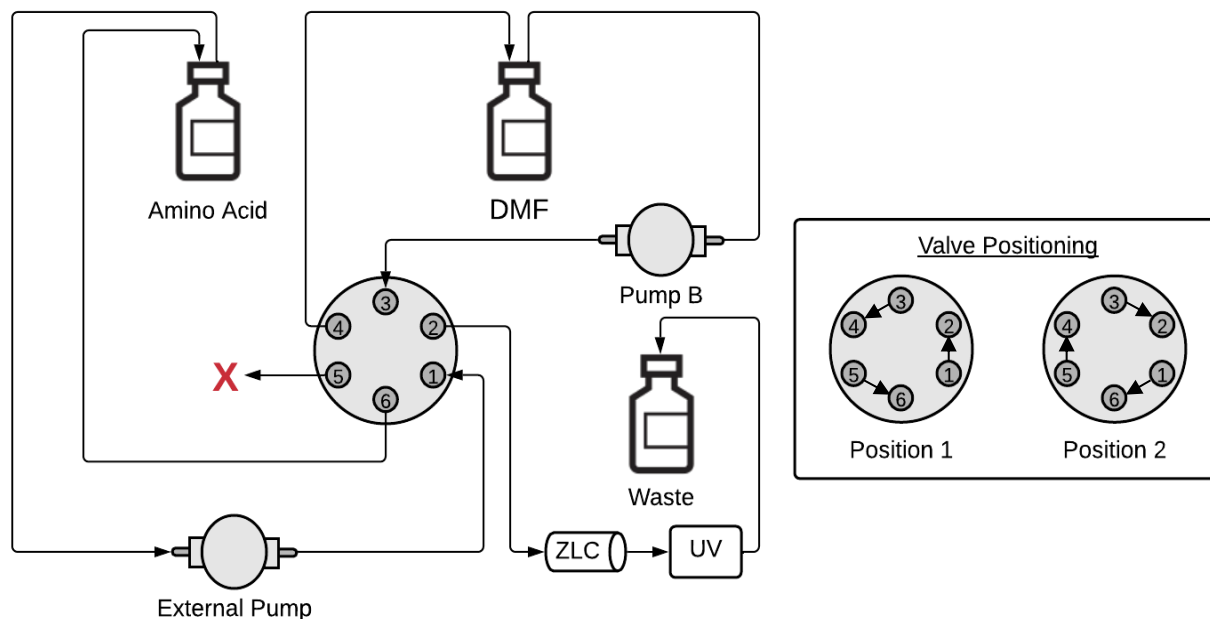


Figure 12. Schematic of 6-Port Valve Configuration

### 3.1.2 Amino Acid Diffusivity in Resin

In order to determine the diffusivity of various amino acids in different resins, HPLC system discussed in the previous section was used with a ZLC column as shown in Figure 13. The ZLC column that was used consisted of a 1-micron screen, a stainless steel 1/4"x 1/16" internal reduced fitting with 1 mm bore and a stainless steel 1/4"x1/16" column end fitting with 0.4 mm bore and 4.6 mm cone without frit. The following experiment was repeated for Fmoc-Gly in fresh PEG and peptide-bound PEG resin. A 0.2 M amino acid solution was made with DMF as the solvent and was placed in a 500 mL glass media storage bottle which was connected to the external pump. 400 mL of pure DMF was added to a second 500 mL glass media storage bottle and connected to pump B. 5 mg of resin were weighed out and added to the column. Then, between 5

and 10 drops of dimethylformamide (DMF) were added to swell the resin. Fresh resin, peptide-bound PEG resin, an empty column, and a column with glass beads were run with flow rates of 1, 1.5 and 2 mL/min. First, the 6-port valve was set in position 2 for 10 minutes so that just the solvent (DMF) was flowing through the detector. At 10 minutes the valve was switched to position 1 to allow both solvent and amino acid to flow through the column. At 40 minutes the washout period was started by switching the valve back to position 1 allowing only solvent to flow through. The washout period continued for 60 minutes until the system returned to baseline. The above is repeated for a total of 9 trials with specific parameters listed in Table 1.

*Table 1. ZLC Experimental Plan*

<b>Experiment</b>	<b>Flow Rates (mL/min)</b>	<b>Number of Runs Per Flow Rate</b>	<b>Total Runs</b>
Fresh PEG Resin	1, 1.5, 2	3	9
Peptide Bound PEG Resin	1, 1.5, 2	3	9
Empty	1, 1.5, 2	3	9
Glass Beads	1,1.5, 2	1	3
<b>Total Runs</b>			<b>27</b>

The product of amino acid and DMF was then separated using a rotary evaporator to conserve and recycle DMF. DMF has a boiling point of 153°C while the boiling points of Fmoc-Gly is 438.8°C, making DMF easily separate by evaporation.<sup>7, 45</sup>



*Figure 13 ZLC Column*

The ZLC data was analyzed using MATLAB (as seen in Appendix A.1), assuming that the resin beads are spherical. Time and Absorption values were recorded, and the absorption values were fitted and standardized using logarithmic function and concentration terms:

$$\ln\left(\frac{C}{C_0}\right) = \ln\left(\frac{C - C_{min}}{C_{max} - C_{min}}\right) \quad (14)$$

Then, the  $\ln(C/C_0)$  is plotted against time; the tail, or the release profile of the residence time distribution curve for different flowrates under different schematics were compared and analyzed. The diffusivity constants were calculated for the linear regions of the release profile under different flowrates and within different resin or column set up to investigate the diffusivity limitations on the ZLC column under different parameters. The graphs with the linear fits of each release profile can be seen in Appendix B. It is assumed that the size of the fresh PEG resin, swelled, was 500 to 800  $\mu\text{m}$  and the peptide-bound PEG resin in Table 2 swelled, had a bead size between 75 and 150  $\mu\text{m}$  based on microscopy imaging. Additionally, the glass beads used were 600 to 710  $\mu\text{m}$  in size.

### 3.1.3 Safety

#### *N, N-Dimethylformamide (DMF)*

N, N-Dimethylformamide (DMF) was used as a solvent throughout this experiment. DMF is considered Hazardous by the 2012 OSHA Hazard Communication Standard (29 CFR 1910.1200). It is only recommended to use as a laboratory chemical, and not advised for use with food, drug, pesticide, or biocidal products. DMF is flammable in liquid and vapor form, harmful in contact with skin, and can cause serious eye irritation. It is harmful if inhaled, may cause respiratory irritation, drowsiness or dizziness, nausea, and vomiting. DMF also causes gastrointestinal discomfort.<sup>46</sup>

DMF is a colorless liquid that is soluble in water and stable under normal conditions. DMF flashes at 58 °C and auto-ignites at 445 °C. The lower and upper explosion limits of DMF are 2.2 volume percent and 15.2 volume percent, respectively. The odor is rotten egg-like. DMF also has a vapor pressure of 4.9 bar at 20°C. The container may explode when heated, and DMF vapors may form explosive mixtures with air. Vapors can travel to the source of ignition and flashback. DMF can decompose into carbon monoxide, carbon dioxide, and nitrogen oxides. Nevertheless, there should be no hazardous reactions under normal processing.<sup>46</sup>

In this experiment, all safety precautions were read and understood before handling DMF. Special instructions were obtained before use, and personal protective equipment such as nitrile gloves and goggles were used. If any DMF came into contact with gloves, gloves were immediately changed, and hands were thoroughly washed. Other good industrial hygiene and safety practices were also used to avoid exposure. Wearing contacts was avoided. DMF was only used in well-ventilated areas and breathing dust, fumes, gas, mist, vapors, and spray were avoided. While storing DMF, DMF was tightly closed, stored in a dry, cool, well-ventilated place, and kept away from heat, spark, open flames, as well as hot surfaces. It is also important that DMF is incompatible with strong oxidizing agents, halogens, halogenated compounds, and reducing agents. No smoking was allowed in the lab. The container was grounded or bonded, and explosion-proof electrical/ventilating/lighting equipment, as well as non-sparking tools, were used. Precautions were also taken to avoid static discharge.<sup>46</sup>

### *Fmoc Glycine*

Fmoc glycine is a white powder that is a strong oxidizing agent not classified as a hazardous substance or mixture according to the GHS and OSHA criteria. For personal protection, personnel should wear protective equipment such as goggles and gloves. It is important to avoid dust

formation and breathing in vapors, mist, or gas. Appropriate exhaust ventilation at places where dust is formed should be provided. To protect the environment, do not let products enter drains. For storage, keep the container tightly closed in a dry and well-ventilated place at a temperature between 2 and 8 degrees Celsius.<sup>2</sup>

## **3.2 Residence Time Distribution Experiments**

The flow and mixing properties of amino acids in the resin were characterized by analyzing residence times. Mytide provided UV data of 13 peptides they have run in the past. From this data, RTDs of the deprotection peaks for each amino acid in the peptide were run to understand the current problems and trends during actual synthesis. Next, Mytide ran numerous experiments using glycine as a tracer amino acid to understand the effect of changing parameters. This section will outline how these experiments were run and the data extraction process.

### **3.2.1 RTD of Current Peptide Synthesis Method**

First, 13 of Mytide's previously synthesized peptides, each composed of different sequence of amino acid residues, were studied using residence time distribution. Each reagent has multiple sets of absorption data under different wavelengths, and the UV resulting in the least noise is chosen for further analysis. Each UV vs. time curve consisted of multiple peaks. For each amino acid, there exists a coupling peak and a deprotecting peak. The residence time distribution and dispersion of both peaks for all 13 peptides were studied.

Python (as seen in Appendix A.2) is used to extract the peptide UV v. time data from Mytide database. Mytide provided the initial codes for data extraction using NumPy and panda library, and the code is edited to extract data for each ID by each wavelength using the panda library. The data extracted are automatically stored as .csv files organized by their ID and then

their wavelength in folders in a specified location. For the 13 peptides studied, the coupling and deprotecting peaks were also separated into individual csv files, saved under each wavelength.

Following data extraction from Python, the UV vs time data that was collected was separated into individual couples and deprotection peaks based on the times of valve switches pulled from the Mytide database if necessary. These individual peaks were then analyzed using the MATLAB code shown in Appendix A.3. First, the .csv files with the individual peaks are imported into MATLAB. Then, the code gives outputs of  $\tau$  and  $\frac{D}{\mu L}$  with  $\tau$  being the residence time in seconds and  $\frac{D}{\mu L}$  being the dispersion time. The code also outputs a graph as seen in Figure 14. In the graph the blue line is the bypass data, the red line is the couple or deprotection peak, the yellow is the reactor, and the purple is the deconvoluted data.

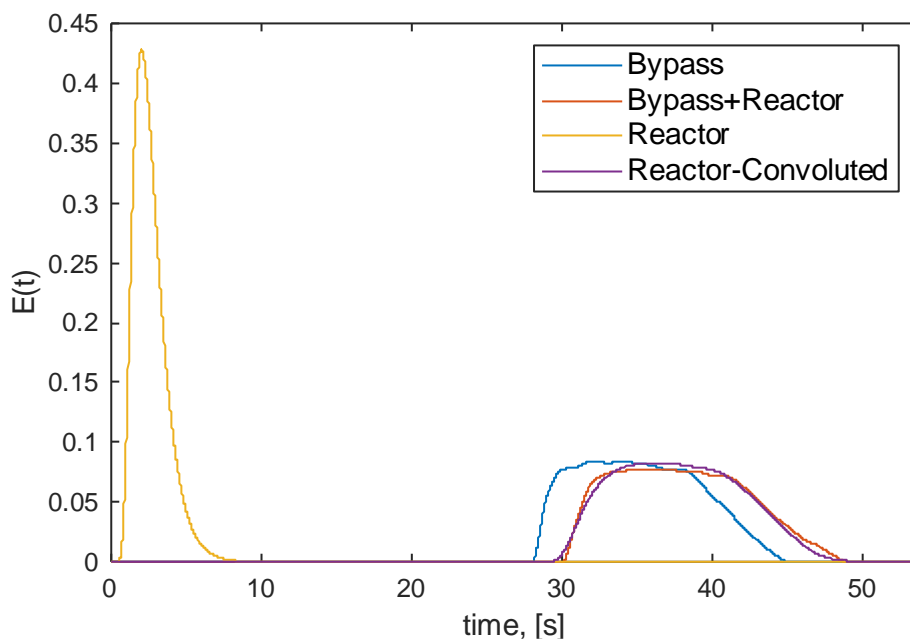


Figure 14 Sample Residence Time Distribution curve obtained from MATLAB

After running the MATLAB code, the collected data was transferred to an Excel sheet. The sheet kept track of peptide number, amino acid being coupled, couple number, residence time and dispersion number. For each peptide, three graphs were made: residence time v. couple number,

dispersion versus couple number, and dispersion versus residence time. This was then analyzed to determine trends among growing peptide chains. Next, a sheet was made for each of the 20 amino acids. These sheets would auto populate the data from the original sheet for their respective amino acid. For example, the Alanine sheet would populate the couple number, residence time, and dispersion number for any data point labeled “Ala” in the original sheet. The same three graphs that were discussed before were made for the individual amino acids as well and then analyzed.

### 3.2.2 RTD Experiments

Residence time distributions were run to determine how long an amino acid remains in the system under different conditions. This set of experiments were run at the Mytide facility and involved injecting a tracer amino acid, glycine, into the reactor and measuring the absorbance versus time of the tracer leaving the system. To understand how given parameters affect residence time, the team had Mytide run the following experiments:

*Table 2. Summary of Residence Time Distribution Experiments*

Run	Type	Headspace?	Oscillation?	Conditions	Total Experiments
N/A (bypass)	Non-convoluted	N (no reactor)	Y + N	Gly diffusion suite through bypass	10
Empty vial	Empty Convoluted	Y (full)	Y + N	Gly diffusion suite through empty reactor	10
Resin 100 mg	Convoluted	Y (partial)	Y + N	Gly diffusion suite at 0, 5, 10, 15, 20 amino acids coupled to resin	50
Glass beads (headspace = 60 mg resin)	Convoluted	Y (partial)	Y + N	Gly diffusion suite in reactor filled with glass beads	10
Glass beads (headspace = 100 mg resin)	Convoluted	Y (partial)	Y + N	Gly diffusion suite in reactor filled with glass beads	10
Glass beads (full)	Convoluted	N	Y + N	Gly diffusion suite in reactor filled with glass beads	10

Each of the runs above were run at five different flowrates with and without oscillation, for a total of 10 experiments for each run. It should be noted that the actual flowrates used my Mytide cannot be disclosed. Therefore, throughout this report the flowrates will be standardized as the flowrate/max flowrate. The following standardized flowrates were used: 0.083, 0.333, 0.583, 0.792, and 1. For simplicity these flows will be denoted as flowrates A-E: A being the minimum flowrate and E being the maximum. The runs with resin have a total of 50 experiments as the glycine tracer was injected at the given flowrates and oscillations when 0, 5, 10, 15, and 20 amino acids were coupled to the resin.

As seen in the Table 2, the team chose to analyze flow rate, headspace, oscillations, effect of a peptide bound resin, and the use of glass beads. This was needed to understand how amino acids flow through the reactor at a variety of parameters. First, flow rate was analyzed to determine if the rate at which the amino acid enters the reactor affects the time it spends in it. The second condition to test was headspace. During normal production, there is some headspace at the top of the reactor. Therefore, it was important to also measure the residence time with and without headspace. Third, during synthesis, there is usually some oscillation to keep the bed fluidized. To understand how this affects the residence time runs both with and without oscillations were measured. Finally, runs were completed with an increasing number of amino acids bound to the resin to understand how a growing peptide chain affects the flow through the reactor. For each experiment, absorbance versus time data was obtained and the residence time and dimensionless dispersion number were obtained using MATLAB code as seen in Appendix A.3.

## Chapter 4 Results

### 4.1 ZLC Results

#### 4.1.1 Amino Acids under Different Flow Rates

First, the normalized ZLC absorption v. time data was analyzed under different flow rates for each column bed used. As shown in Figure 15, flowrate heavily affects the initial release profile of amino acids, specifically the initial five minutes of release. In fresh resins and empty columns, the higher the flow rate, the faster the initial amino acid release. In peptide bound resins, the initial release profile is similar under all flowrates for the first minute of release, then demonstrated phenomenon similar to that of fresh resin and empty columns one to five minutes after release. The release profile of the glass bead column demonstrated a different behavior, with the 1 mL/min giving fastest release for the first three minutes, and 1.5 mL/min giving the slowest release.

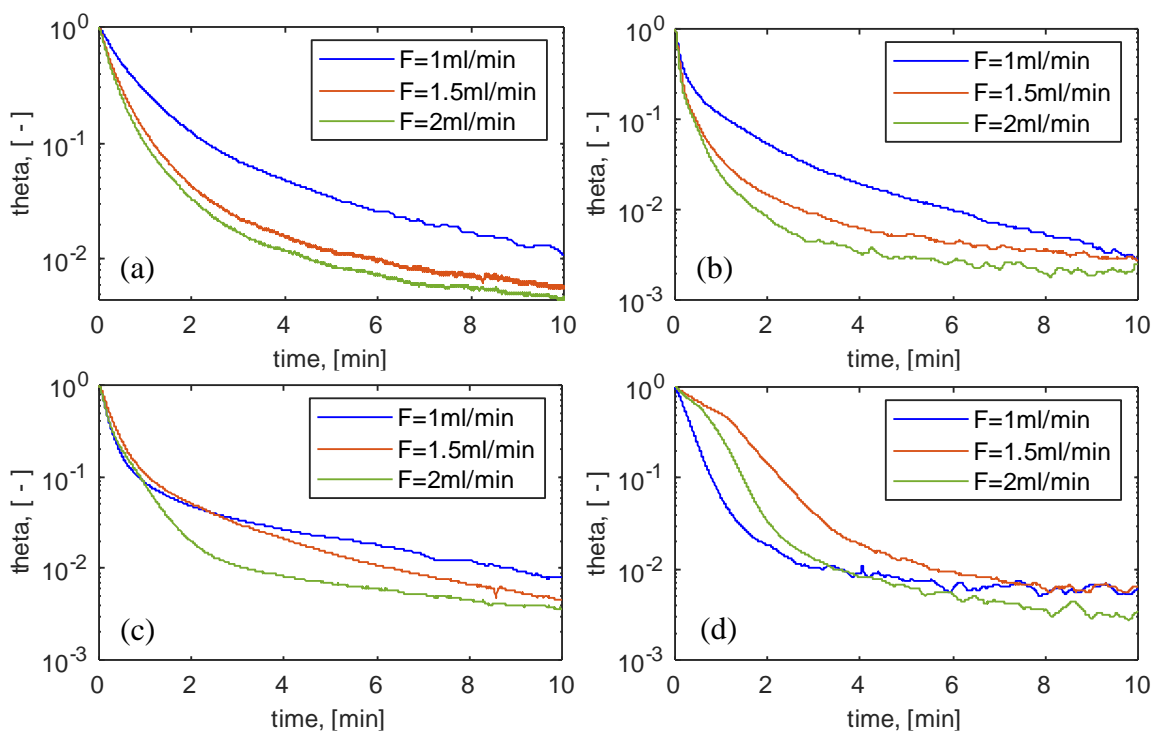


Figure 15. ZLC normalized absorption v. time release profile for (a) fresh resin, (b) empty, (c) peptide bound resin, and (d) glass bead filled columns under different flowrates

As illustrated in Figure 15, after the initial five minutes of release, flow rate had less impact on the release profile. For each ZLC column bed schematic, the release profile under different flow rates approached similar rate of release, suggesting the release profile is less affected by kinematics after the initial wash out period.

#### 4.1.2 Amino Acids under Different Bed Schematics

The release profiles under different ZLC column bed schematics were then analyzed under different flow rates. All flowrates demonstrated similar behavior; Figure 16 below was selected as a depiction of the behaviors observed. All of the release profiles can be seen in Appendix C.

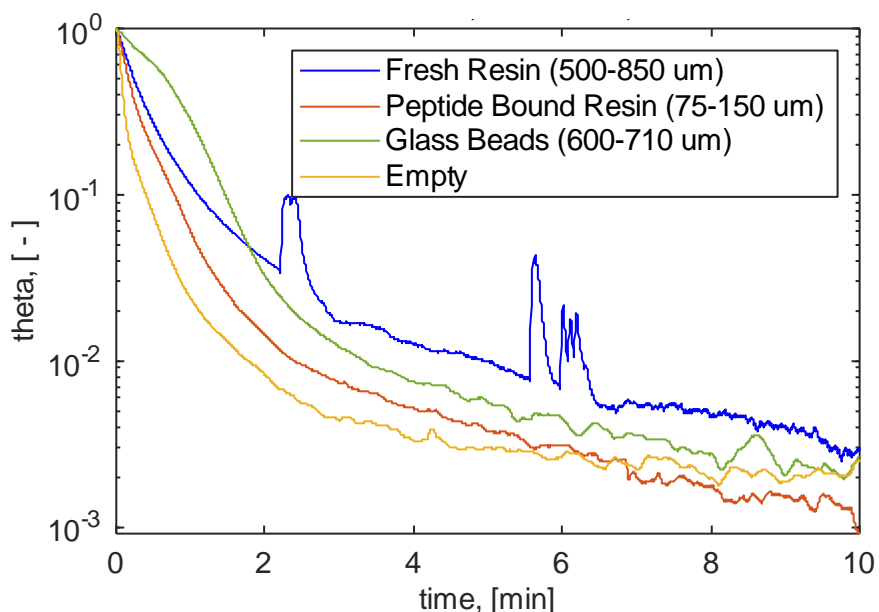


Figure 16. ZLC release profile for different bed schematics at 2 mL/min flow rate

As illustrated in Figure 16 above, fresh resin (500 to 850  $\mu\text{m}$ , swollen) required more time to release the amino acid compared to peptide bound resin (75 to 150  $\mu\text{m}$ , swollen). The initial washout first two minutes after release demonstrated that empty column releases the amino acids at the fastest rate, followed by peptide bound resin, fresh resin, and then glass bead-filled column.

Two minutes after release, the release profile of class bead and empty columns slowly approaches zero, while the fresh resin and peptide bound resin approaches similar rates of release. Generally, the slope of the release profiles stabilized five minutes after release, suggesting that after 5 minutes, the release profile for fresh resin and peptide bound resin are mostly diffusion limited.

#### 4.1.2 Diffusivity under Different Flow Rates and Bed

From the release profiles, the diffusivities were calculated for all ZLC experiments. The diffusivity under different flowrates and bed schematic area shown in Table 3 below.

*Table 3. ZLC Diffusivity under different flowrates and column bed schematics*

Column Bed	Flow Rate (mL/min)	Average Diffusivity (cm <sup>2</sup> /s)
<b>Fresh Resin</b>	1.0	$4.85 \times 10^{-7}$
	1.5	$3.28 \times 10^{-7}$
	2.0	$4.37 \times 10^{-7}$
<b>Peptide Bound Resin-</b>	1.0	$8.57 \times 10^{-9}$
	1.5	$1.25 \times 10^{-8}$
	2.0	$3.83 \times 10^{-9}$
<b>Glass Bead</b>	1.0	$1.62 \times 10^{-7}$
	1.5	$3.26 \times 10^{-7}$
	2.0	$2.91 \times 10^{-7}$

Theoretically, flow rate should not influence the diffusivity. However, the diffusivity measured varies with flow rate. There is also no apparent trend in how the flowrate varies the diffusivity comparing the diffusivity measured for all column bed schematics. On the other hand, the diffusivity of the amino acid in fresh resin is larger than that of the peptide bound resin, which is expected. The amino acids also have larger diffusivity in fresh resin than glass beads, and larger diffusivity in glass beads than peptide bound resins.

## 4.2 Residence Time Distribution Results

### 4.2.1 Residence Time and Dispersion of Amino Acids in Peptide Synthesis

Mytide Therapeutics provided data for 13 sample peptides. The first two peptides were 26 amino acids long and the rest were 14 amino acids long. Table 4 below illustrates the sequence of each peptide and the corresponding sequence. This data was then used to determine if residence time and dispersion number changed as the peptide chain grew on the resin.

*Table 4. Sample Peptides and corresponding amino acid sequence*

Peptide No.	Amino Acid Sequence	Synthesis Difficulty
1	APLGAQLIPRHPCRELVDLTYTQRIS	0.99
2	NQILQITLASKGVGDAGVVVLKYZTM	0.92
3	QIFIFDKSYTALAK	0.87
4	AGAHFGGPGAPGPG	1.29
5	KTDNNELRIHRLQN	1.01
6	TDRSNTVPKTDNNE	1.06
7	FRMTSAALFALLL	0.82
8	KTDNNELRIHRLQN	1.01
9	KTDNNELRIHRLQN	1.01
10	NFALGCEEFKTFNV	0.91
11	PAHAPQGQALAPRS	1.06
12	FDKSYTALAKNFLK	0.9
13	FRMTSAALFALLL	0.82

RTDs were run using the UV data from the deprotection step for each amino acid in the peptide. Figure 17 shows results comparing residence time to couple number. For simplicity, only graphs from four of the sample peptides are shown here as the rest also followed similar trends. The rest of the graphs can be seen in Appendix D. It was expected that as the peptide chain grew, the residence time would increase. This trend was seen in peptide 1, as well as peptides 7 and 13. However, for the most part the residence times followed trends similar to those of peptide 5 and 10 where they remained somewhat stable at around 36 seconds, regardless of couple number.

Finally, one peptide, peptide 11, had a decreasing residence time with increasing couple number. In general, most residence times were found to be between 36 to 40 seconds with some outliers 50 seconds and higher. It should be noted that these residence times were determined without deconvoluting the data with a bypass. This is strictly using raw peptide synthesis data which may be why the values are so high.

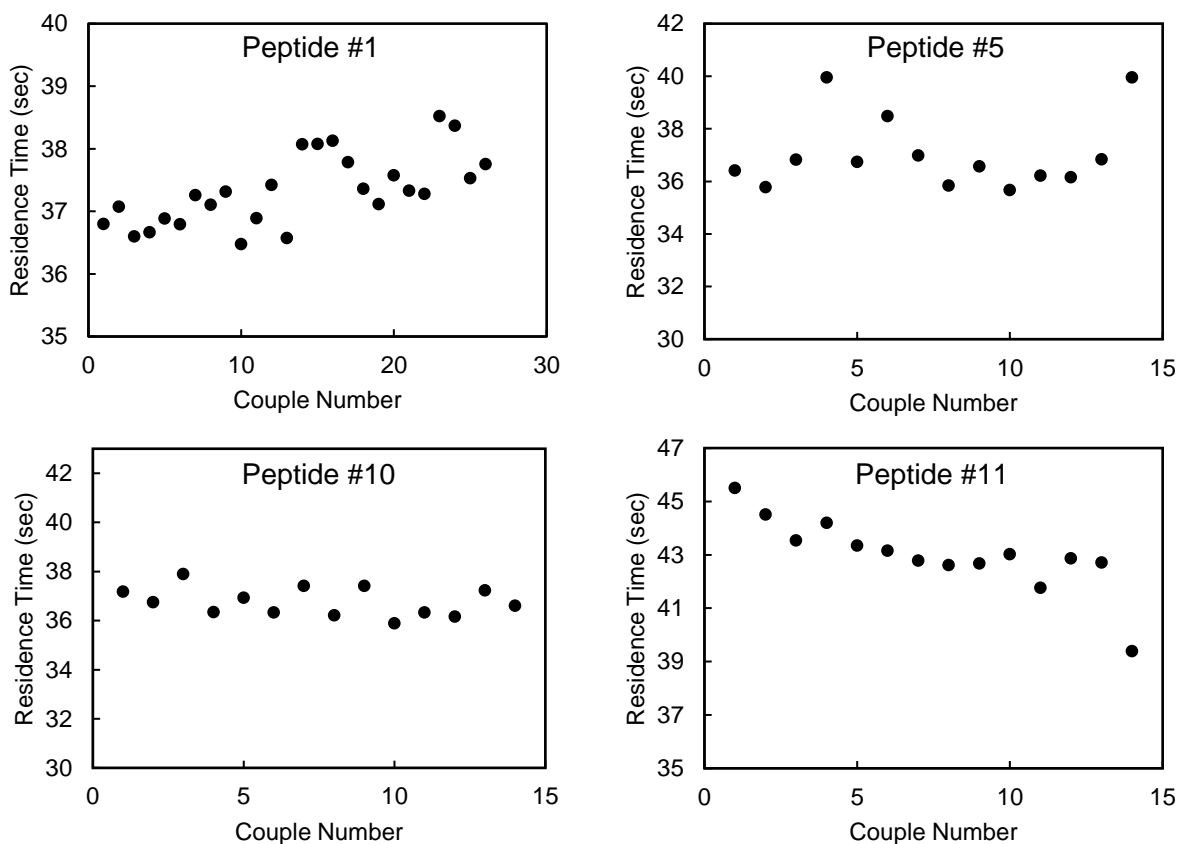


Figure 17. Residence Times Versus Amino Acid Couple Number for Four Sample Peptides

Along with residence time, dispersion number was also analyzed. Figure 18 below shows graphs of dispersion number versus couple number from the same peptides analyzed above. The graphs for the rest of the peptides can be seen in Appendix E. It appeared that the dispersion graphs followed similar trends to their respective residence time graphs. As seen below, peptide 1 had increasing dispersion with couple number, peptides 5 and 10 were somewhat stable, and peptide

11 had a decreasing trend. It was found that the dispersion numbers for these peptides were less consistent with values than the residence time values ranging anywhere from 0.0001 to 0.026.

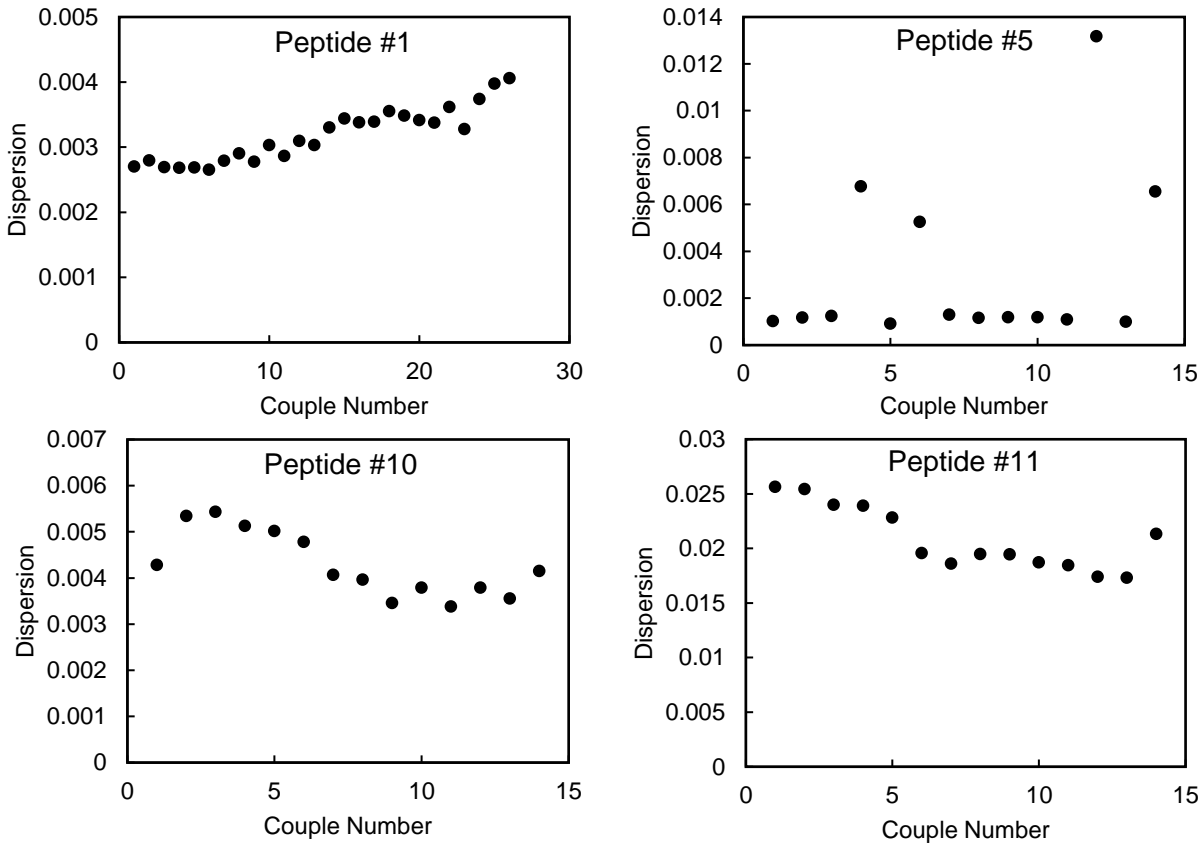


Figure 18. Dispersion Number Versus Couple Number for Four Sample Peptides

It can be seen in the previous two graphs that the residence time and dispersion number follow similar trends for their respective peptides. Therefore, graphs of dispersion versus residence time were also created to understand how these two parameters are related. This was proven to be true as seen in Figure 19. It was found that as residence time increases so does the dispersion number. However, as seen in the previous graphs some of the dispersion numbers are much higher than the rest. So, there is not a direct correlation between dispersion number and residence time and therefore there must be other factors contributing to dispersion number. Here dispersion is represented by the Bodenstein number in which  $Bo = 0$  represents the ideal state of a continuous-

stirred reactor and  $Bo = \infty$  represents continuous flow with no back mixing. The dispersion numbers shown here indicate that there is limited back mixing and the reactor is operating very close to an ideal CSTR.<sup>53</sup>

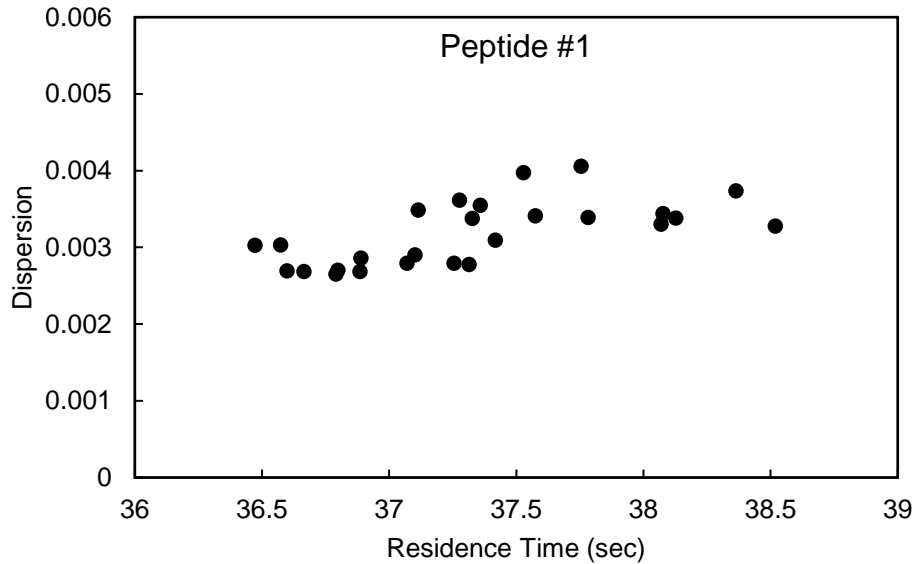


Figure 19. Dispersion Number Versus Residence Time for Four Sample Peptides

## 4.2.2 Residence Time and Dispersion in RTD Experiments

### 4.2.2.1 Effect of Flowrate

First, the effect of flowrate was analyzed as seen in Appendix F.1. It was found that as flow rate increased the residence time decreased. For all flowrates except the minimum (flow A), the residence times ranged from 0.07 to 10 seconds. For the flowrate A the residence times ranged from 6.4 to 31 seconds for resin and glass bead runs, which were significantly higher than the rest of the values. This indicated that this flow was far too slow of a flowrate to be used. Therefore, the minimum value was determined to be an unreasonable flowrate and was excluded from the remaining graphs in this section. This allowed for trends among reasonable flowrates (flows B-E)

to be examined and made it easier to see the trends within the graphs. However, graphs including the minimum flow rate can be seen in Appendix F for reference.

This trend with flowrate is also very clear in the residence time graphs extracted from MATLAB. For example, as seen in Figure 20, as flowrate increased the graph became sharper and the tail shortened. Ideal residence time distributions are sharp curves like that for flow A. This further shows that higher residence times are more favorable for synthesis.

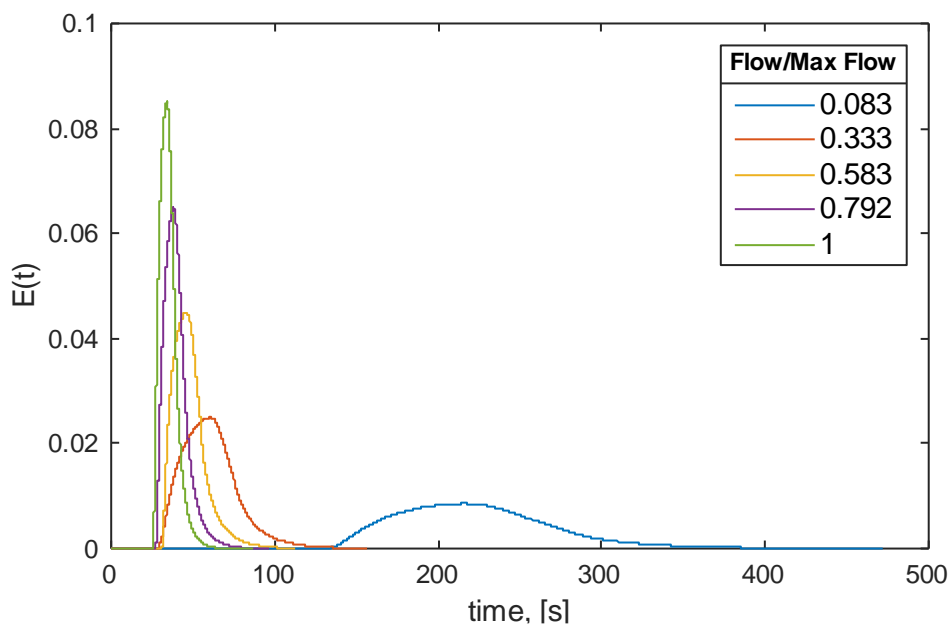


Figure 20. Residence time distributions of the five flowrates used

Furthermore, it can be noted that the runs with resin in the reactor had higher residence times than runs with the glass beads, and the empty reactor had the lowest residence times. This can be seen in Figure 21 as the “X” denotes the average value and the whiskers show distribution of residence times for these experiments. It should be noted that the resin had three outliers between 5 and 9 seconds that aren’t pictured here. Dispersion was also investigated with respect to flowrate. A graph of dispersion versus residence time for resin filled, glass bead filled, and empty reactors can be seen in Appendix F. Unlike residence time there was not a trend for

dispersion versus residence time. However, like the residence times, the dispersion was found to be generally higher for the resin filled reactor and the empty reactor than the glass bead filled reactor.

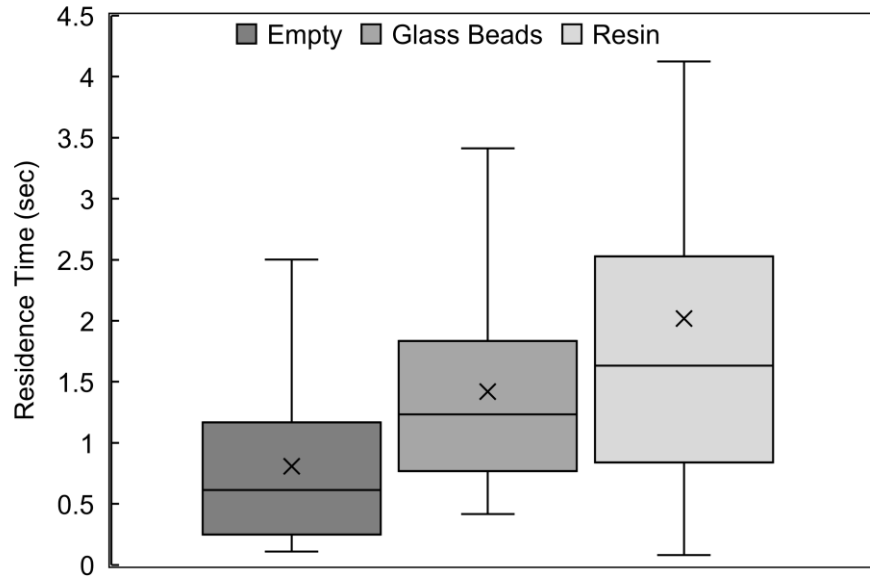


Figure 21. Box and whisker plot showing average residence times and distribution of residence times for empty, glass bead, and resin filled column

#### 4.2.2.2 Effect of Oscillation

Next, the effect of oscillation was investigated. Figure 22 shows the average residence times of the runs with 60 mg of glass beads, 100 mg of glass beads, and full glass beads. A graph containing the residence times at each flowrate for each fill can be seen in Appendix F.2. First, the 60 mg runs with oscillations were found to have the lowest residence times. The 60 mg runs without oscillations also had very low residence times but one outlier at flow B increased the average. As for the 100 mg runs, the average residence time was lower when oscillations were present. On the other hand, the full glass bead runs with oscillations had a higher average residence time. Considering all of this, the 60 mg and 100 mg glass beads with oscillation had the overall lowest residence times and were found to be the ideal cases here.

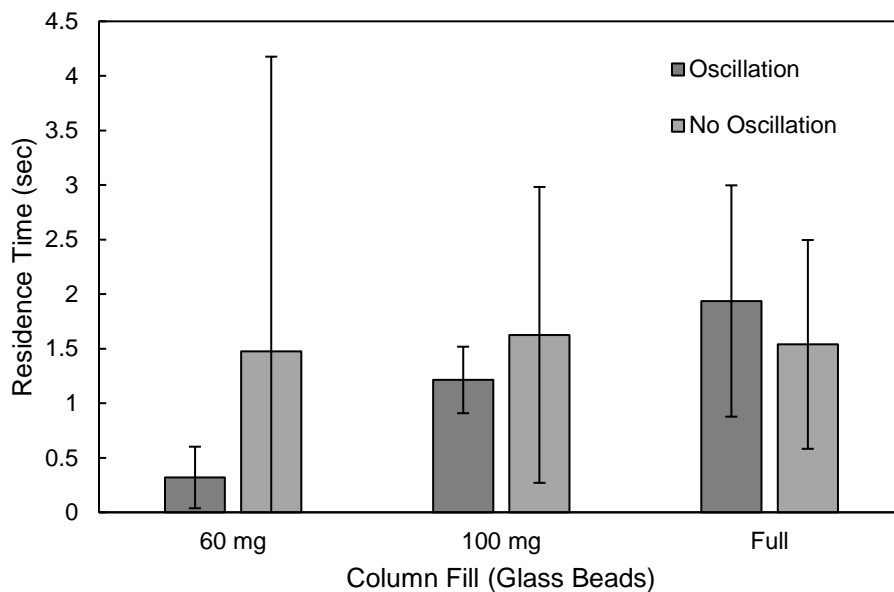


Figure 22. Average residence times for a glass bead filled reactor with and without oscillations

Oscillation was also explored with resin in the reactor. As seen in Appendix F.2, the runs without oscillations had overall higher residence times at each flowrate. To confirm this, the average residence time at each of these four flows was calculated as seen in Figure 23. It was found that the average residence time without oscillations was about double that with oscillations for every flow except the flow C. However, this higher average can be explained by the one outlier seen in the graph in Appendix F.2 at this flowrate. This outlier is also accounted for by the large error bars seen in the bottom graph for this set of data. If this point was excluded this average would be lower and would likely follow the trend better. In general, oscillation was found to be beneficial in helping the amino acid flow through the reactor.

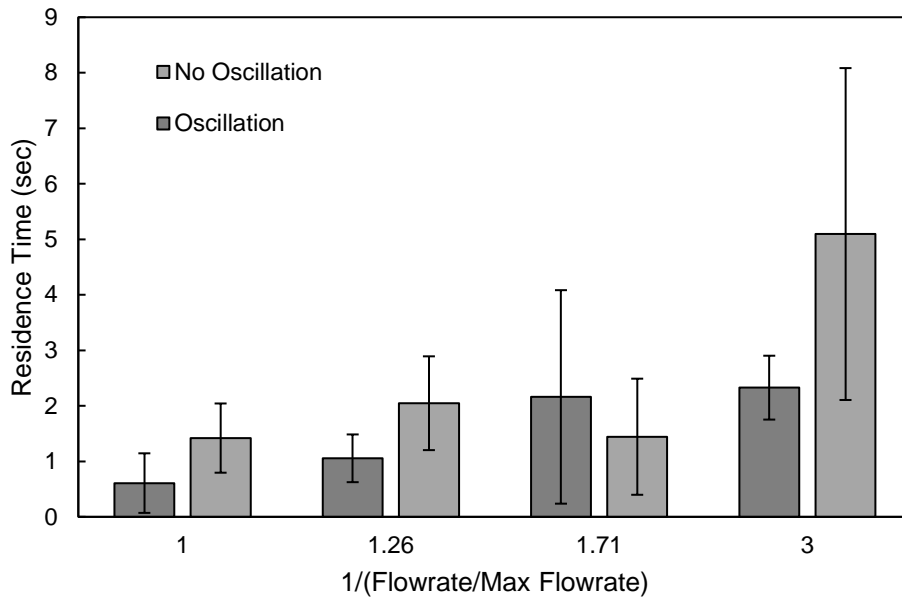


Figure 23. Average residence times for a resin filled reactor with and without oscillations

#### 4.2.2.3 Effect of Headspace

Next, the effect of headspace was examined. The effect on residence time was previously determined in section 4.2.2.2. That is, the 60 mg and 100 mg runs with oscillations were found to be the lowest. Knowing that, this section will focus on the effect that headspace has on dispersion as there was a clear difference. As seen in Figure 24, when there was no headspace, the dispersion was significantly lower than when there was headspace. Also, as the headspace in the reactor increased, this trend stayed true as the 60 mg glass bead runs had significantly higher dispersion than the 100 mg runs. Moreover, of the full glass bead runs, the oscillated runs had lower dispersion than the non-oscillated runs, once again highlighting the benefit of using oscillations. A graph showing the effect of oscillations on dispersion for the glass bead runs can be seen in Appendix F.

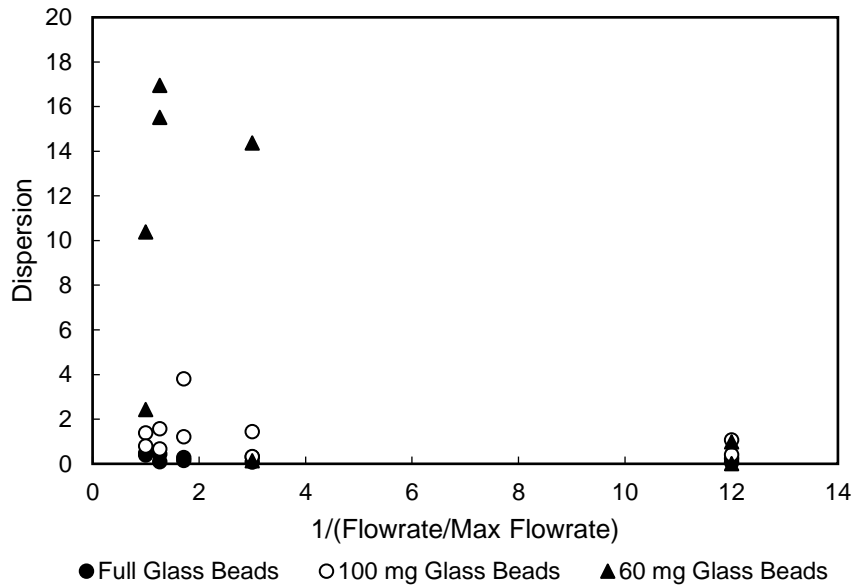


Figure 24. Dimensionless dispersion number with respect to headspace for a glass bead filled reactor

This trend can also be seen in the MATLAB residence time distribution graphs in Figure 25. The residence time distribution curve was calculated by subtracting the bypass from the reactor. Dispersion directly correlates to the shape of the RTD graph. Lower dispersion is represented by a sharper peak. As seen below, the full glass bead run has a nice sharp peak, then the 100 mg glass bead run was a little broader with a longer tail, and the 60 mg glass bead run had the broadest curve and the longest tail.

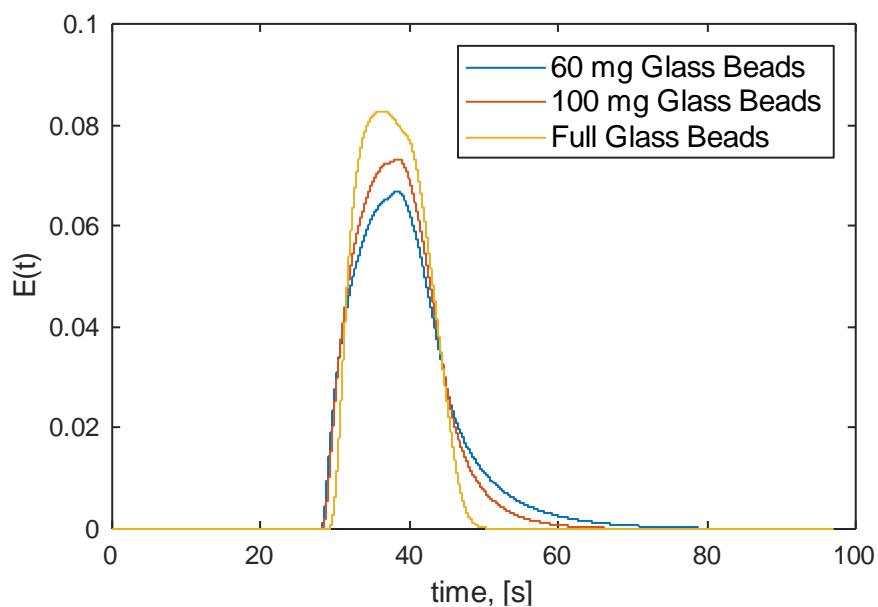


Figure 25. Residence time distributions extracted from MATLAB for a full glass bead reactor, a 100 mg glass bead reactor, and a 60 mg glass bead reactor

#### 4.2.2.4 Effect of a Growing Peptide

Finally, the effect of a growing peptide was investigated. Experiments were run at each flow rate when 0, 5, 10, 15, and 20 amino acids were coupled to the resin, with and without oscillation. First a graph was made for no oscillation, which can be seen in Figure 26. Overall, the residence time was found to be the highest when 15 amino acids were coupled to the resin. When 20 amino acids were coupled there was not a clear trend. For the flowrate A it had the highest residence time, for flowrates B and C it was the third highest, for the flowrate D it was the second highest, and for flowrate E it was the second lowest. The 10 coupled amino acids experiments consistently had the third or second highest residence times. When 5 amino acids were coupled the residence times were always the second lowest except for flowrates A-C and was the lowest for flowrates D and E. Finally, when the resin was fresh with no amino acids, it had the lowest residence times except for flow D when it was the second lowest and at flow E when it was the

second highest. Despite a few outliers, overall, this data followed what was expected. That is, as the peptide grows on the resin, the residence time increases.

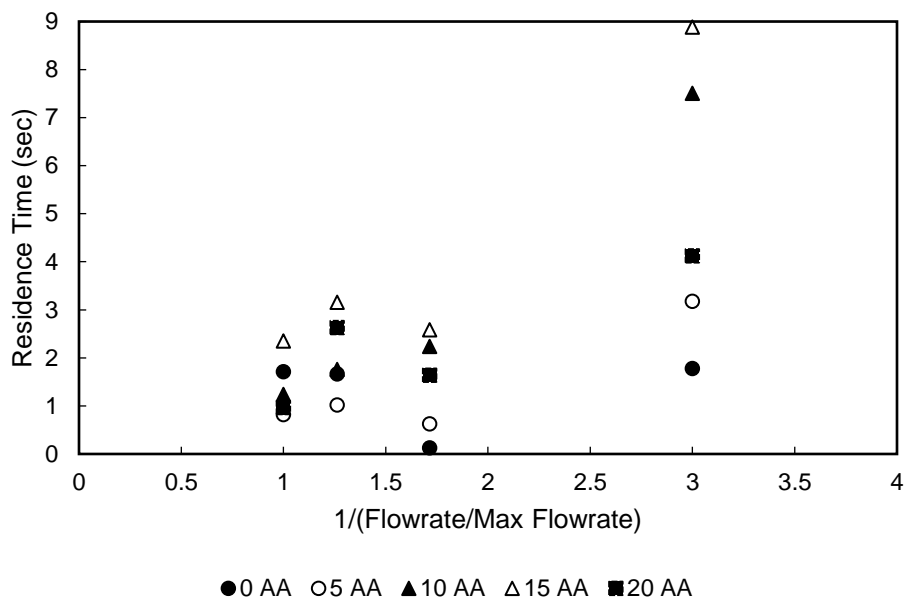


Figure 26. Effect of growing peptide on resin with no oscillation

The same effect was looked at with oscillation. A graph of residence time versus flowrate for the oscillating runs can be seen in Appendix F.4. Looking at this graph, the use of oscillations clearly has an effect on the data as this does not follow the same trends seen above. The 15 and 10 amino acid runs had the lowest residence times, the 5 amino acid runs were consistently in the middle, and the 0 and 20 amino acid runs were the highest.

Continuing with this, the residence times were generally lower with oscillation, despite one outlier (0 AA) at flow C on the oscillations graph. Also, oscillation appears to help lower residence time as the peptide grows on the resin. This comparison can be further proven by looking at the average residence times for peptide growth in Figure 27. Here, it can be seen, that despite the high average for 0 AA with oscillations (due to outlier), the residence times are generally lower than

when there are oscillations. Furthermore, without oscillations the average residence time increased as the peptide grew while with oscillations the residence time decreased.

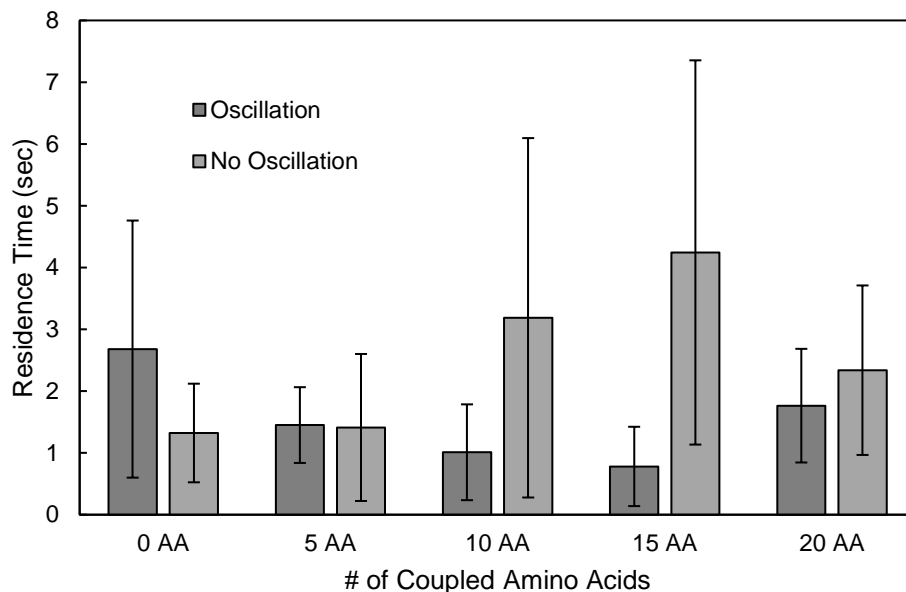


Figure 27. Average residence times when there are 0, 5, 10, 15, and 20 amino acids coupled to the resin with respect to oscillation

Another take away from this data was that the difference between residence times was lower among the number of coupled amino acids when there were oscillations. This means that not only were the residence times lower, but peptide growth didn't have as much of an effect on the residence time when oscillations were present. For example, Figure 28 is a box and whisker plot showing the average residence times and distribution of residence times for a growing peptide at flow D with and without oscillations. On this graph the average value is represented by an "X" and the five stages of peptide growth (0, 5, 10, 15, and 20 amino acids) are represented by the whiskers and the circles. The end of the whiskers are the lowest and highest residence times of the five stages and the three circles within the box are the residence times of the other 3 stages. This graph clearly shows that the distribution among the residence times is significantly smaller when there are oscillations than without. Ultimately this shows that when oscillations are present the

residence time is both lower and is not affected by peptide growth as much as when there aren't oscillations.

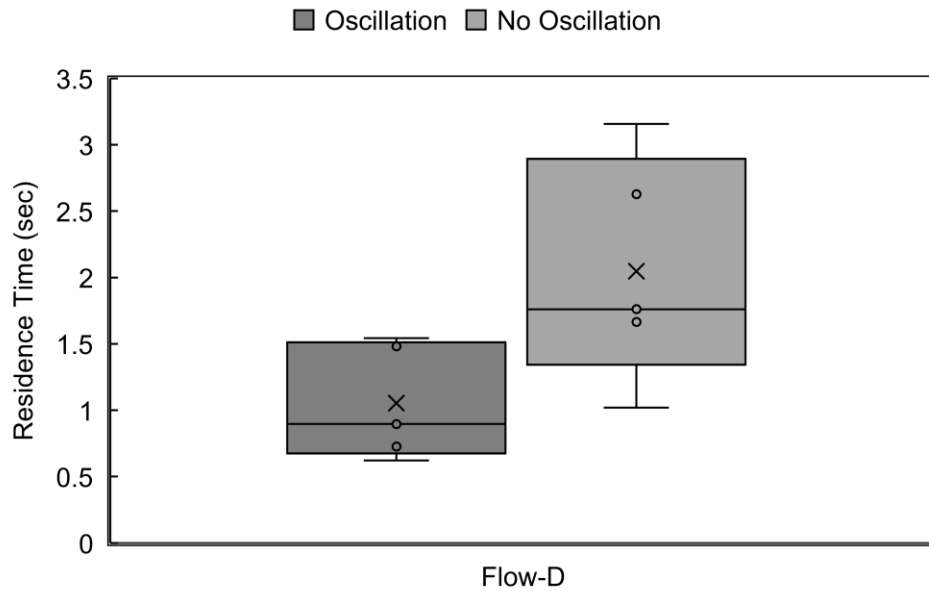


Figure 28. Box and whisker plot showing average residence times and distribution of residence times for a growing peptide at flow  $D$  with respect to oscillation

## Chapter 5 Discussion

### 5.1 ZLC

From the release profiles of amino acid in different column beds under different flowrates, the effect of flowrate and diffusion on the time it takes to wash out all amino acids was observed. First, as shown Figure 15, increasing the flowrate does reduce the time required to release amino acid initially. This phenomenon could be explained by of the volume the resin occupies. For instance, fresh resin occupies more volume than the peptide-bound resin because of its bead size; the peptide bound resin is more compact than the fresh resin. This reduces the time it takes for the solution to travel across the resin in the column. However, this phenomenon observed was not applicable to the glass bead column bed. One potential explanation is that the column bed was filled according to the mass; all the column beds have the same mass before swelling. While the resins were able to swell and occupy volume, the glass beads have fixed volume that may leave cross sections of the column unoccupied, with glass beads moving due to motion. Then, the column bed does not have the same structure throughout the length for the experiment. Additionally, only 1 run under each flowrate were performed for the ZLC experiments ran with glass bead filled column due to time limitations. Having more runs may eliminate potential statistical errors.

Another trend that was observed from the ZLC experiments was how the release profiles were heavily impacted by diffusional limitations approximately 5 minutes after release. As illustrated by Figure 16, the rate of amino acid release after 5 minutes gradually stabilized, with the non-resin columns approaching a rate of zero and the resin columns approaching a similar, steady rate of release. Diffusional limitations were further confirmed by the diffusivity in Table 3. ZLC Diffusivity under different flowrates and column bed schematics where the fresh and peptide bound resins have much smaller diffusivity constants compared to the glass bead column.

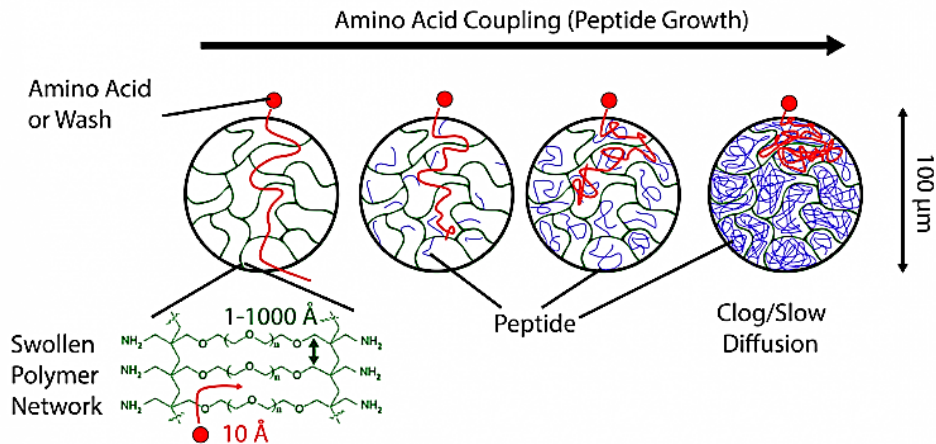


Figure 29. Fresh v. peptide bound resin polymer network

Additionally, the amino acid had higher diffusivity in fresh resin compared to peptide-bound resin. While reducing the volume by using a more compact resin reduces the time necessary for the initial wash out, the structure of the polymer network reduces the diffusivity. As illustrated in Figure 29, amino acids or wash passes through the resin bead more easily if the resin is less clogged; if the resin is peptide bounded, the swollen bead network is more complex, slowing the diffusion within the resin bead.

## 5.2 Residence Time

From the residence time and dispersion, some general trends were observed that improved the system. First, the residence time decreased with increasing flow rate to a certain point. At flow rate A, the residence time was significantly larger than at the other flow rates. As can be seen in Appendix F.1. The four other flow rates only continue to have a slight decrease in residence time with increasing flow rate. This is likely due to the chromatographic effect of the system. Here  $\tau$  or the residence time is equal to  $\tau_{\text{liquid}}$  plus  $\tau_{\text{solid}}$  and  $\tau_{\text{liquid}}$  is equal to volume over flow. Although increasing the flow decreases  $\tau_{\text{liquid}}$ , no matter how much the flow is increased  $\tau$

can't be decreased below  $\tau_{\text{solid}}$ . Due to the diffusional limitations of the amino acid through the resin, even if the flow rate continues to increase the residence time would only decrease an inconsequential amount since it is mainly controlled by the peptide itself after the flow rate is raised to a certain point. Once the flow rate is brought up to that point, running the system at anything above that will not significantly decrease the synthesis time and will rather just lead to more waste due to an increase in the amount of solvent needed. Second, removing headspace caused the RTDs to become sharper and have less of a tail as can be seen in Figure 25. This is due to the decrease in dispersion within the reactor since the reactor has a higher volume of resin within it. Third, the experiment runs with oscillations overall had lower residence time. For the runs with an increasing number of amino acids coupled to the resin, the runs without oscillations had an increase in residence time with an increasing number of amino acids but the runs with oscillations did not. These lower residence times with oscillations are most likely due to this making the system well-mixed and therefore it acts more like a continuous-stirred reactor (CSTR) than how typical SPPS reactors act which is more like a packed-bed reactor (PBR).

## Chapter 6 Conclusions & Recommendations

Through residence time distribution and ZLC column experiments, we made the following key findings. In order to optimize SPPS and reduce the time it takes to release amino acids or wash:

1. Increasing flow rate reduces residence time. But the top three flowrates (C-E) had relatively the same low residence times. To minimize waste, flow C should be used as it will use less solvent while still having low residence times.
2. The headspace within the column should be reduced to decrease dispersion, tailing and holdup in the column.
3. Oscillations reduce residence time by fluidizing the column bed effectively promoting mixing similar to a CSTR.
4. High flow rate is helpful in reducing the initial washout time. However, after the initial washout period, diffusion limitations reduce the impact of flow rate on washout.

To continue the study on diffusional limitations in SPPS, we recommend establishing a COMSOL Multiphysics Model on the SPPS reactor or column. The model can provide simulations and estimate how diffusion limits the washout of amino acids or other solutions, which can be utilized to optimize the SPPS process. Additionally, it's recommended to continue residence time distribution experiments. Specifically, experiments should be run with resin at different headspaces to provide further understanding on how headspace impacts dispersion and flow through the reactor during SPPS. Furthermore, we recommend supplementary experiments with fresh, and peptide-bound resin of the same size. This will provide a more intricate understanding of how flow rate and diffusion impact the release profile of amino acids and other solvents from

the resin. Additionally, having resins of the same size can eliminate the effect of chain length and aggregation on the release profile. Furthermore, experiments can be done with different amino acids protected with Fmoc to explore the effect of size or chemical nature of diffusing species on the release profile.

All of the findings listed above were new analyses provided to Mytide. By applying the findings to their SPPS process, Mytide can reduce the amount of waste generated, thereby reducing the cost of synthesis. Additionally, reducing the waste in production aligns with United Nation's Sustainable Development Goal 12 and Goal 13: Responsible Consumption and Production and Climate Action, respectively.<sup>53</sup> While reducing the waste and cost of SPPS, our findings also supported global sustainable goals and made peptide therapeutics more accessible to the public.

## References

1. AAPPTEC. Peptide Synthesis Resins. *AAPPTEC*.
2. AnaSpec, Inc. *SDS. Fmoc-Gly-OH*; AnaSpec, Inc., 2021.
3. F. G.; Guiochon, G. General HETP Equation for the Study of Mass-Transfer Mechanisms in RPLC <https://pubs.acs.org/doi/pdf/10.1021/ac060203r> (accessed 2022 -04 -18).  
<https://doi.org/10.1021/ac060203r>.
4. Barth, H. Chromatography Fundamentals, Part V: Theoretical Plates: Significance, Properties, and Uses <https://www.chromatographyonline.com/view/chromatography-fundamentals-part-v-theoretical-plates-significance-properties-and-uses> (accessed 2021 -10 -15).
5. Brandani, S.; Mangano, E. The Zero Length Column Technique to Measure Adsorption Equilibrium and Kinetics: Lessons Learnt from 30 Years of Experience. *Adsorption* **2021**, *27* (3), 319–351. <https://doi.org/10.1007/s10450-020-00273-w>.
6. Brandani, S.; Ruthven, D. M. Analysis of ZLC Desorption Curves for Liquid Systems. *Chemical Engineering Science* **1995**, *50* (13), 2055–2059. [https://doi.org/10.1016/0009-2509\(95\)00048-A](https://doi.org/10.1016/0009-2509(95)00048-A).
7. Chemical Book. Fmoc-Glycine Product Description [https://www.chemicalbook.com/ChemicalProductProperty\\_US\\_CB4288480.aspx](https://www.chemicalbook.com/ChemicalProductProperty_US_CB4288480.aspx) (accessed 2021 -11 -04).
8. Coin, I.; Beyermann, M.; Bienert, M. Solid-Phase Peptide Synthesis: From Standard Procedures to the Synthesis of Difficult Sequences. *Nat Protoc* **2007**, *2* (12), 3247–3256. <https://doi.org/10.1038/nprot.2007.454>.
9. COMSOL. Diffusion Coefficient Definition <https://www.comsol.com/multiphysics/diffusion-coefficient#:~:text=A%20typical%20diffusion%20coefficient%20for,%2D9%20m%2F5.> (accessed 2021 -10 -15).
10. Dickson, L. Diffusion [https://chem.libretexts.org/Bookshelves/Physical\\_and\\_Theoretical\\_Chemistry\\_Textbook\\_Maps/Supplemental\\_Modules\\_\(Physical\\_and\\_Theoretical\\_Chemistry\)/Kinetics/09%3A\\_Diffusion](https://chem.libretexts.org/Bookshelves/Physical_and_Theoretical_Chemistry_Textbook_Maps/Supplemental_Modules_(Physical_and_Theoretical_Chemistry)/Kinetics/09%3A_Diffusion) (accessed 2021 -10 -14).
11. Fogler, H. S. *Elements of Chemical Reaction Engineering*, Fifth edition.; Prentice Hall: Boston, 2016.
12. García-Ramos, Y.; Paradís-Bas, M.; Tulla-Puche, J.; Albericio, F. ChemMatrix® for Complex Peptides and Combinatorial Chemistry. *J. Peptide Sci.* **2010**, *16* (12), 675–678. <https://doi.org/10.1002/psc.1282>.
13. Isidro-Llobet, A., Kenworthy, M. N., Mukherjee, S., Kopach, M. E., Wegner, K., Gallou, F., Smith, A. G., & Roschangar, F. (2019). Sustainability Challenges in Peptide Synthesis and Purification: From R&D to Production. *The Journal of Organic Chemistry*, *84*(8), 4615–4628. <https://doi.org/10.1021/acs.joc.8b03001>
14. Kruss Scientific. Diffusion coefficient <https://www.kruss-scientific.com/en-US/know-how/glossary/diffusion-coefficient> (accessed 2021 -10 -14).
15. Marshall Scientific. Agilent 1100 HPLC G1315B DAD Detector | Marshall Scientific <https://www.MarshallScientific.com/product-p/ag-dad.htm> (accessed 2021 -12 -07).
16. Millipore Sigma. Base Resins for Peptide Synthesis. *Millipore Sigma*. n.d.

17. Muttenthaler, M.; King, G. F.; Adams, D. J.; Alewood, P. F. Trends in Peptide Drug Discovery. *Nat Rev Drug Discov* **2021**, *20* (4), 309–325. <https://doi.org/10.1038/s41573-020-00135-8>.
18. Marshall Scientific. HP Agilent 1100 HPLC G1316A Column Compartment | Marshall Scientific <https://www.MarshallScientific.com/product-p/ag-colc.htm> (accessed 2021 -12 -07).
19. Matrix Innovation. ChemMatrix® Resin <https://www.matrix-innovation.com/ChemMatrix®-resin/> (accessed 2021 -10 -14).
20. Merrifield, B. Solid Phase Peptide Synthesis. In *Nobel Lecture*; The Rockefeller University, 1987.
21. Marshall Scientific. Agilent 1100 HPLC G1379A Degasser | Marshall Scientific <https://www.MarshallScientific.com/product-p/ag-mdg.htm> (accessed 2021 -12 -07).
22. Marshall Scientific. Agilent 1100 HPLC G1312A Binary Pump | Marshall Scientific <https://www.MarshallScientific.com/product-p/ag-bp.htm> (accessed 2021 -12 -07).
23. Itoh, K.; Yamada, A. Personalized Peptide Vaccines: A New Therapeutic Modality for Cancer. *Cancer Science* **2006**, *97* (10), 970–976. <https://doi.org/10.1111/j.1349-7006.2006.00272.x>.
24. Jaradat, D. M. M. Thirteen Decades of Peptide Synthesis: Key Developments in Solid Phase Peptide Synthesis and Amide Bond Formation Utilized in Peptide Ligation. *Amino Acids* **2018**, *50* (1), 39–68. <https://doi.org/10.1007/s00726-017-2516-0>.
25. Gao, Y.; Muzzio, F. J.; Ierapetritou, M. G. A Review of the Residence Time Distribution (RTD) Applications in Solid Unit Operations. *Powder Technology* **2012**, *228*, 416–423. <https://doi.org/10.1016/j.powtec.2012.05.060>.
26. Fields, G. B. Introduction to Peptide Synthesis. *Current Protocols in Protein Science* **2001**, *26* (1). <https://doi.org/10.1002/0471140864.ps1801s26>.
27. Eloul, S.; Kätelhön, E.; Compton, R. G. When Does Near-Wall Hindered Diffusion Influence Mass Transport towards Targets? *Phys. Chem. Chem. Phys.* **2016**, *18* (38), 26539–26549. <https://doi.org/10.1039/C6CP05716K>.
28. Creative Proteomics. Main High-Performance Liquid Chromatography (HPLC) Components - Creative Proteomics <https://www.creative-proteomics.com/pronalyse/main-hplc-components.html> (accessed 2021 -10 -14).
29. MIT. Diffusivity <https://abaqus-docs.mit.edu/2017/English/SIMACAEMATRefMap/simamat-c-diffusivity.htm> (accessed 2021 -10 -14).
30. Moss, J. A. Guide for Resin and Linker Selection in Solid-Phase Peptide Synthesis. *Current Protocols in Protein Science* **2005**, *40* (1), 18.7.1-18.7.19. <https://doi.org/10.1002/0471140864.ps1807s40>.
31. Nature Education. Essentials of Cell Biology <https://www.nature.com/scitable/ebooks/essentials-of-cell-biology-14749010/how-do-cells-decode-genetic-information-into-14751777/> (accessed 2022 -01 -30).
32. Nemeč, D.; Levec, J. Flow through Packed Bed Reactors: 1. Single-Phase Flow. *Chemical Engineering Science* **2005**, *60* (24), 6947–6957. <https://doi.org/10.1016/j.ces.2005.05.068>.
33. Netrabukkana, R.; Lourvanji, K.; Rorrer, G. Diffusion of Glucose and Glucitol in Microporous and Mesoporous Silicate/Aluminosilicate Catalysts. *Industrial & Engineering Chemistry Research* **1996**, *35* (2), 458–464.

34. Pavličič, A.; Ceglar, R.; Pohar, A.; Likozar, B. Comparison of Computational Fluid Dynamics (CFD) and Pressure Drop Correlations in Laminar Flow Regime for Packed Bed Reactors and Columns. *Powder Technology* **2018**, *328*, 130–139. <https://doi.org/10.1016/j.powtec.2018.01.029>.
35. Pearson, E. R. Personalized Medicine in Diabetes: The Role of ‘Omics’ and Biomarkers. *Diabetic Medicine* **2016**, *33* (6), 712–717. <https://doi.org/10.1111>.
36. Pietsch, S.; Schönherr, M.; Kleine Jäger, F.; Heinrich, S. Measurement of Residence Time Distributions in a Continuously Operated Spouted Bed. *Chemical Engineering & Technology* **2020**, *43* (5), 804–812. <https://doi.org/10.1002/ceat.201900453>.
37. Petrou, C.; Sarigiannis, Y. Peptide Synthesis: Methods, Trends, and Challenges. In *Peptide Applications in Biomedicine, Biotechnology and Bioengineering*; Koutsopoulos, S., Ed.; Woodhead Publishing, 2018; pp 1–21. <https://doi.org/10.1016/B978-0-08-100736-5.00001-6>.
38. Place, 877-9-Consci 877-926-6724 619-690-7300 12778 Brookprinter; Poway; Ca 92064. Agilent 1100 Series G1315B DAD <https://conquerscientific.com/cq-product/agilent-1100-series-g1315b-dad/> (accessed 2021 -12 -07).
39. Place, 877-9-Consci 877-926-6724 619-690-7300 12778 Brookprinter; Poway; Ca 92064. Agilent 1100 Series G1379A Micro Vacuum Degasser <https://conquerscientific.com/cq-product/agilent-1100-series-g1379a-micro-vacuum-degasser/> (accessed 2021 -12 -07).
40. Raja, P.; Barron, A. High Performance Liquid chromatography [https://chem.libretexts.org/Bookshelves/Analytical\\_Chemistry/Physical\\_Methods\\_in\\_Chemistry\\_and\\_Nano\\_Science\\_\(Barron\)/03%3A\\_Principles\\_of\\_Gas\\_Chromatography/3.02%3A\\_High\\_Performance\\_Liquid\\_chromatography](https://chem.libretexts.org/Bookshelves/Analytical_Chemistry/Physical_Methods_in_Chemistry_and_Nano_Science_(Barron)/03%3A_Principles_of_Gas_Chromatography/3.02%3A_High_Performance_Liquid_chromatography) (accessed 2021 -10 -14).
41. Russell, J. *IGenetics*, 3rd ed.; 2010.
42. Simon, M. D.; Heider, P. L.; Adamo, A.; Vinogradov, A. A.; Mong, S. K.; Li, X.; Berger, T.; Policarpo, R. L.; Zhang, C.; Zou, Y.; Liao, X.; Spokoyny, A. M.; Jensen, K. F.; Pentelute, B. L. Rapid Flow-Based Peptide Synthesis. *Chembiochem* **2014**, *15* (5), 713–720. <https://doi.org/10.1002/cbic.201300796>.
43. Stawikowski, M.; Fields, G. B. Introduction to Peptide Synthesis. *Curr Protoc Protein Sci* **2002**, *CHAPTER*, Unit-18.1. <https://doi.org/10.1002/0471140864.ps1801s26>.
44. Place, 877-9-Consci 877-926-6724 619-690-7300 12778 Brookprinter; Poway; Ca 92064. Agilent/HP 1100 Series G1313A ALS Autosampler <https://conquerscientific.com/cq-product/agilenthp-1100-series-g1313a-als-autosampler/> (accessed 2021 -12 -07).
45. PubChem. N,N-Dimethylformamide <https://pubchem.ncbi.nlm.nih.gov/compound/6228> (accessed 2021 -11 -04).
46. Regulatory Affairs. *SDS N, N-Dimethylformamide-D7*; Thermo Fisher Scientific, 2018.
47. Sheffield Hallam University. Chromatography - Introductory theory <https://teaching.shu.ac.uk/hwb/chemistry/tutorials/chrom/chrom1.htm> (accessed 2021 -10 -15).
48. Silva, JoséA. C.; Rodrigues, A. E. Analysis of ZLC Technique for Diffusivity Measurements in Bidisperse Porous Adsorbent Pellets. *Gas Separation & Purification* **1996**, *10* (4), 207–224. [https://doi.org/10.1016/S0950-4214\(96\)00021-7](https://doi.org/10.1016/S0950-4214(96)00021-7).
49. Slominsky, P. A.; Shadrina, M. I. Peptide Pharmaceuticals: Opportunities, Prospects, and Limitations. *Mol. Genet. Microbiol. Virol.* **2018**, *33* (1), 8–14. <https://doi.org/10.3103/S0891416818010123>.
50. Sorolla, A.; Wang, E.; Golden, E.; Duffy, C.; Henriques, S. T.; Redfern, A. D.; Blancafort, P. Precision Medicine by Designer Interference Peptides: Applications in Oncology and

- Molecular Therapeutics. *Oncogene* **2020**, 39 (6), 1167–1184. <https://doi.org/10.1038/s41388-019-1056-3>.
51. Thermo Fisher Scientific. Overview of Crosslinking and Protein Modification - US [www.thermofisher.com/us/en/home/life-science/protein-biology/protein-biology-learning-center/protein-biology-resource-library/pierce-protein-methods/overview-crosslinking-protein-modification.html](http://www.thermofisher.com/us/en/home/life-science/protein-biology/protein-biology-learning-center/protein-biology-resource-library/pierce-protein-methods/overview-crosslinking-protein-modification.html) (accessed 2022 -04 -18).
  52. Thornhill, D. Packed Beds [http://faculty.washington.edu/finlayso/Fluidized\\_Bed/FBR\\_Fluid\\_Mech/packed\\_beds\\_fbr.htm](http://faculty.washington.edu/finlayso/Fluidized_Bed/FBR_Fluid_Mech/packed_beds_fbr.htm) (accessed 2021 -10 -15).
  53. Turton, R.; *Analysis, Synthesis, and Design of Chemical Processes*, 5th edition.; Ed.; Prentice Hall international series in the physical and chemical engineering sciences; Prentice Hall: Boston, 2018.
  54. United Nations (UN). Take Action for the Sustainable Development Goals. *United Nations Sustainable Development*.
  55. Žuvela, P.; Skoczylas, M.; Jay Liu, J.; Bączek, T.; Kaliszan, R.; Wong, M. W.; Buszewski, B. Column Characterization and Selection Systems in Reversed-Phase High-Performance Liquid Chromatography. *Chem. Rev.* **2019**, 119 (6), 3674–3729. <https://doi.org/10.1021/acs.chemrev.8b00246>.

# Appendices

## Appendix A: Codes

### Appendix A.1: MATLAB Code for ZLC analysis

```
1 %% ZLC Analysis
2 - close all
3 - clear
4 - clc
5
6 %% Procedure:
7 % 1) Run raw_plots_rawdata.m to make sure your data looks good. Also,
8 % extrat t0min (when valve switched to desorb mode) if you don't know it
9 % 2) use the same code to determine your bounds where your data is linear
10 % (e.g. 2-10 minutes, 30-60 minutes, etc.). This value is highly dependent
11 % 3) use the same code to find Imin (the asmpotic limit on I vs t)
12 % on the loading and sensitivity of the detector
13 % 4) run this code with the proper inputs gathered from 1-2 above
14
15 %% Inputs
16 - File = 'wang-2-290-2.csv';
17 - t0min = 40; % Just before drop
18 - tbounds = [5 7]; % min Linear region
19 - Imin = -33;
20 - Model = 1; % 1 = sphere LT
21
22 % File = 'nitrilechemmatrix-21-290.csv';
23
24 %% Guesses
25 - DR2 = 1e-1; % D/R^2 [=] sec^-1
26 - L0 = 10; % dimesnionless, 1 - 1000 (bigger = better)
27
28
29 %% Parse Input Data
30 - x0 = [L0 log10(DR2)];
31
32 %% Fit ZLC
33 - X=ZLC(tbounds,x0,t0min,File,Model,Imin);
```

## Appendix A.2. Python Code for data extraction

```
1 import csv
2 import os
3 import pandas as pd
4 from data_handling_edited import collect_ids, load_peptide_metadata, load_synth_data, load_lcms_data
5 from parse_synth_2 import parse_synth_data
6 import requests
7
8 uuids = collect_ids('uuid1.csv')
9
10 print(uuids)
11 type(uuids)
12
13 # Generate result using pandas
14 list = ["uv275", "uv280", "uv290", "uv300", "uv310",
15        "uv330", "uv340", "uv350", "uv455"]
16 a=0
17
18 for idx, uuid in enumerate(uuids):
19
20     # load data from the database
21     peptide_meta = load_peptide_metadata(uuid)
22     all_synth_data = load_synth_data(uuid)
23
24     # uv
25     synth_name = all_synth_data[0]['synth meta']['expt_name']
26     uv = all_synth_data[0]['synth data']['data']['uv']
27     time = all_synth_data[0]['synth data']['data']['time']
28
29     # parse synthesis data
30     parsed_synth_data = parse_synth_data(uuid, all_synth_data)
31
32     x = 1
33
34     # export to csv file
35
36     # create folder
37     a+=1
38     newpath = 'uuid'+str(a)
39     if not os.path.exists(newpath):
40         os.mkdir(newpath)
41
42     initial_data = {}
43
44     for i in range(9):
45         df = pd.DataFrame(initial_data, columns = ['time',str(list[i])])
46         df['time'] = time
47         result = uv.get(list[i])
48         df[list[i]]= result
49         df.to_csv( newpath+'/'+newpath+'-'+str(list[i])+'.csv', index=False,encoding='utf-8')
50         for j in range(len(all_synth_data[0]['synth data']['peaks'])):
51             if result:
52                 df = pd.DataFrame(initial_data, columns = ['time',str(list[i])+'-'+str(j)])
53                 left = all_synth_data[0]['synth data']['peaks'][j]['couples' or 'deprotects'][0]['t_left']
54                 right = all_synth_data[0]['synth data']['peaks'][j]['couples' or 'deprotects'][0]['t_right']
55                 leftindex = time.index(left)
56                 rightindex = time.index(right)
57                 partofTime = time[leftindex:rightindex+1]
58                 df['time'] = [round(x-leftindex,3) for x in partofTime ]
59                 df[str(list[i])+'-'+str(j)]= result[leftindex:rightindex+1]
60                 path1 = newpath+'/'+newpath+'-'+str(list[i])+'/'
61                 if not os.path.exists(path1):
62                     os.mkdir(path1)
63                 df.to_csv( newpath+'/'+newpath+'-'+str(list[i])+'-'+str(j)+'.csv', index=False,encoding='utf-8')
64
65 print(uv)
```

## Appendix A.3. MATLAB Code for RTD analysis

```
%% Solve RTD for each File

% Reactor
data = readtable(fn_reactor);
data=table2array(data);
    t_reactor = data(:,1)-data(1,1); % [s]
    c_reactor = data(:,2); % [arb]

% Bypass
data = readtable(fn_bypass);
data=table2array(data);
    t_bypass = data(:,1)-data(1,1); % [s]
    c_bypass = data(:,2); % [arb]

% Deconvolution and Dispersion Model Fit
[t,Ein,Eout,E_reactor,E_convolved,x] = RTD_deconv(t_bypass,c_bypass,...
    t_reactor,c_reactor,[npoints, tau_guess, DuL_guess]);

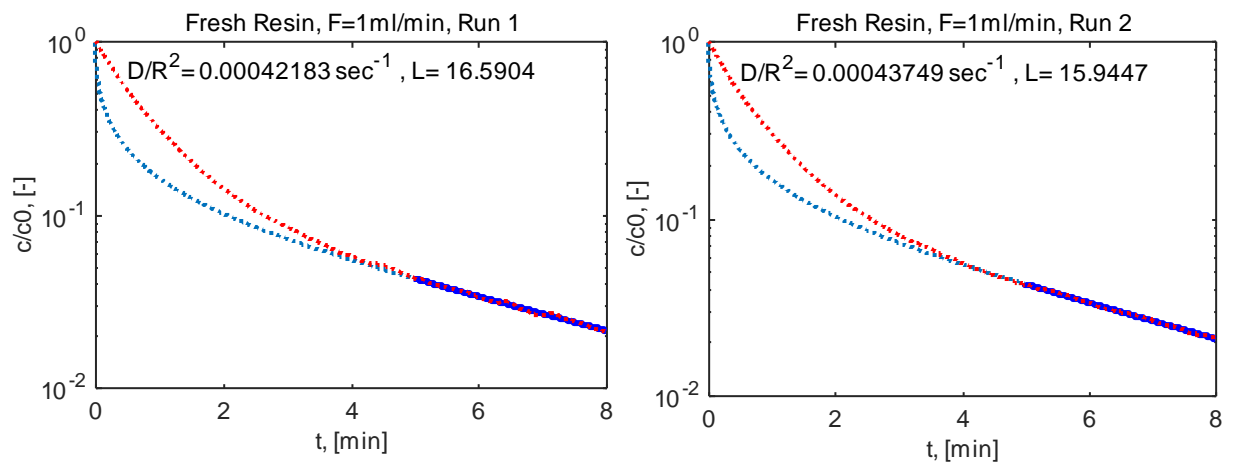
% Model Outputs
tau = x(1);
DuL = x(2);

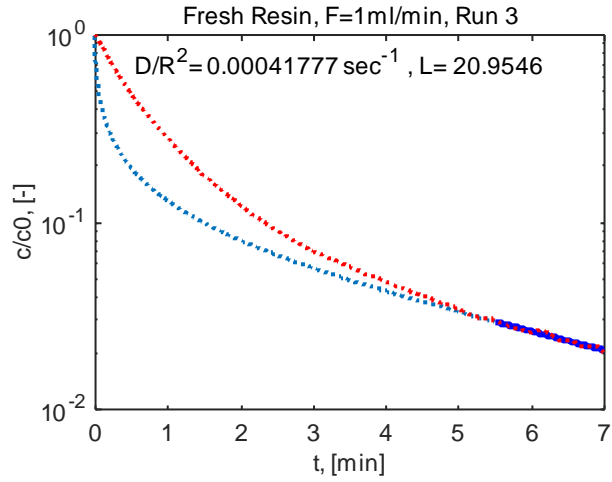
plot(t,Ein,t,Eout,t,E_reactor,t,E_convolved)
xlabel('time, [s]')
ylabel('E(t)')
legend('Bypass','Bypass + Reactor','Reactor','Reactor-Convolved')

%% Outputs
disp(['tau = ', num2str(tau), ' s'])
disp(['D/uL = ', num2str(DuL)])
```

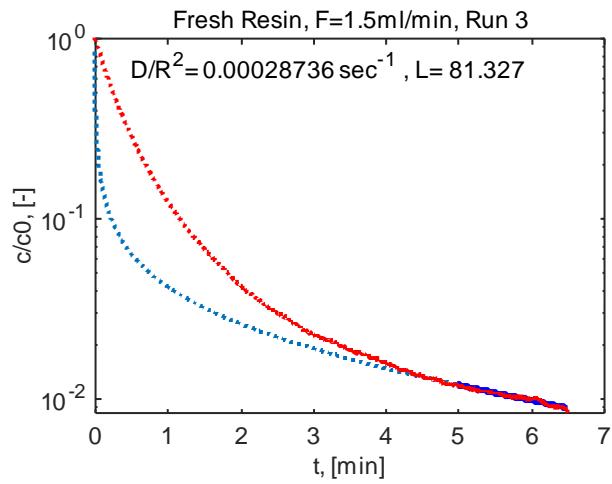
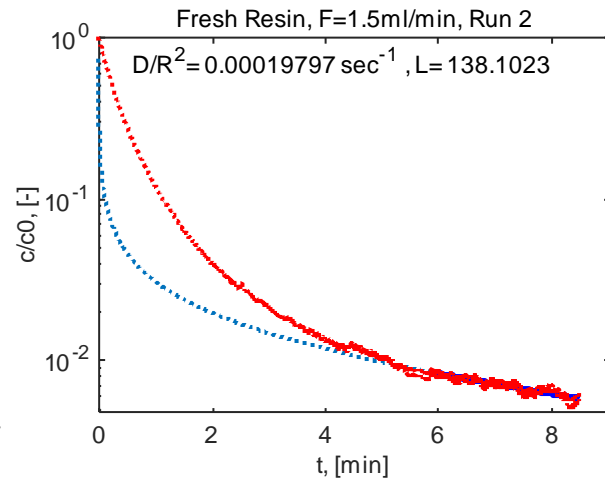
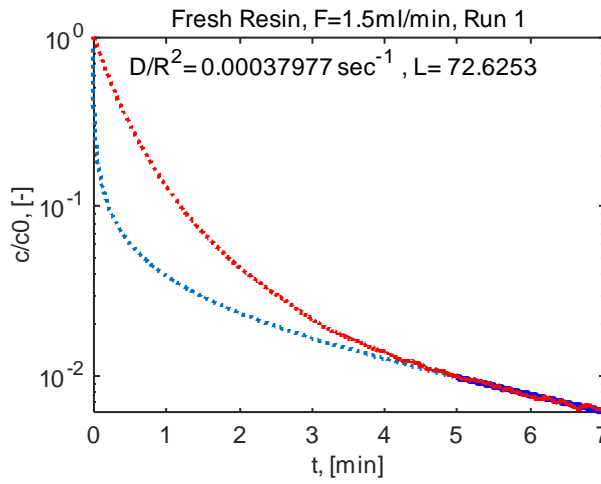
## Appendix B: ZLC Diffusion Fits

*Fresh Resin, 1 ml/min*

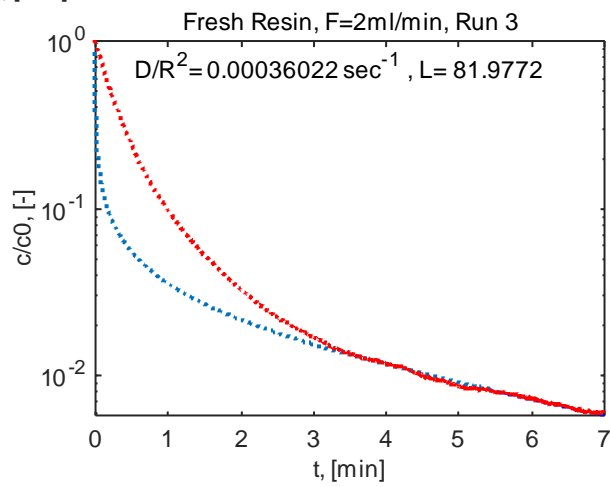
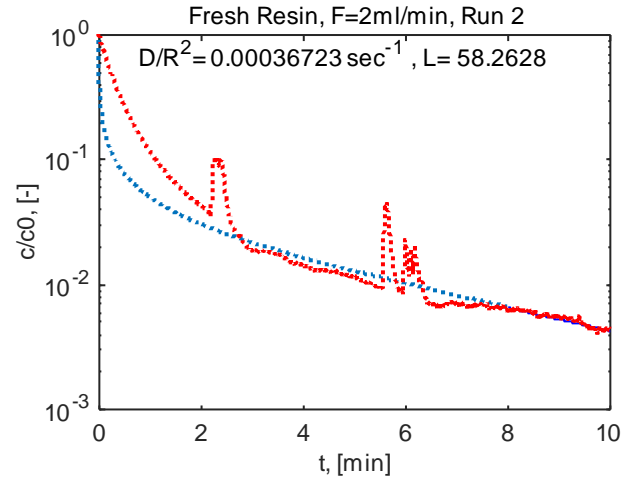
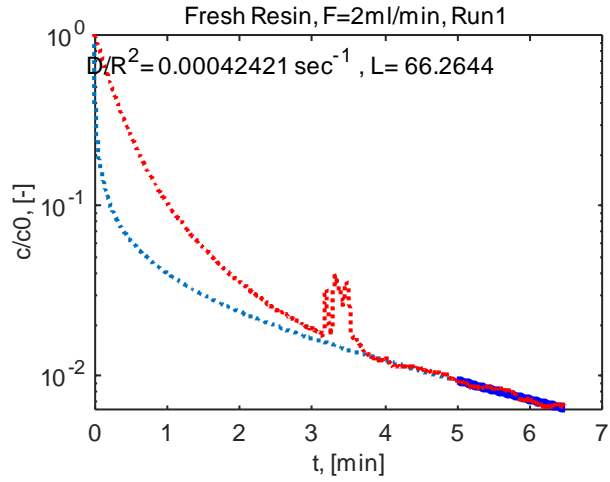




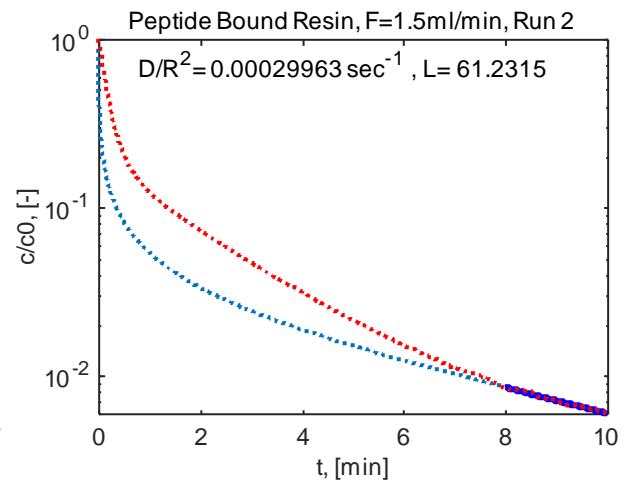
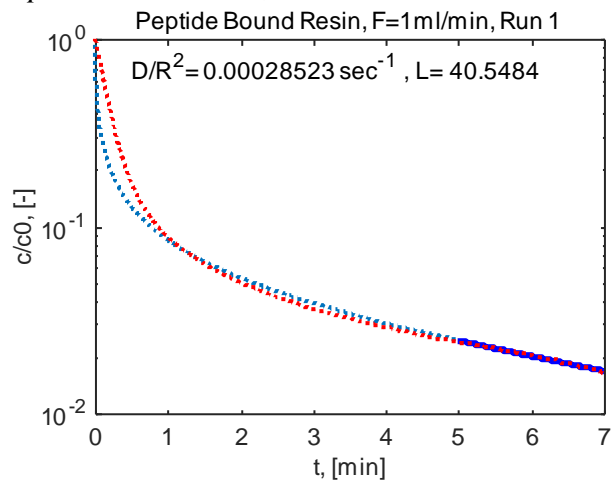
*Fresh Resin, 1.5 ml/min*

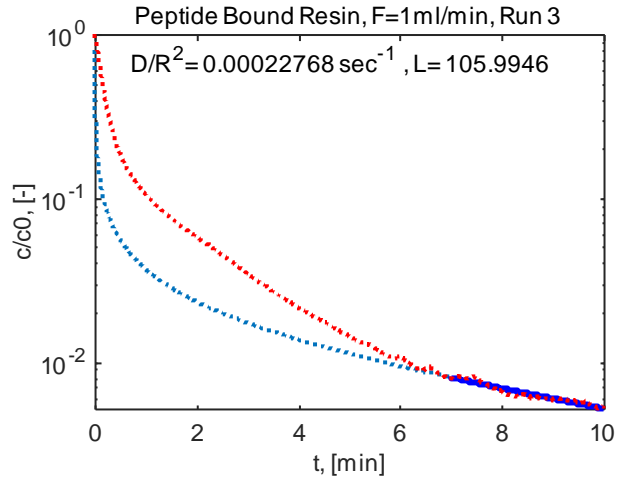


*Fresh Resin, 2 ml/min*

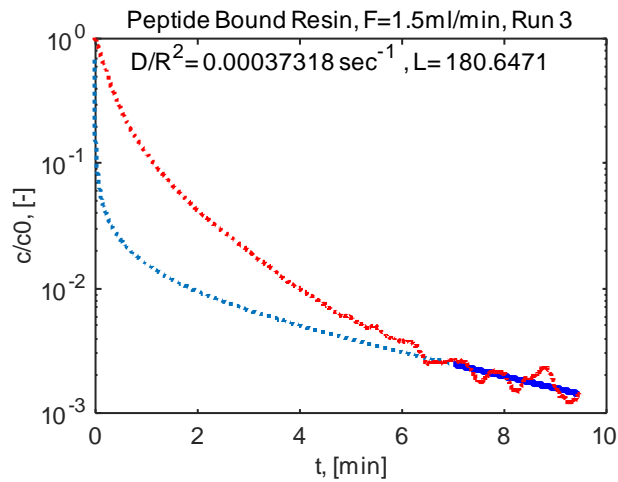
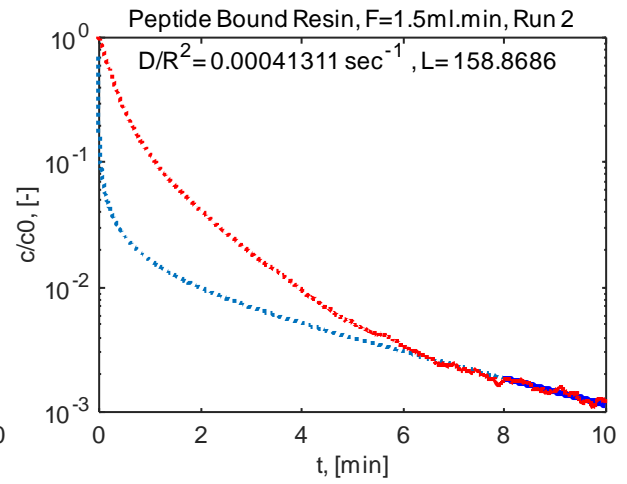
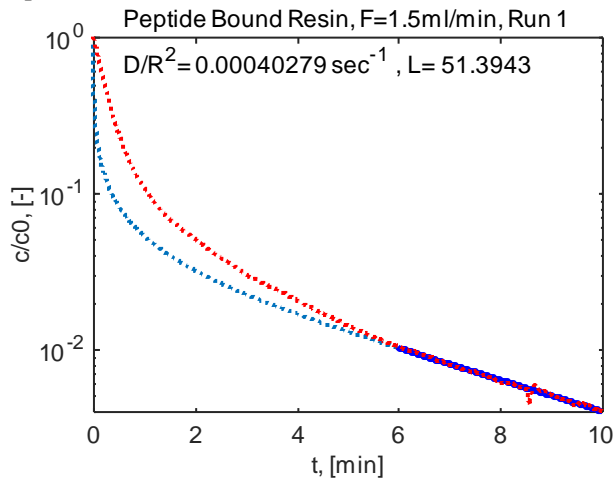


*Peptide Bound Resin, 1 ml/min*

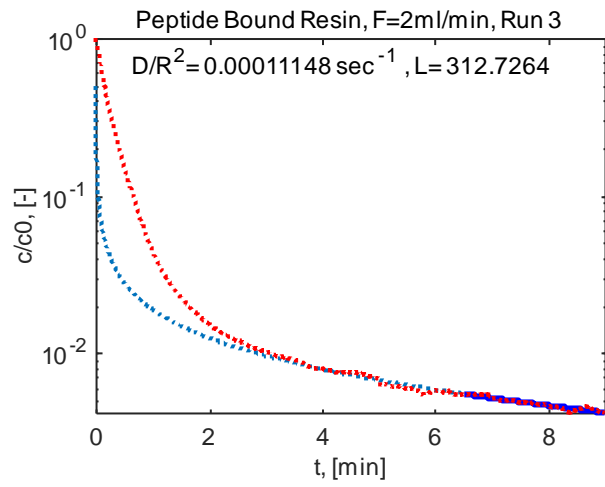
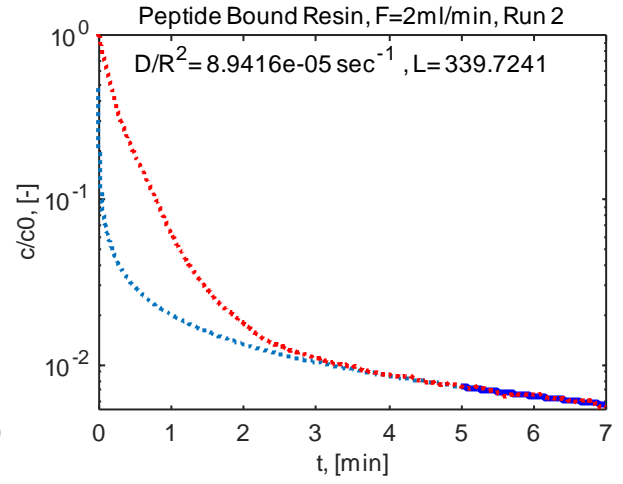
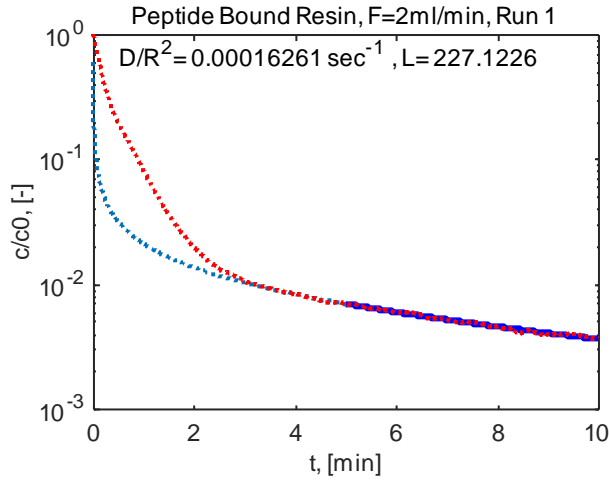




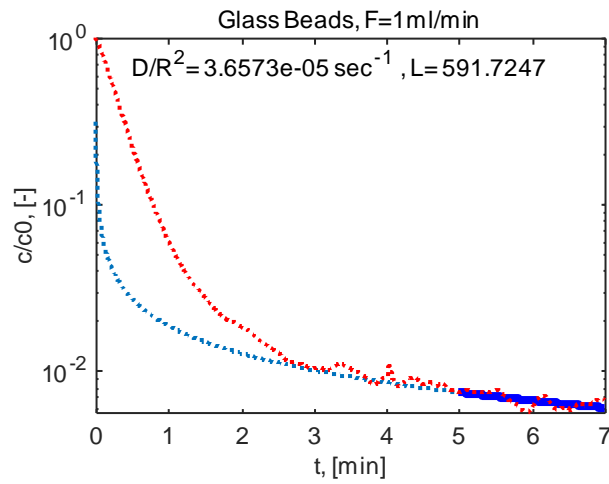
*Peptide Bound Resin, 1.5 ml/min*



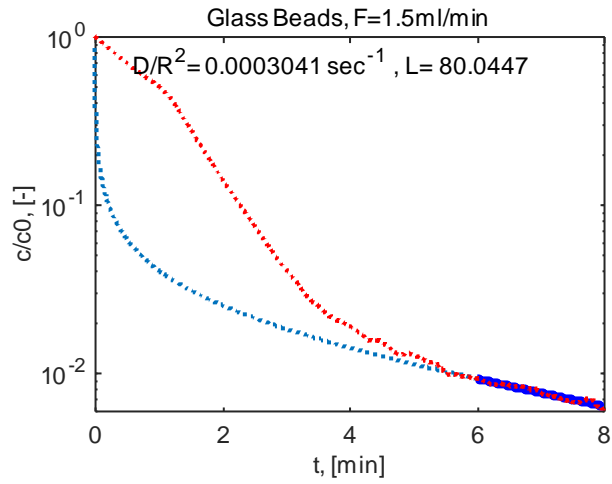
*Peptide Bound Resin, 2 ml/min*



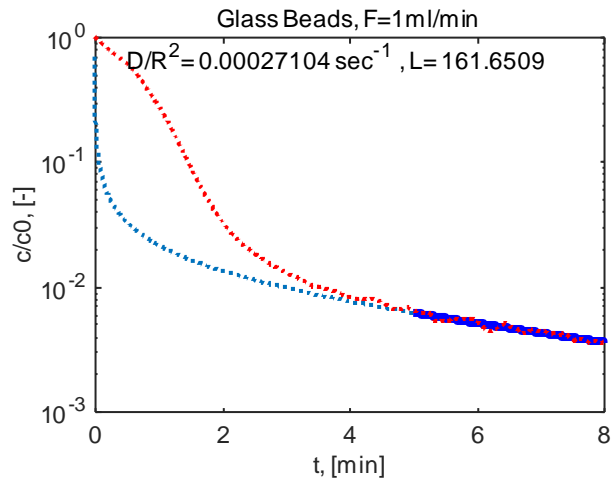
*Glass Beads, 1 ml/min*



*Glass Beads, 1.5 ml/min*



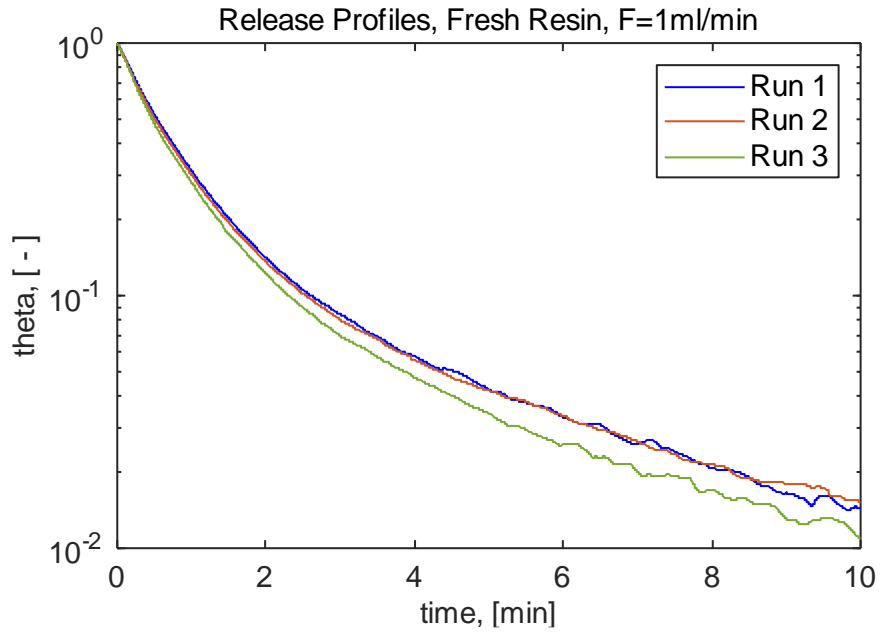
*Glass Bead,s 2 ml/min*



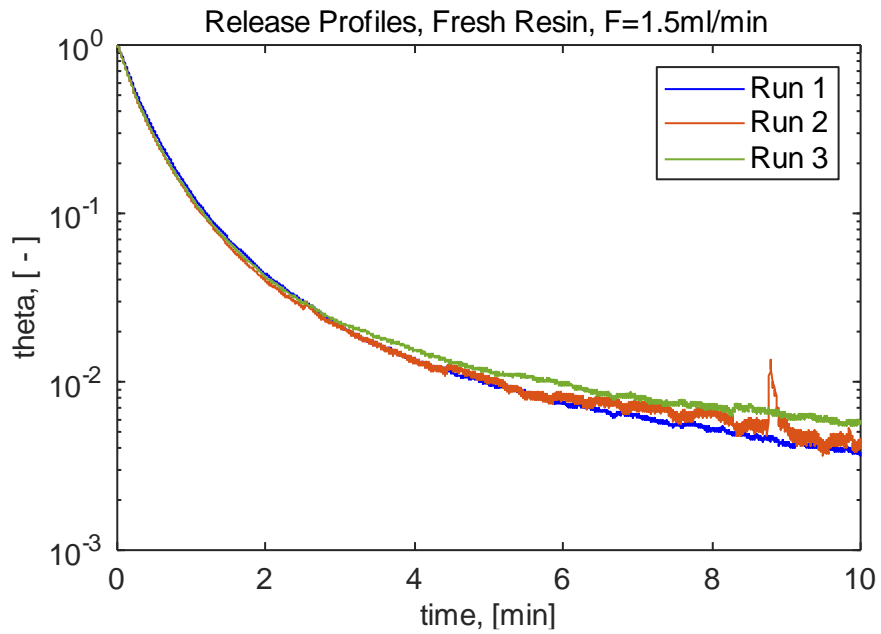
## Appendix C: ZLC Release Profiles

### Fresh Resin:

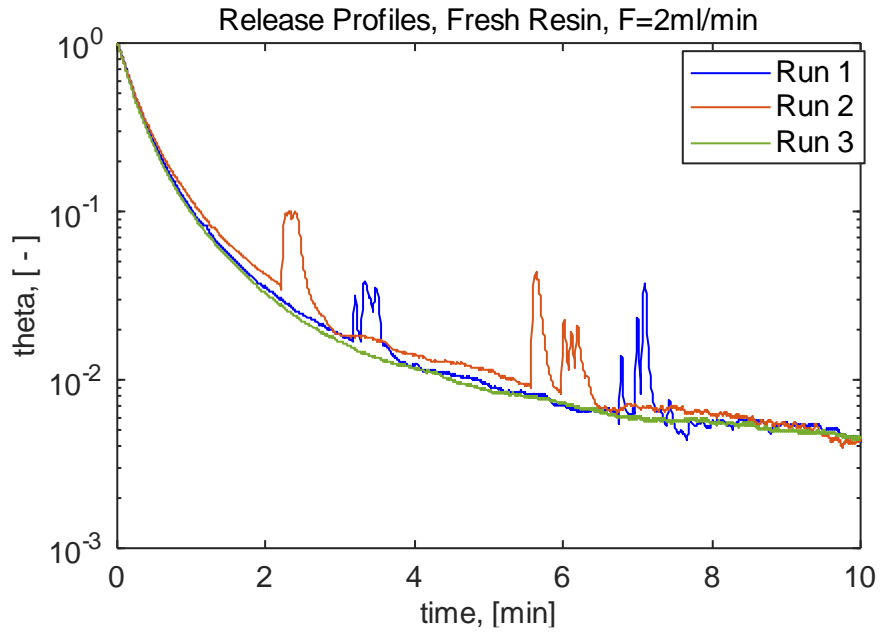
*Fresh Resin, 1 ml/min*



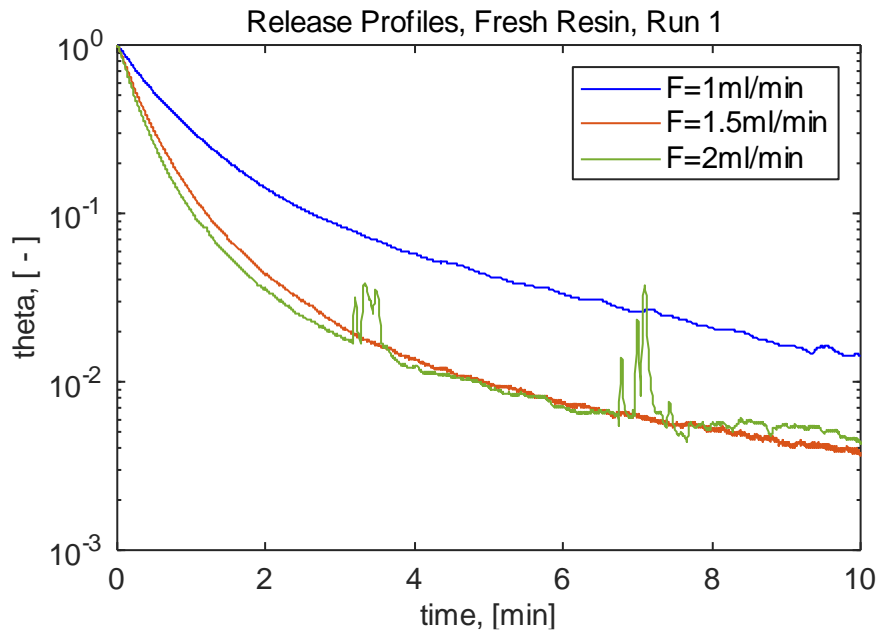
*Fresh Resin, 1.5 ml/min*



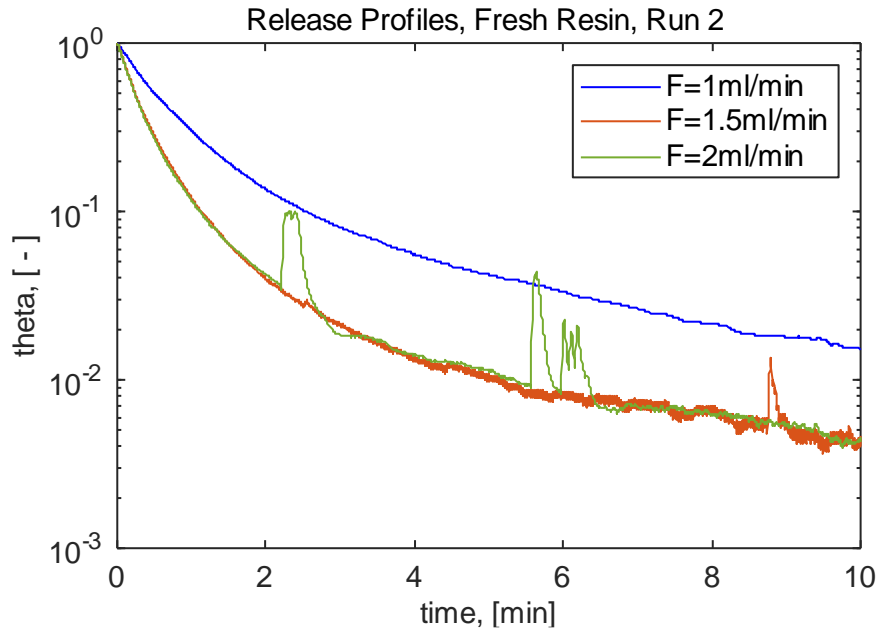
*Fresh Resin, 2 ml/min*



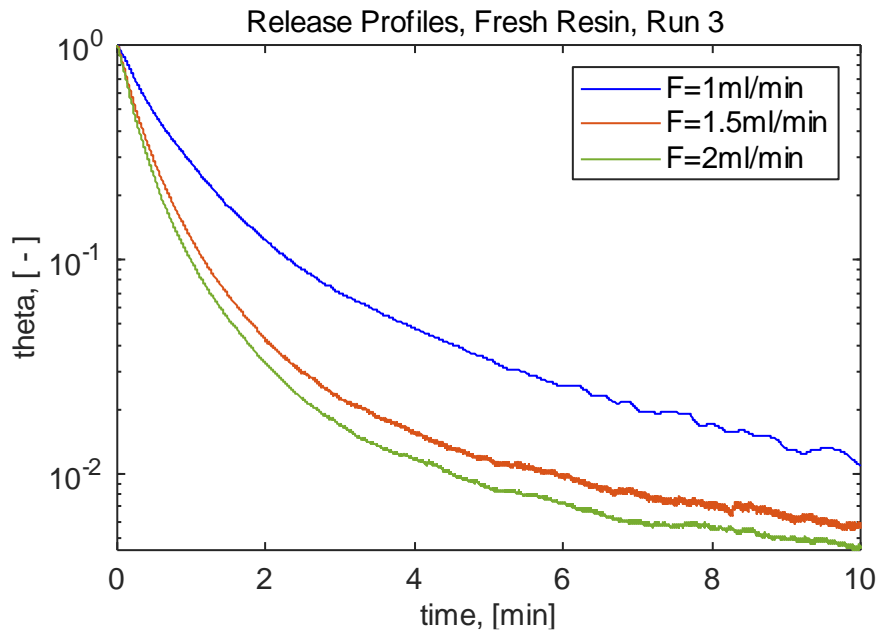
*Fresh Resin, All Flowrates, Run 1*



*Fresh Resin, All Flowrates, Run 2*

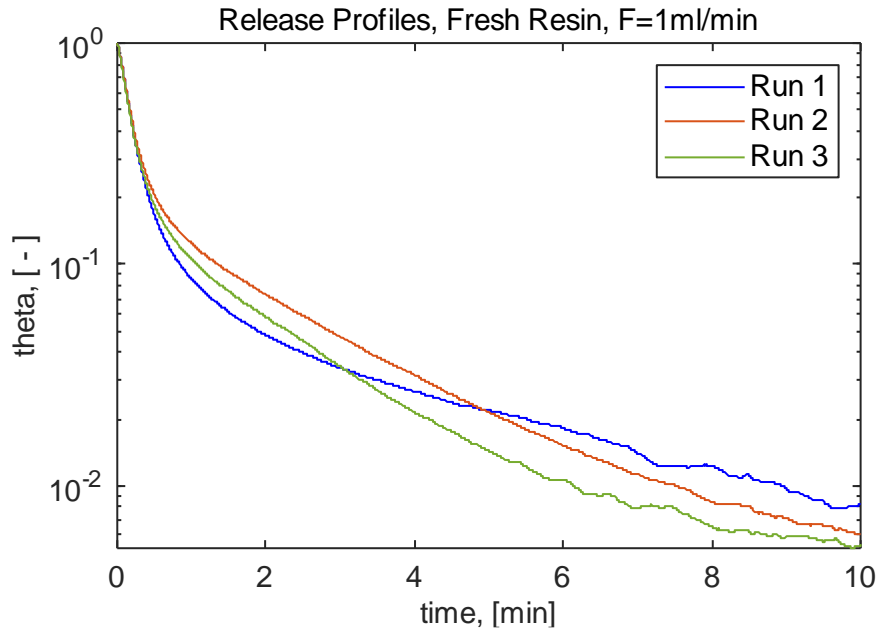


*Fresh Resin, All Flowrates, Run 3*

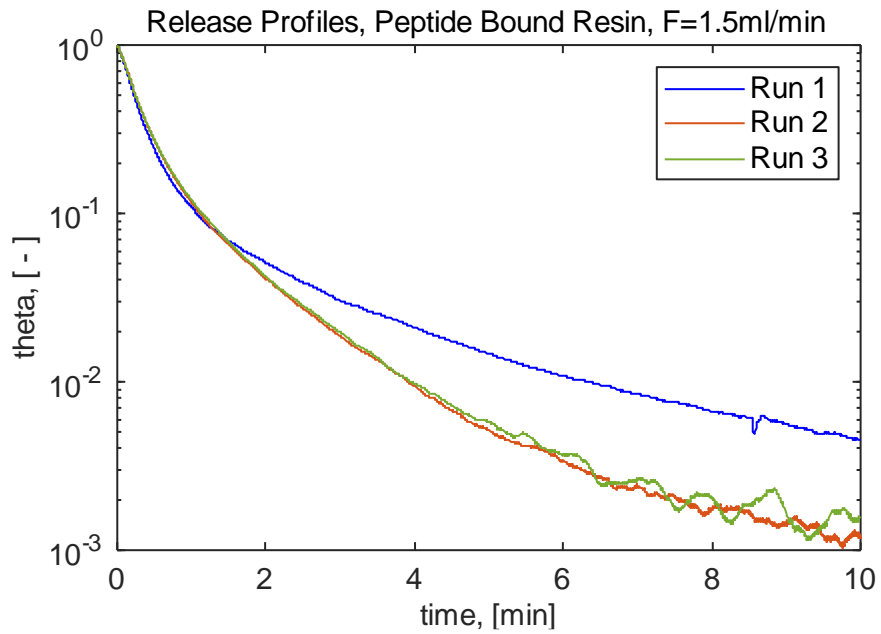


**Peptide Bound Resin:**

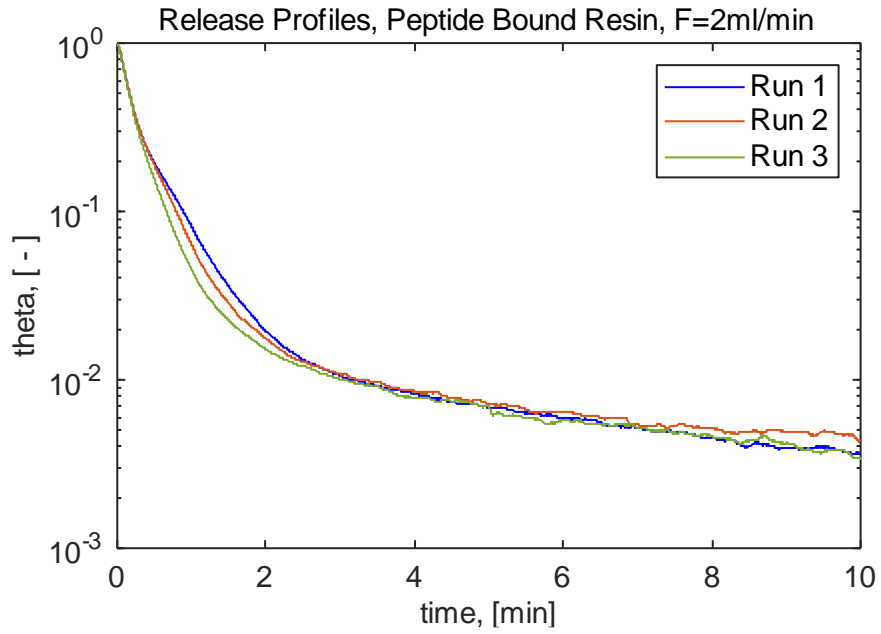
*Peptide Bound Resin, 1 ml/min*



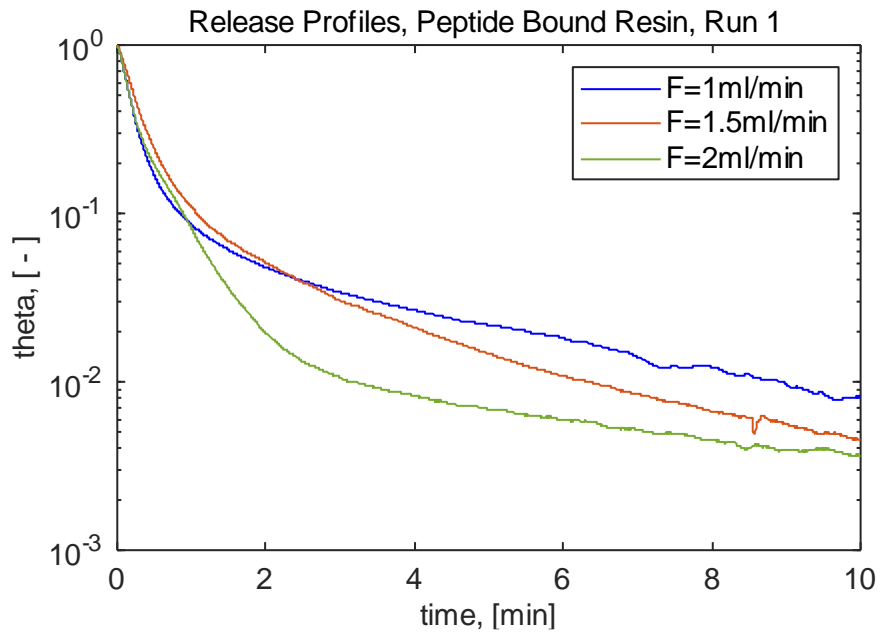
*Peptide Bound Resin, 1.5 ml/min*



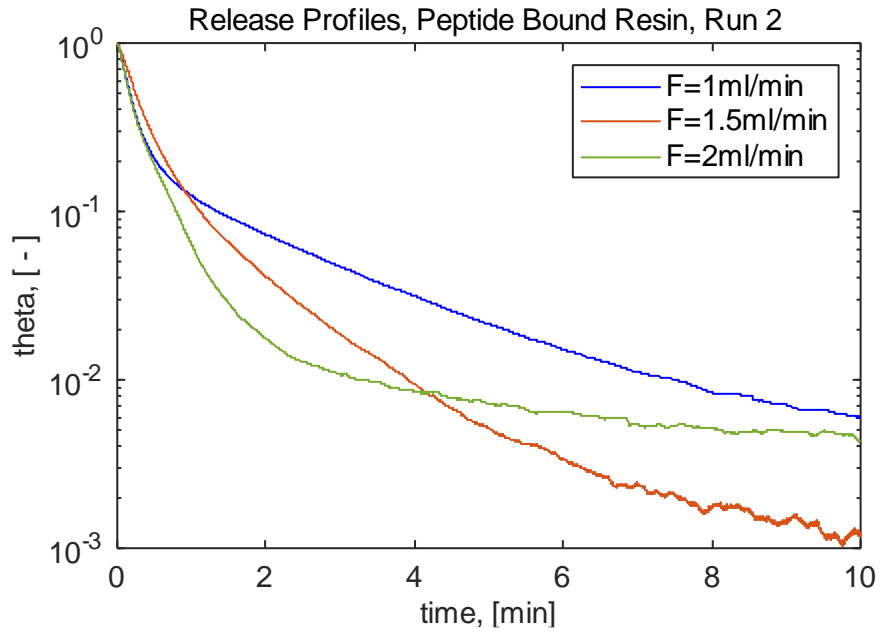
*Peptide Bound Resin, 1.5 ml/min*



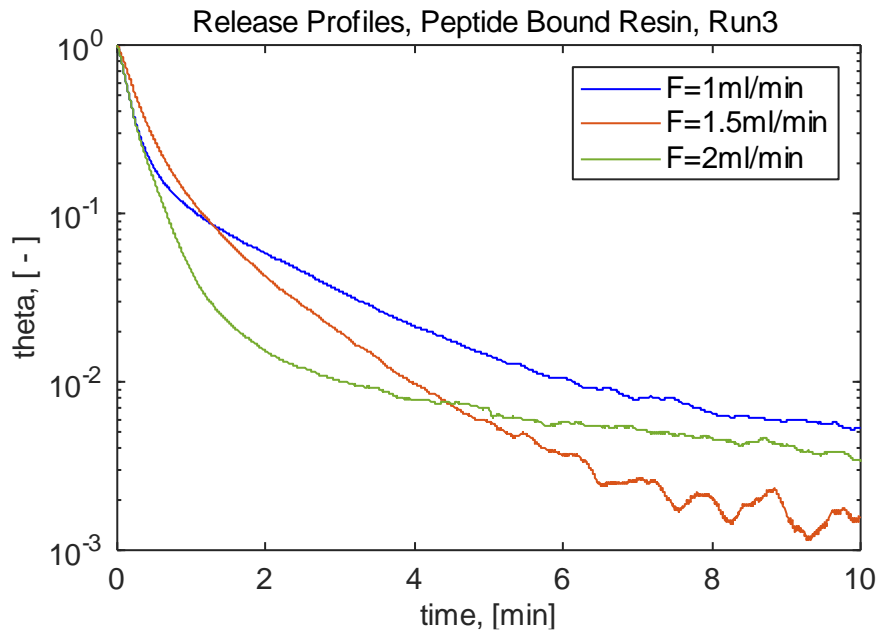
*Peptide Bound Resin, All Flowrates, Run 1*



*Peptide Bound Resin, All Flowrates, Run 2*

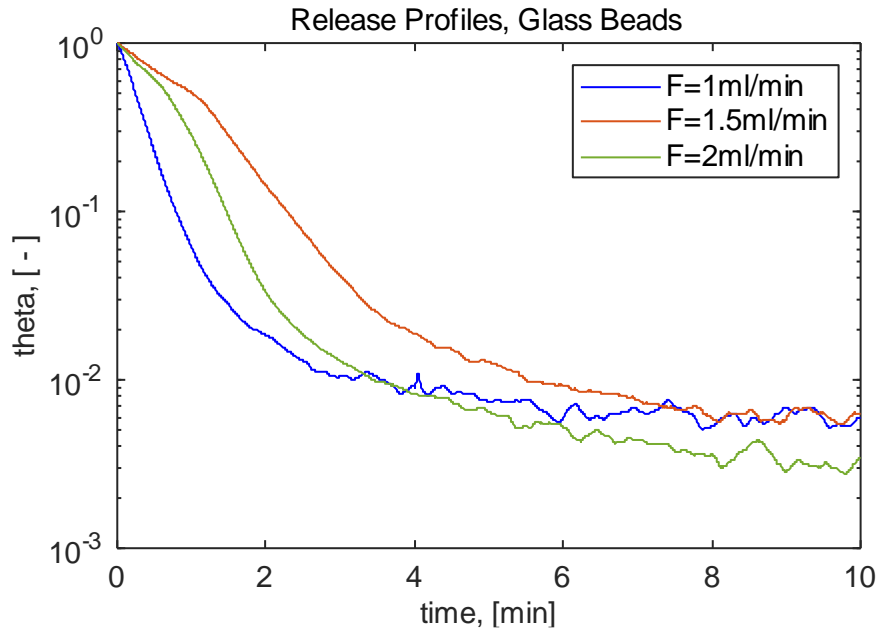


Peptide Bound Resin, All Flowrates, Run 3



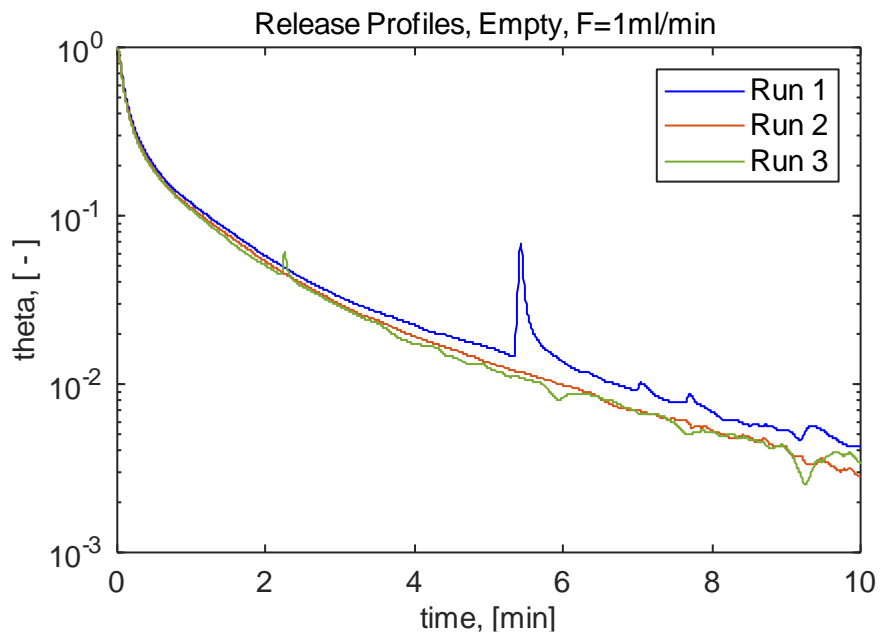
**Glass Beads:**

Glass Beads, All Flowrates

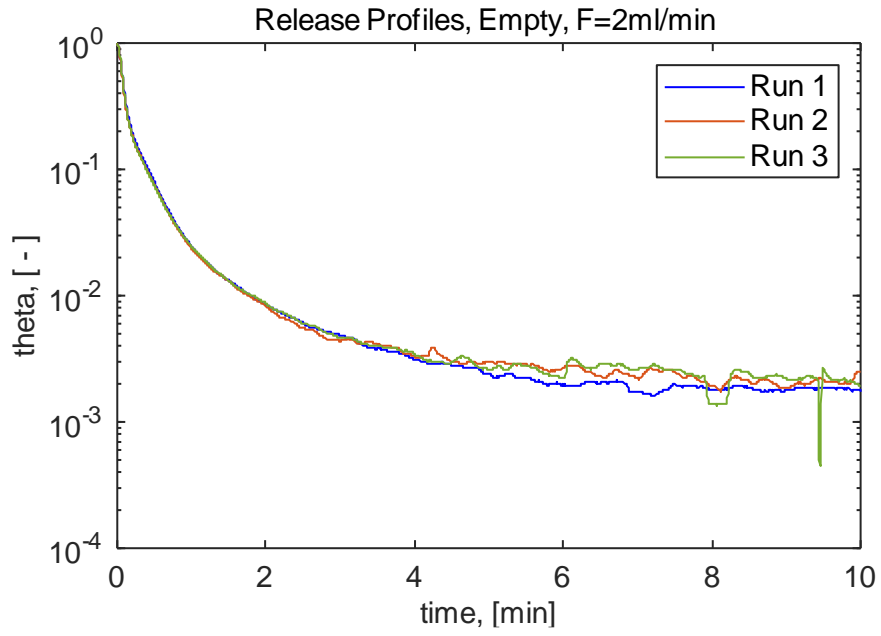


**Empty:**

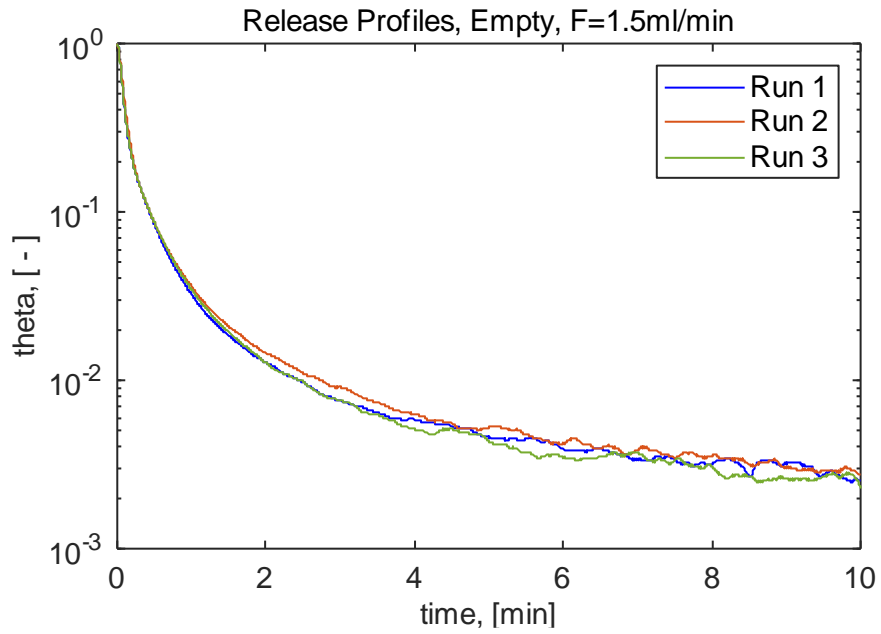
*Empty, 1 ml/min*



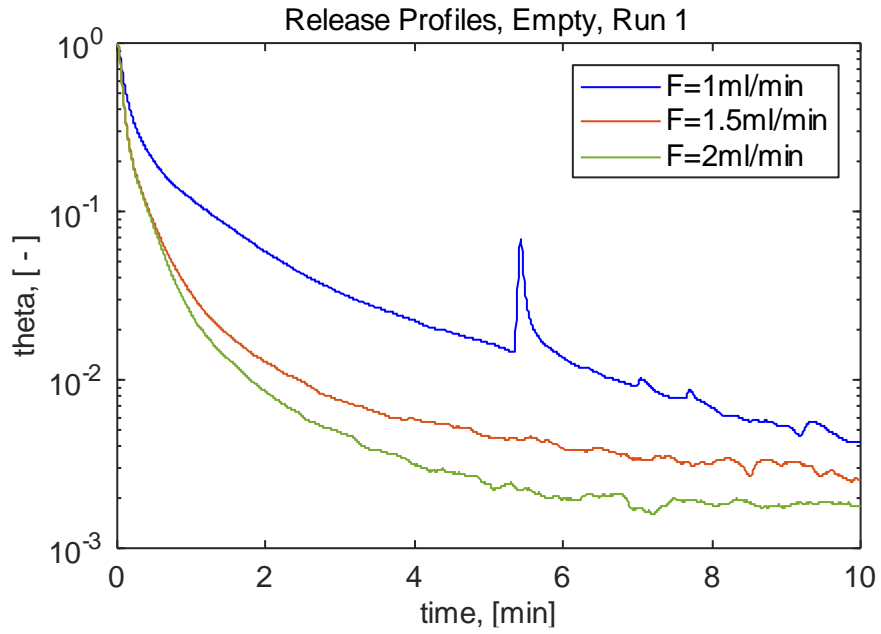
*Empty, 1.5 ml/min*



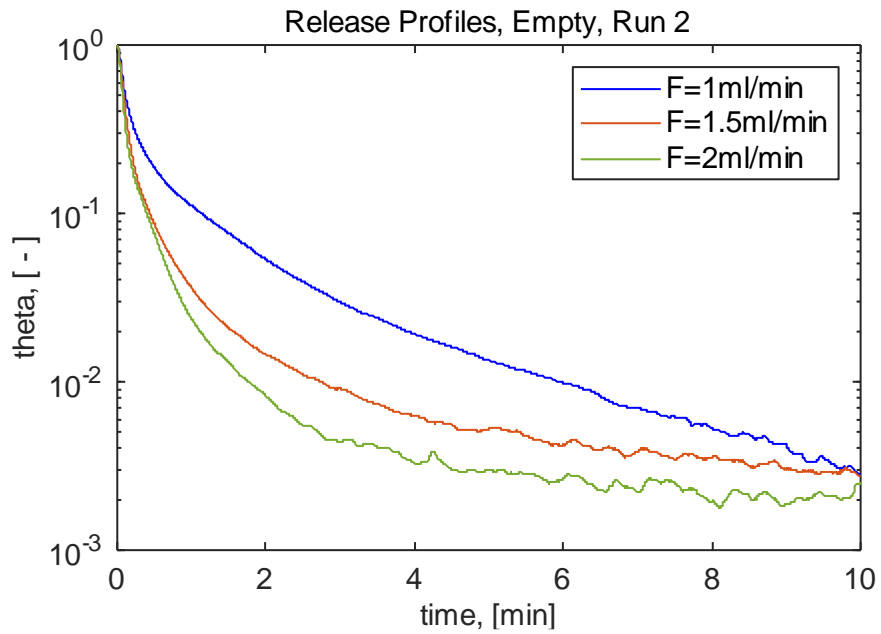
*Empty, 2 ml/min*



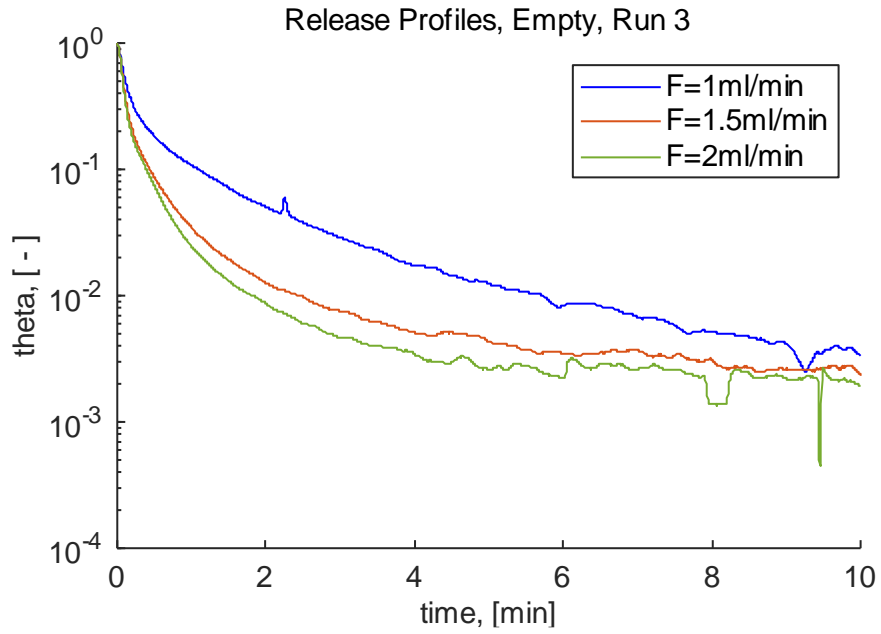
*Empty, All Flowrates, Run 1*



*Empty, All Flowrates, Run 2*

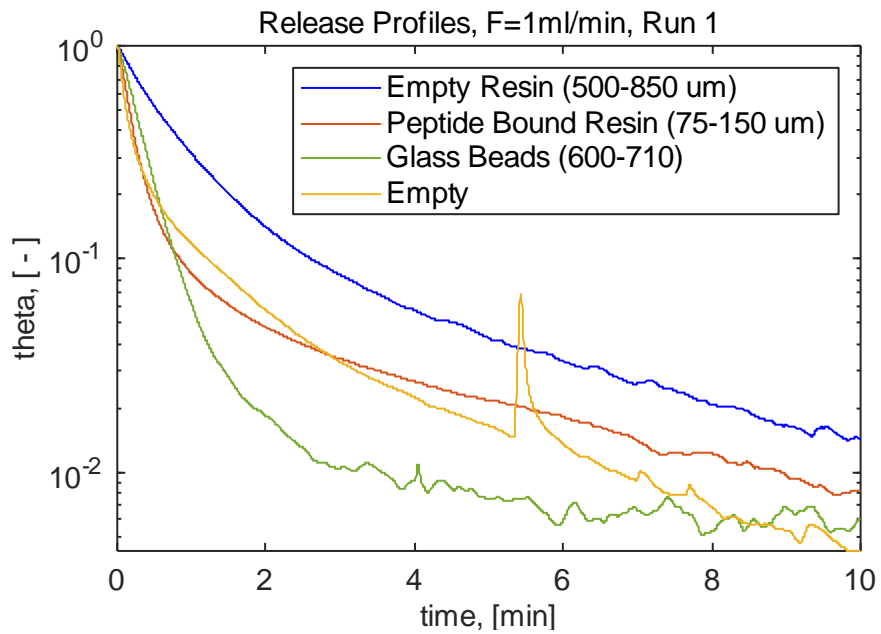


*Empty, All Flowrates, Run 3*

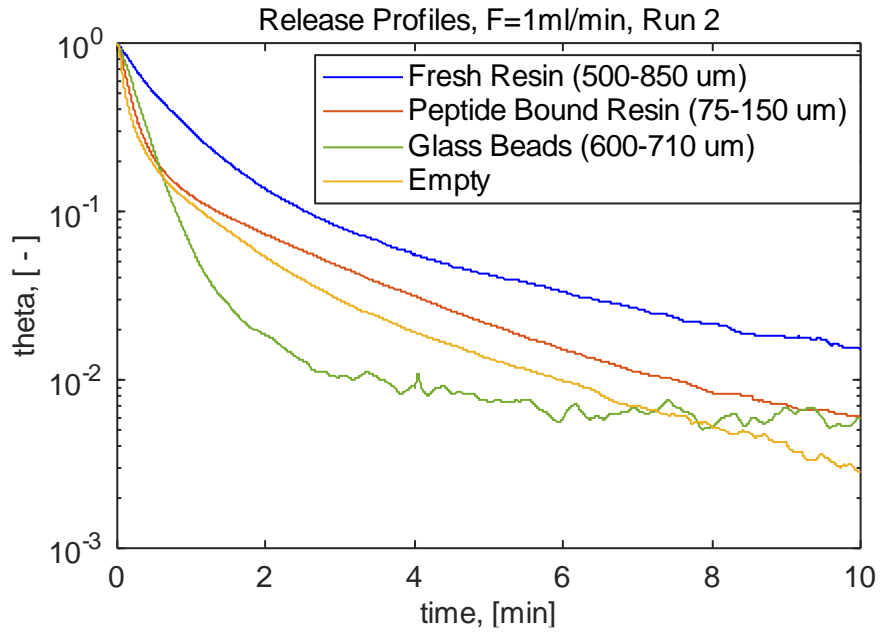


**All Reactor Fills:**

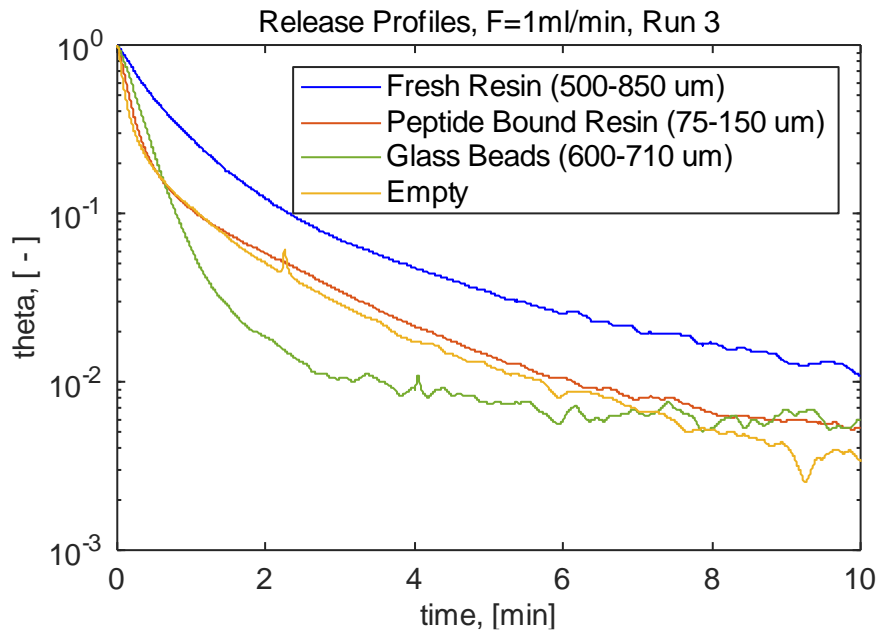
*All Fills, 1 ml/min, Run 1*



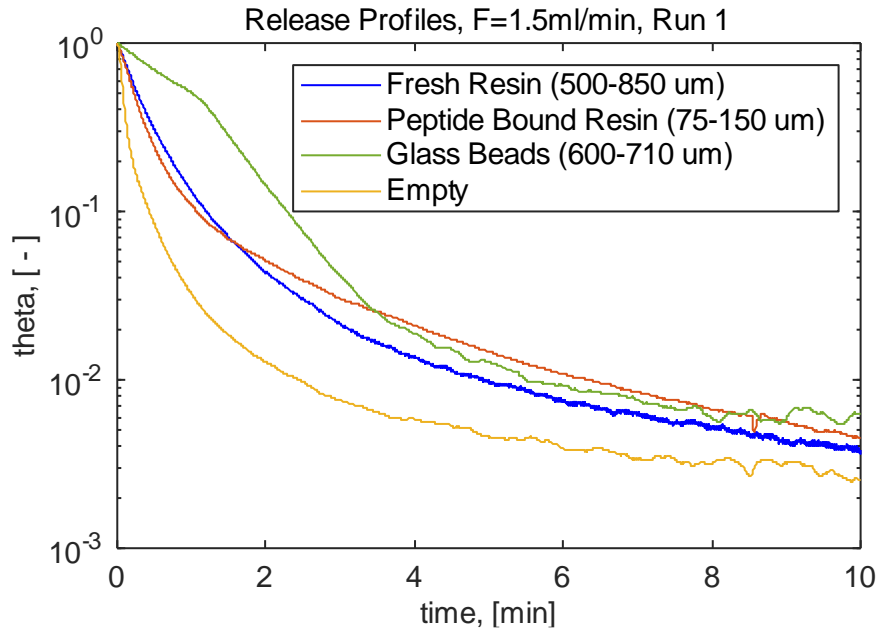
*All Fills, 1 ml/min, Run 2*



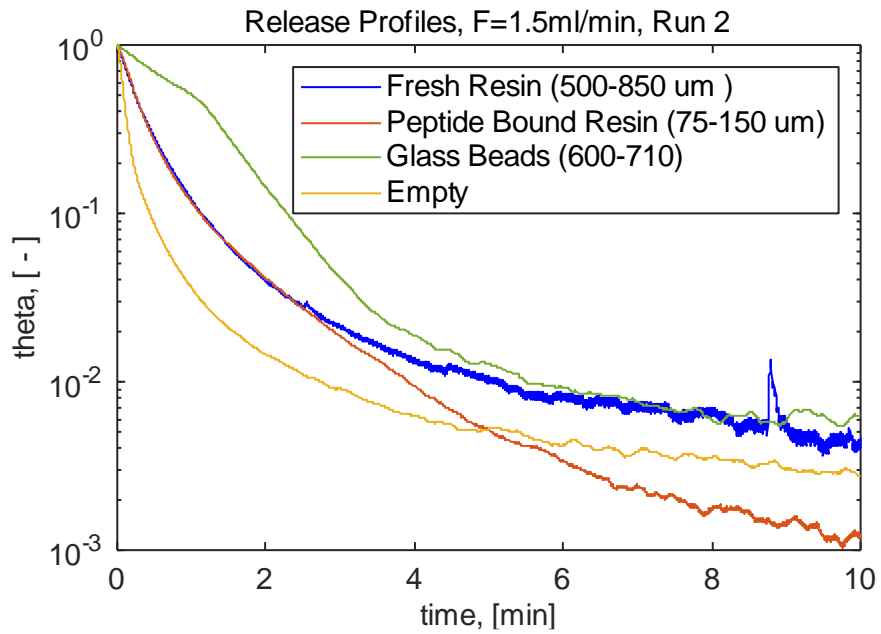
*All Fills, 1 ml/min, Run 3*



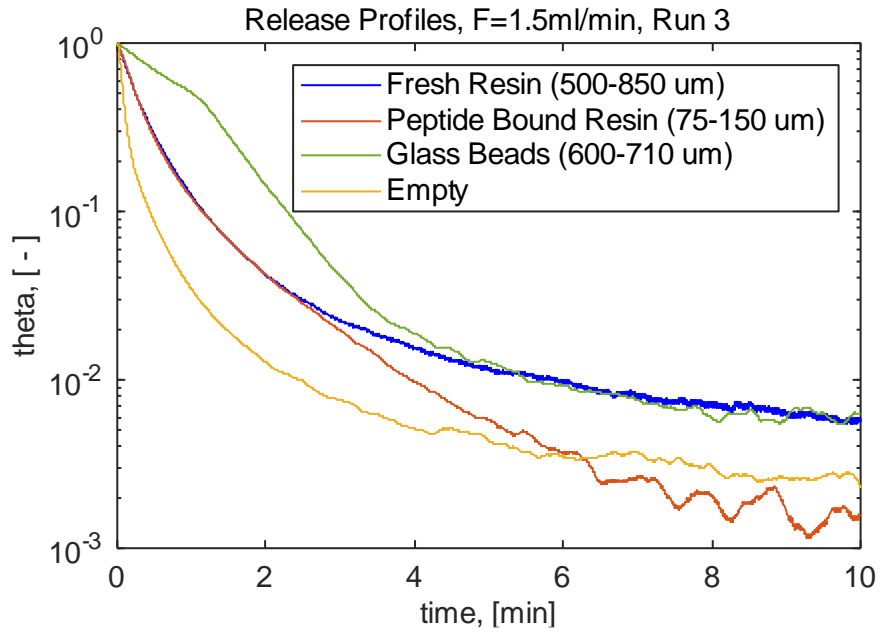
*All Fills, 1.5 ml/min, Run 1*



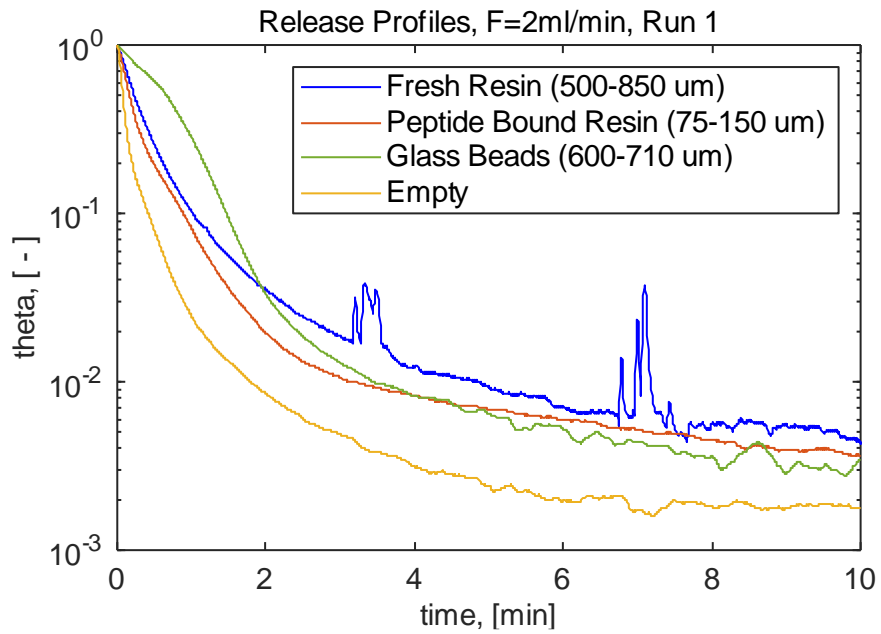
*All Fills, 1.5 ml/min, Run 2*



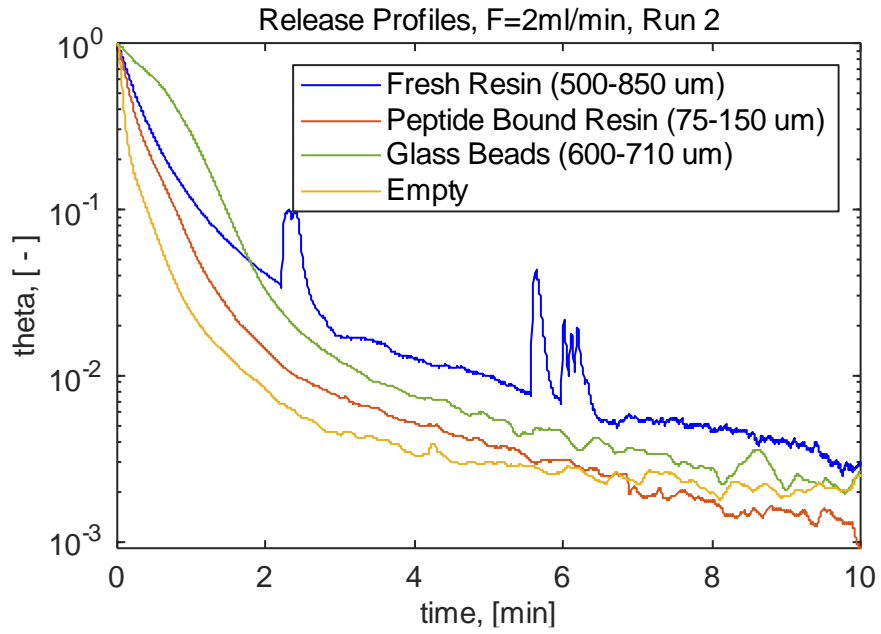
*All Fills, 1.5 ml/min, Run 3*



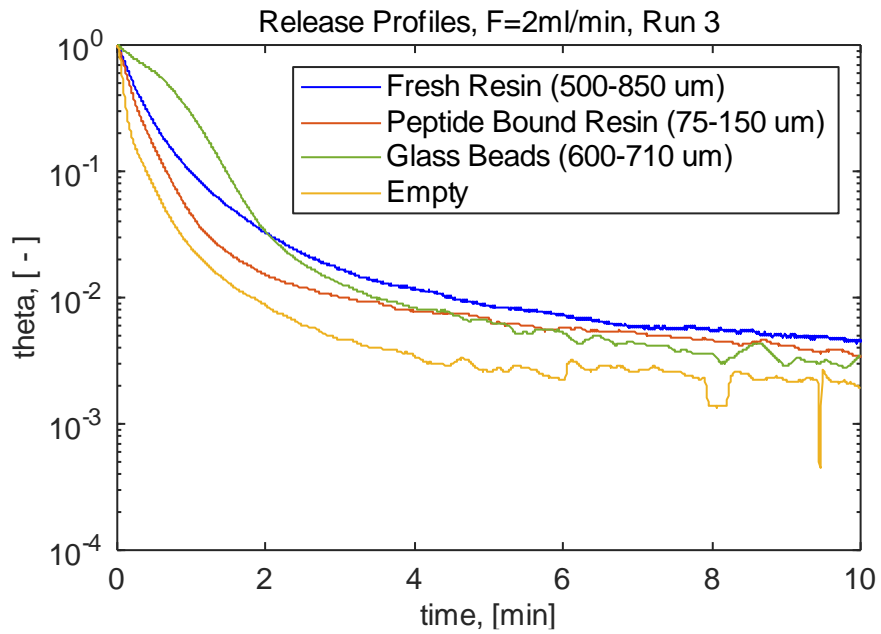
*All Fills, 2 ml/min, Run 1*



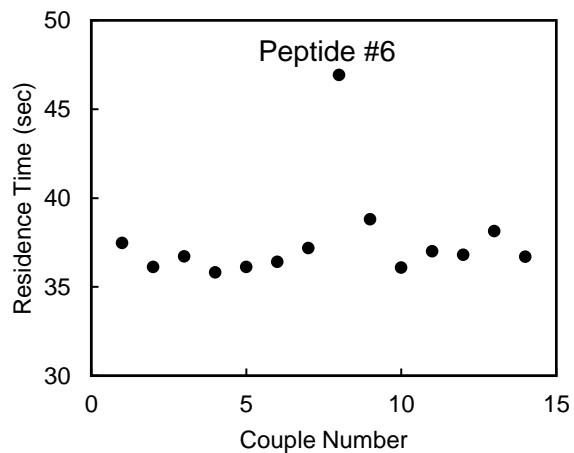
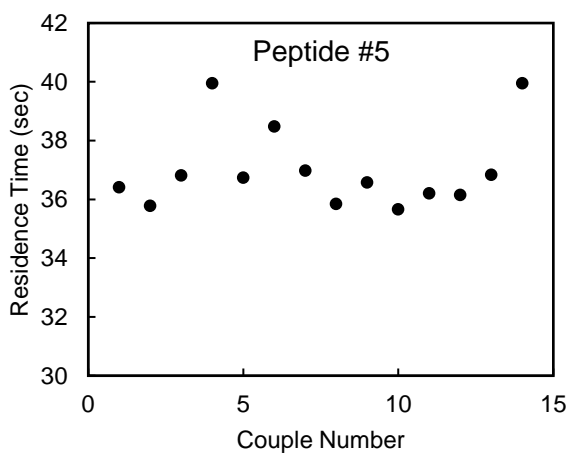
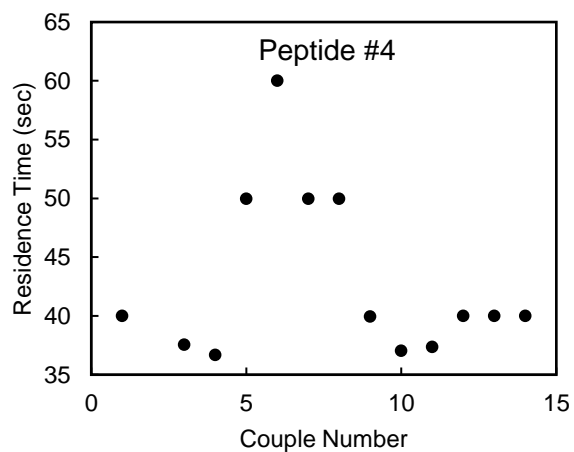
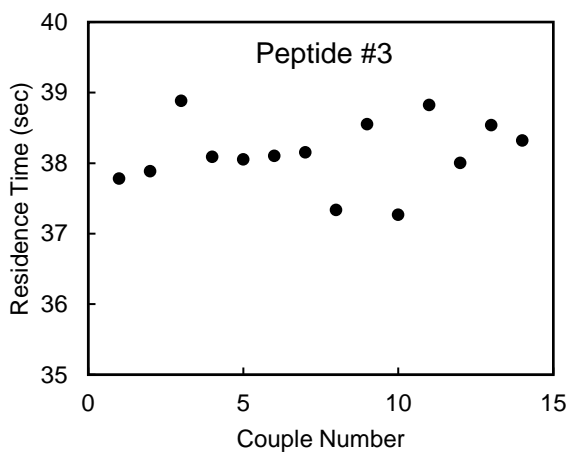
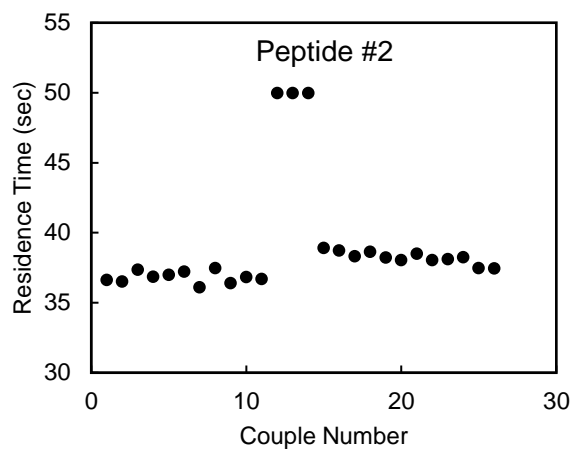
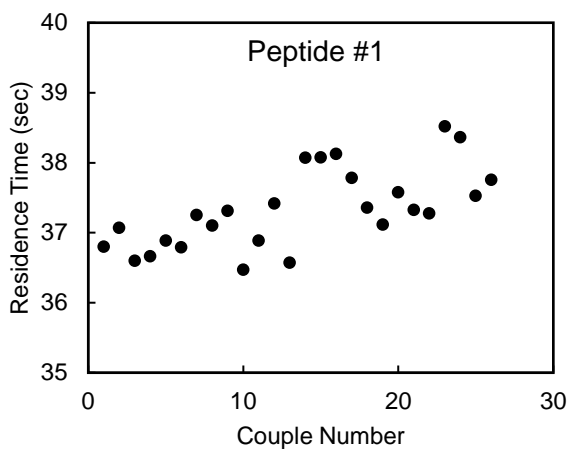
*All Fills, 2 ml/min, Run 2*

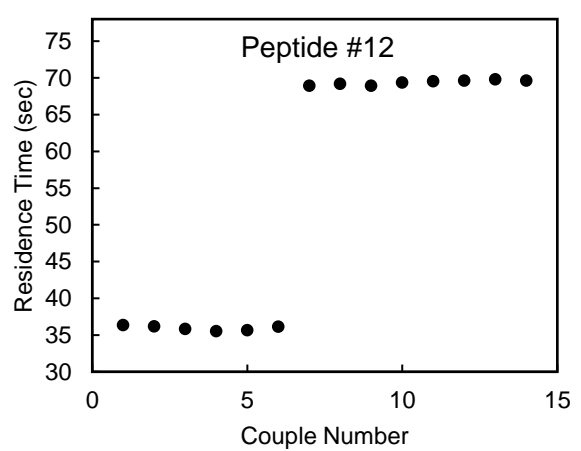
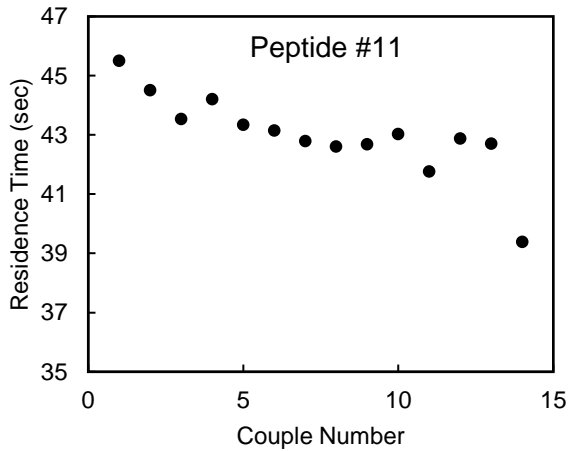
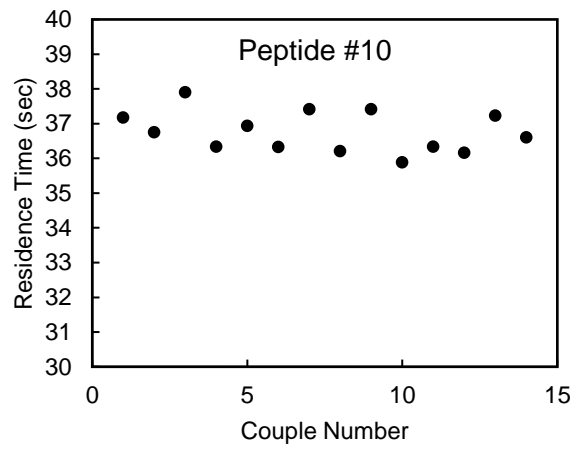
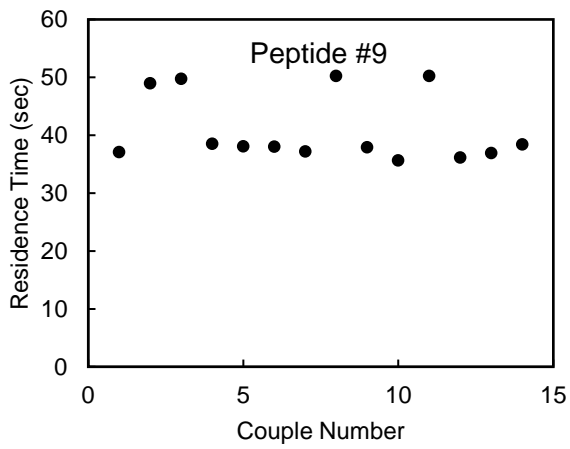
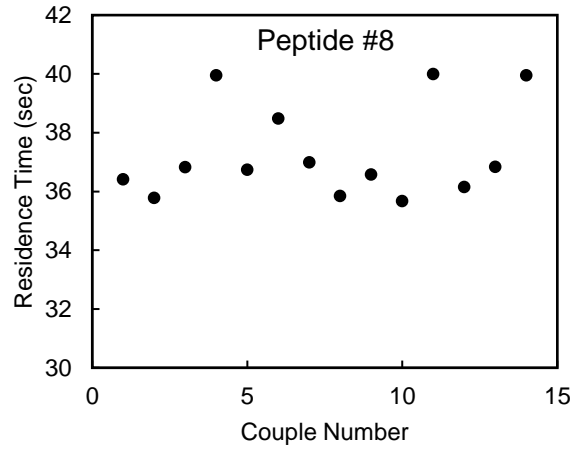
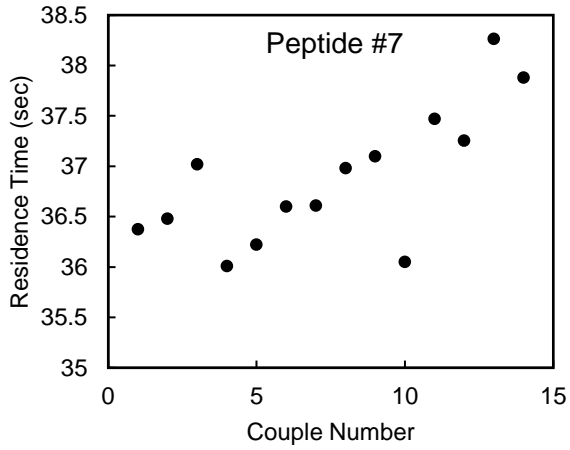


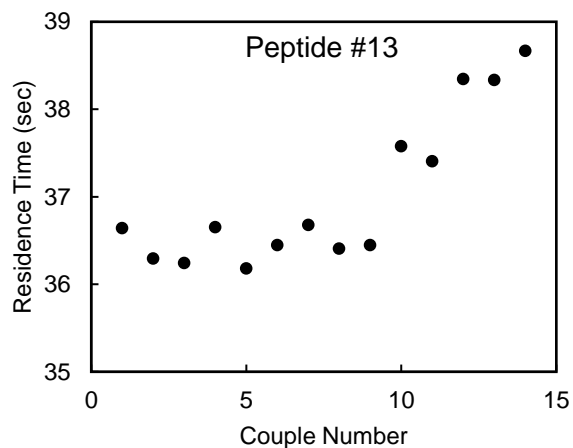
All Fills, 2 ml/min, Run 3



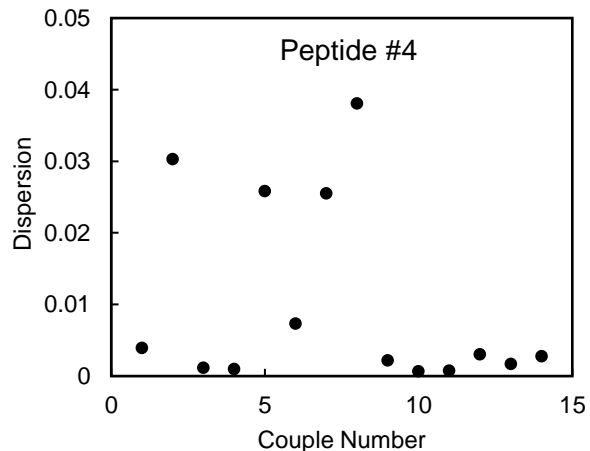
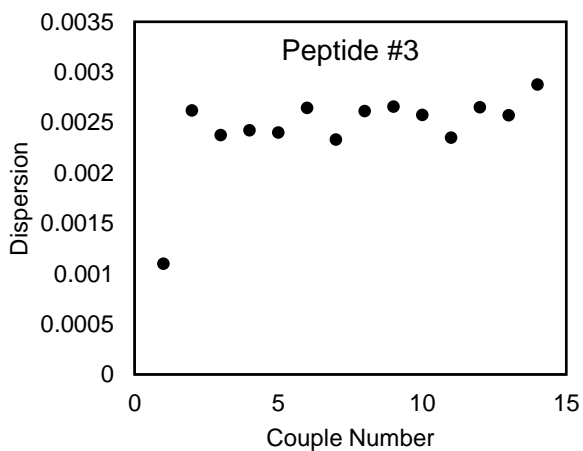
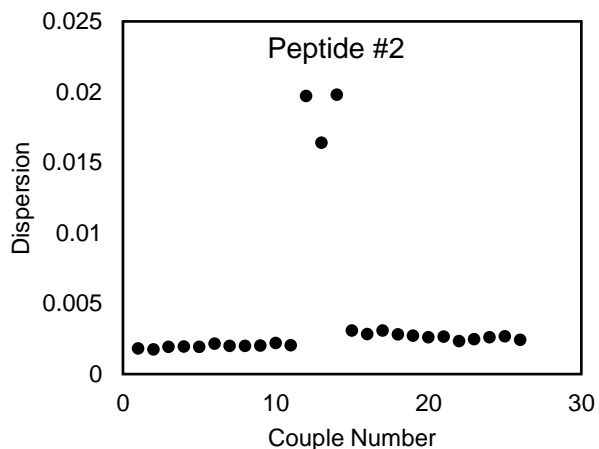
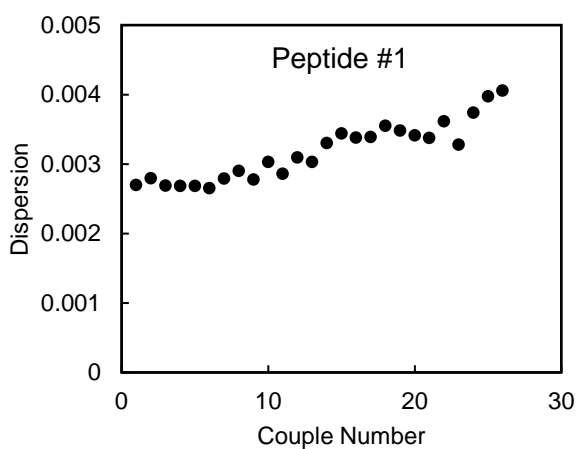
## Appendix D: Residence Time Graphs for Peptide Deprotection Peaks

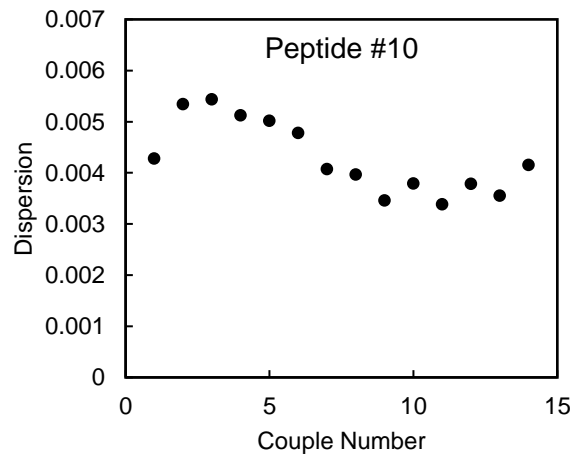
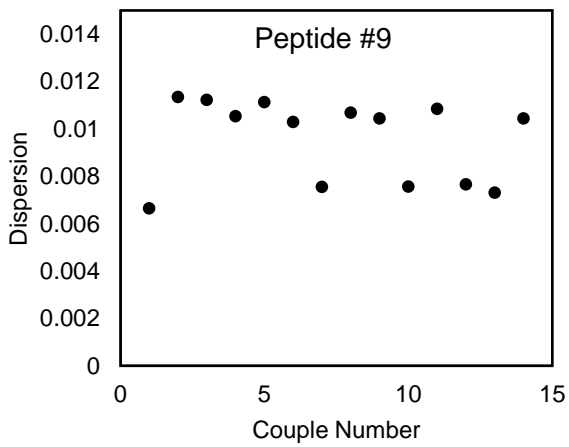
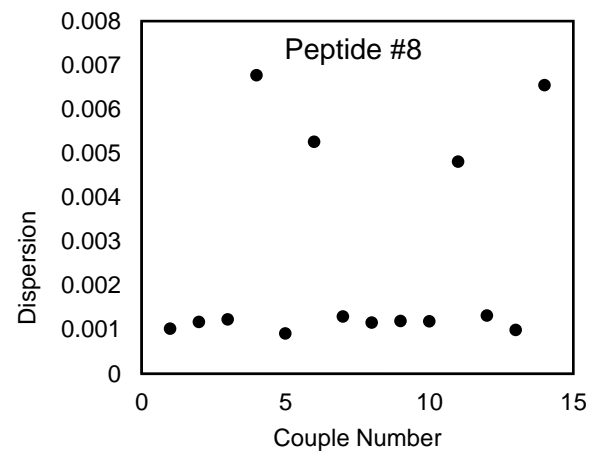
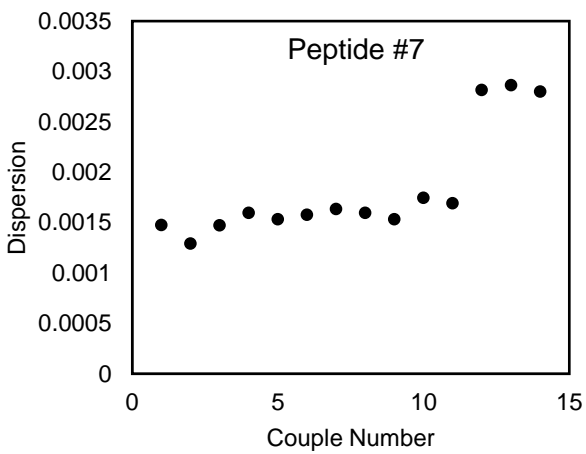
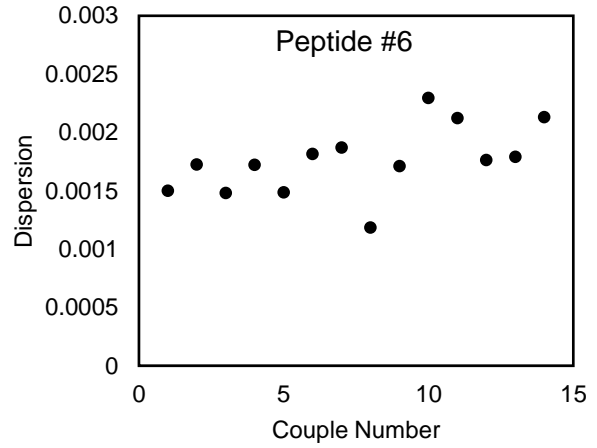
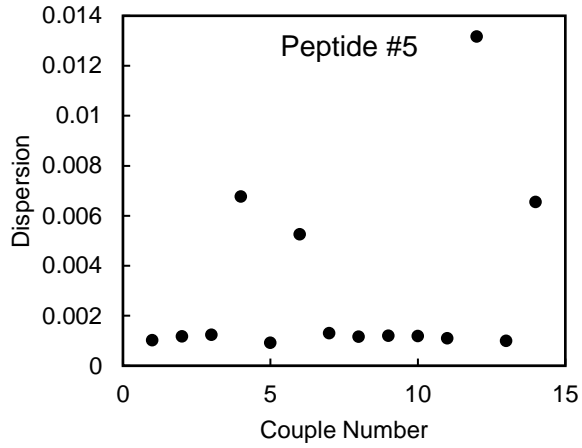


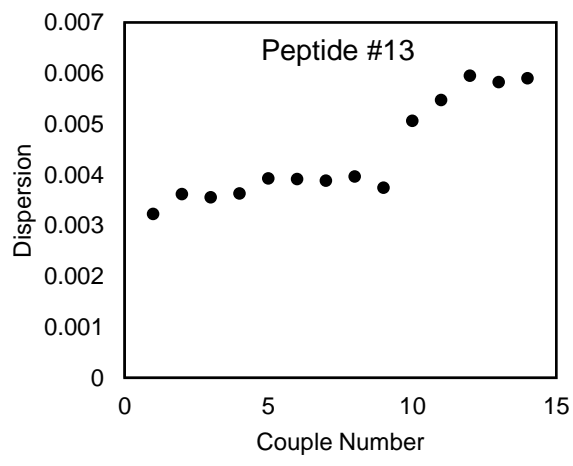
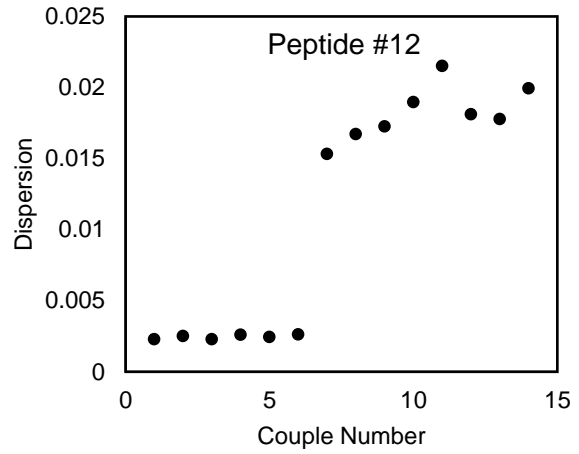
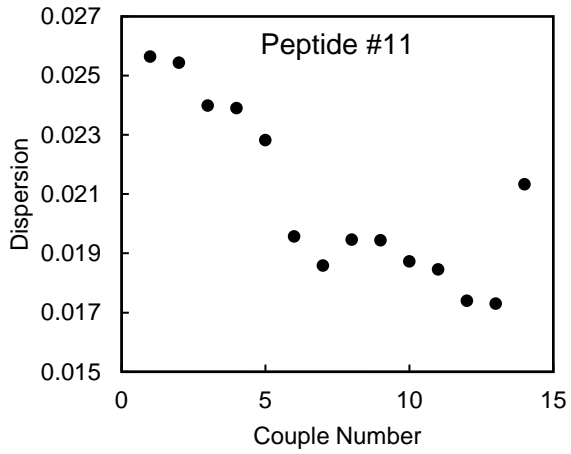




### Appendix E: Dimensionless Dispersion Graphs for Peptide Deprotection Peaks

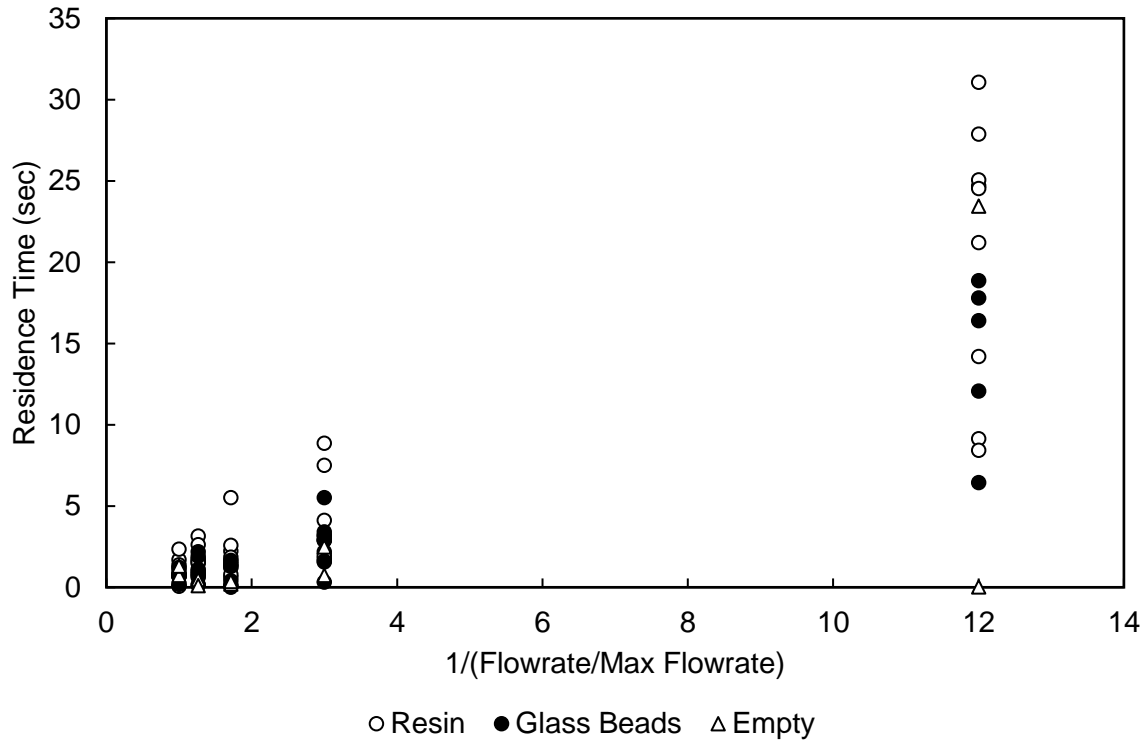






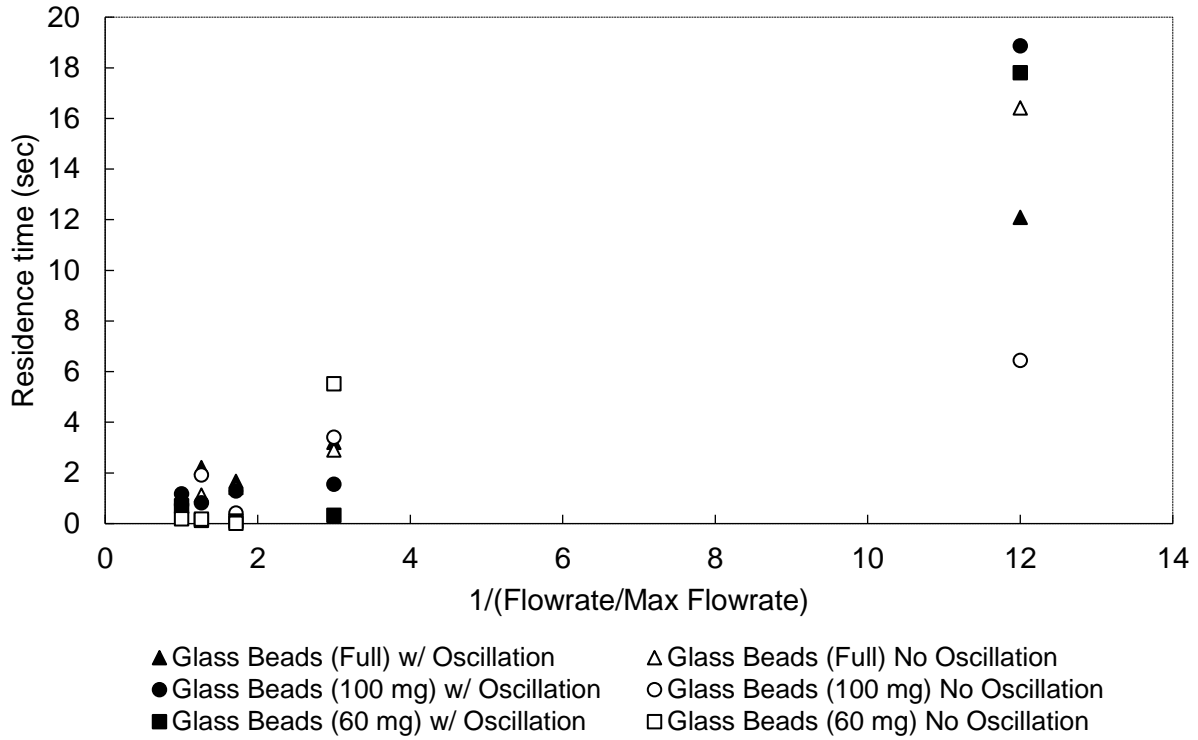
## Appendix F: Residence Time Experiment Graphs

### Appendix F.1: Flowrate Graph

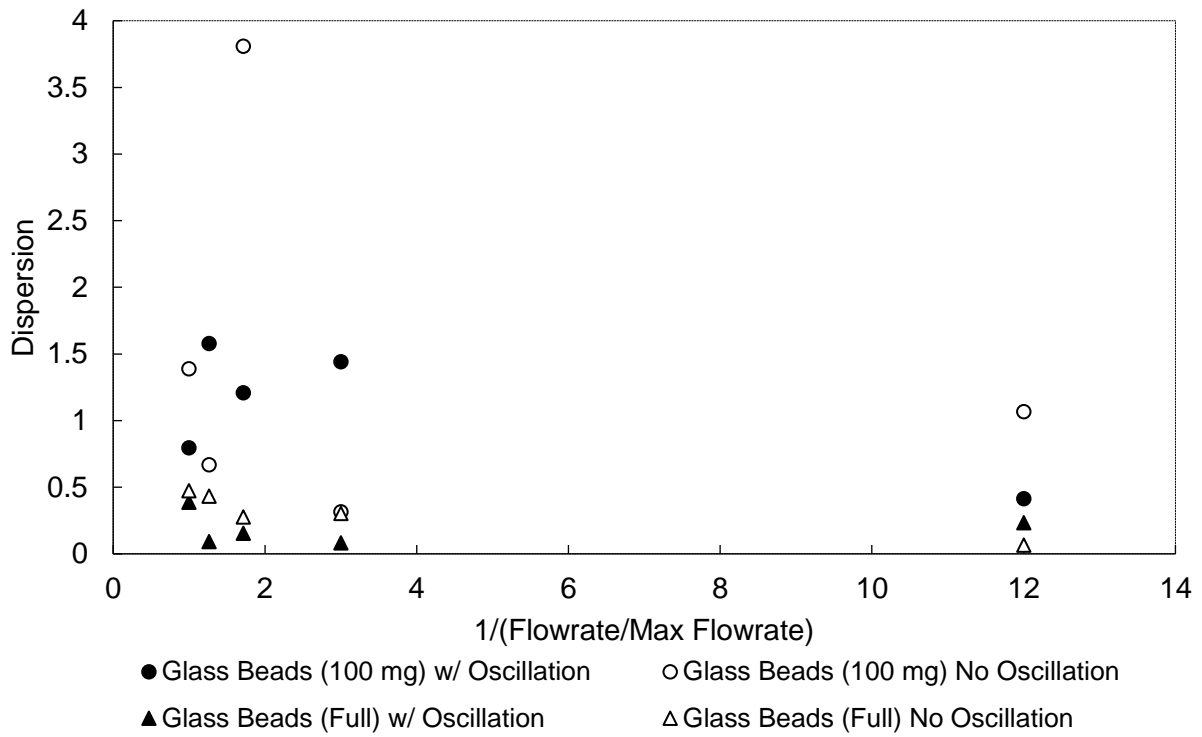


### Appendix F.2: Oscillation Graphs

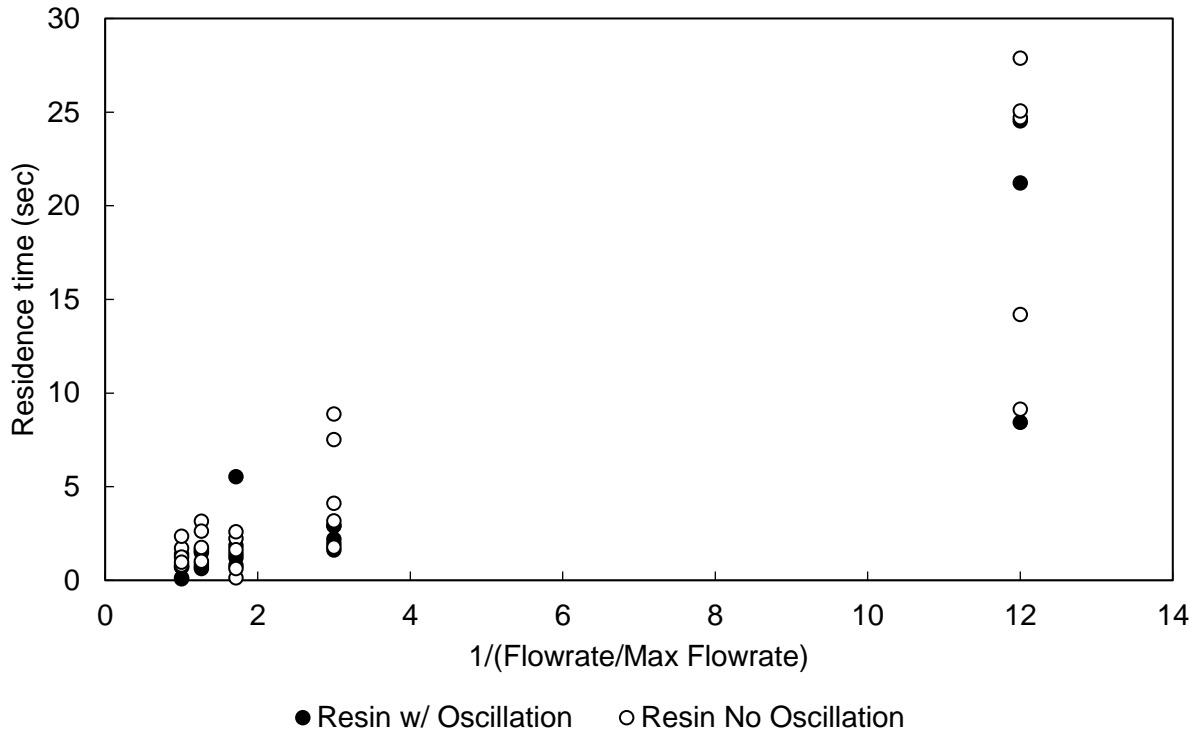
*Effect of oscillation on residence time with glass beads:*



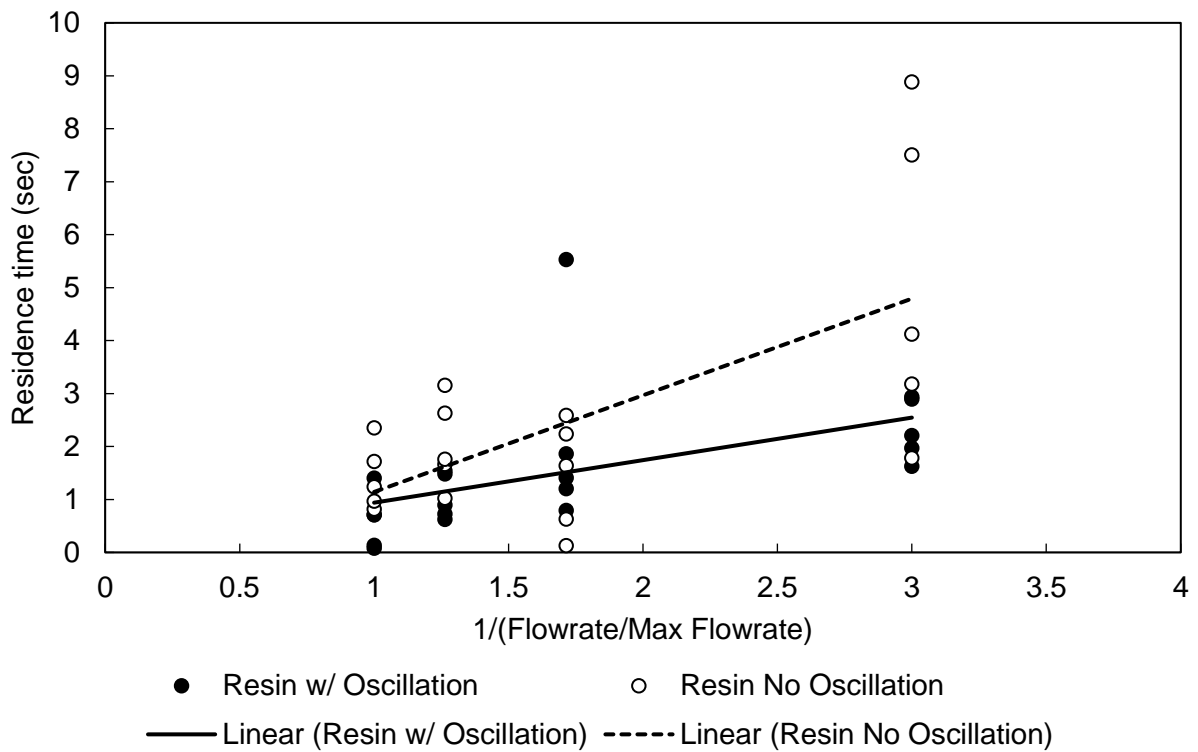
*Effect of oscillation on dimensionless dispersion number with glass beads:*



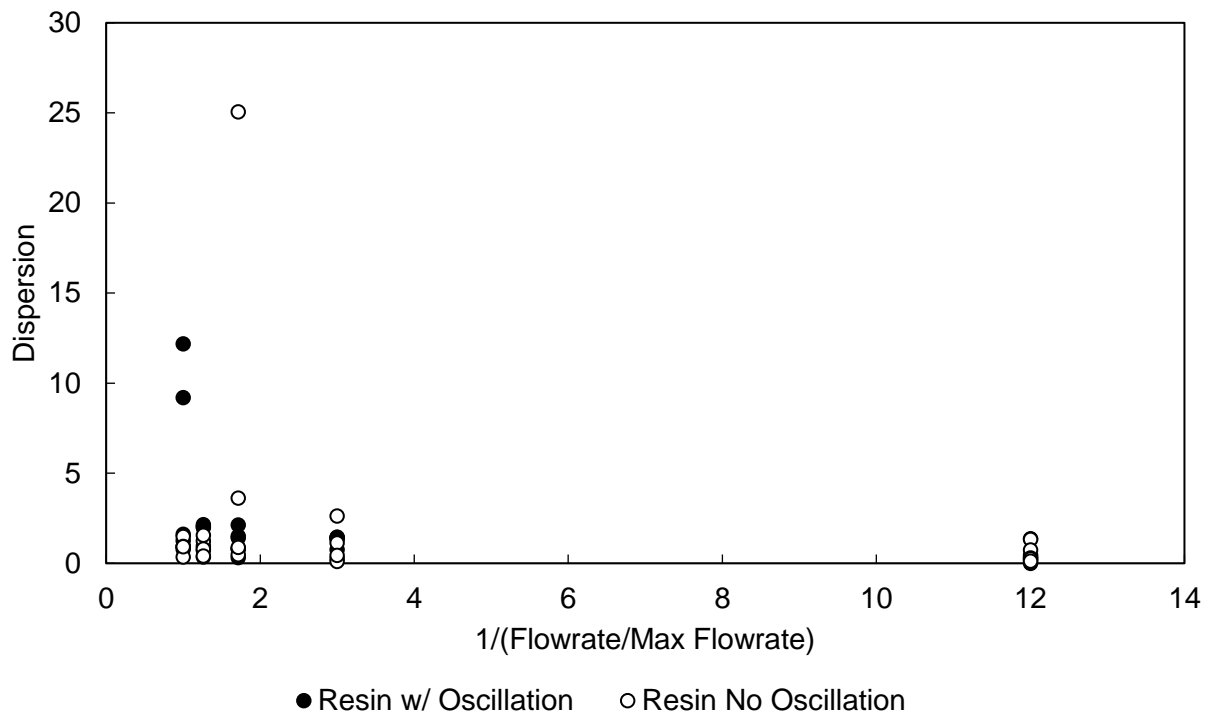
*Effect of oscillation on residence time with resin (Flows A-E):*



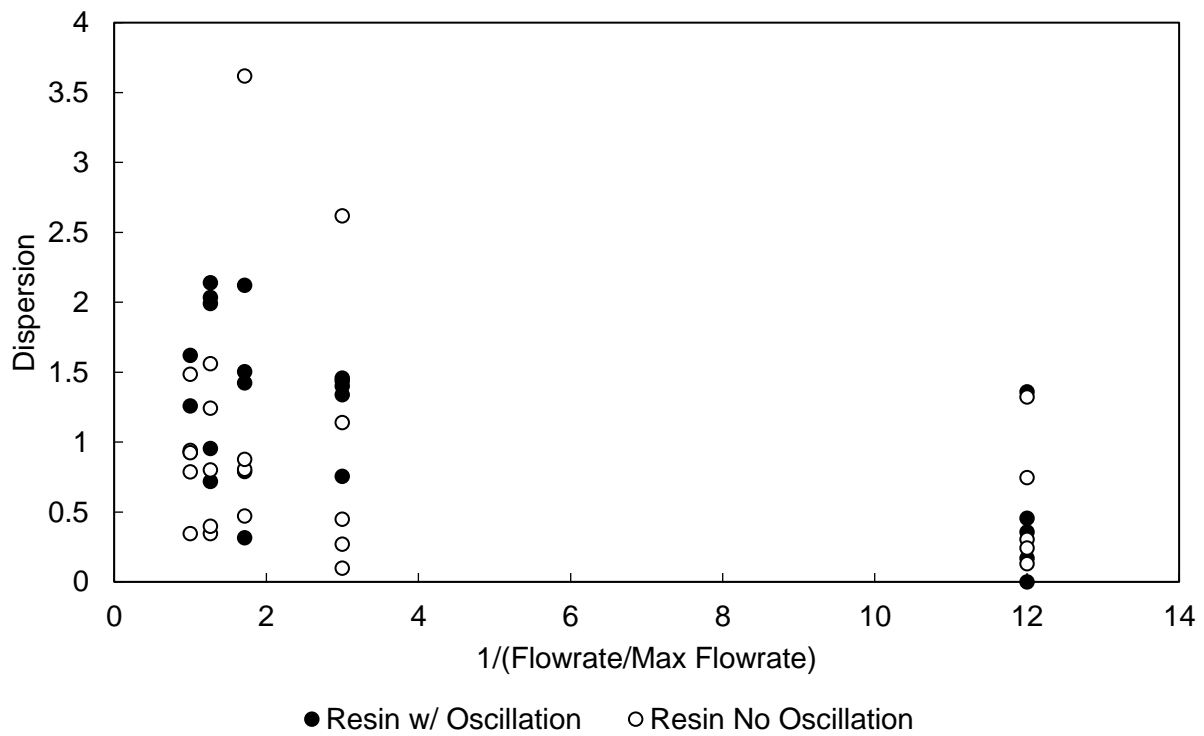
Effect of oscillation on residence time with resin (Flows B-E):



Effect of oscillation on dimensionless dispersion number with resin:

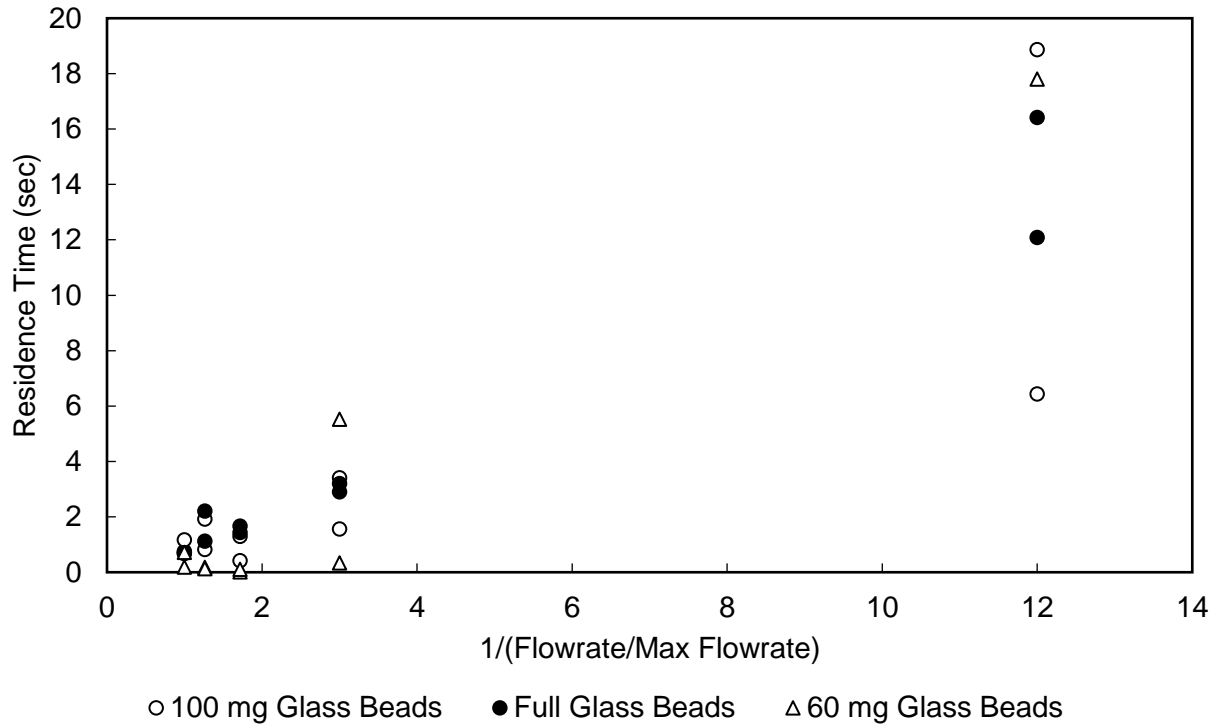


*Effect of oscillation on dimensionless dispersion number with resin (excluding outliers):*

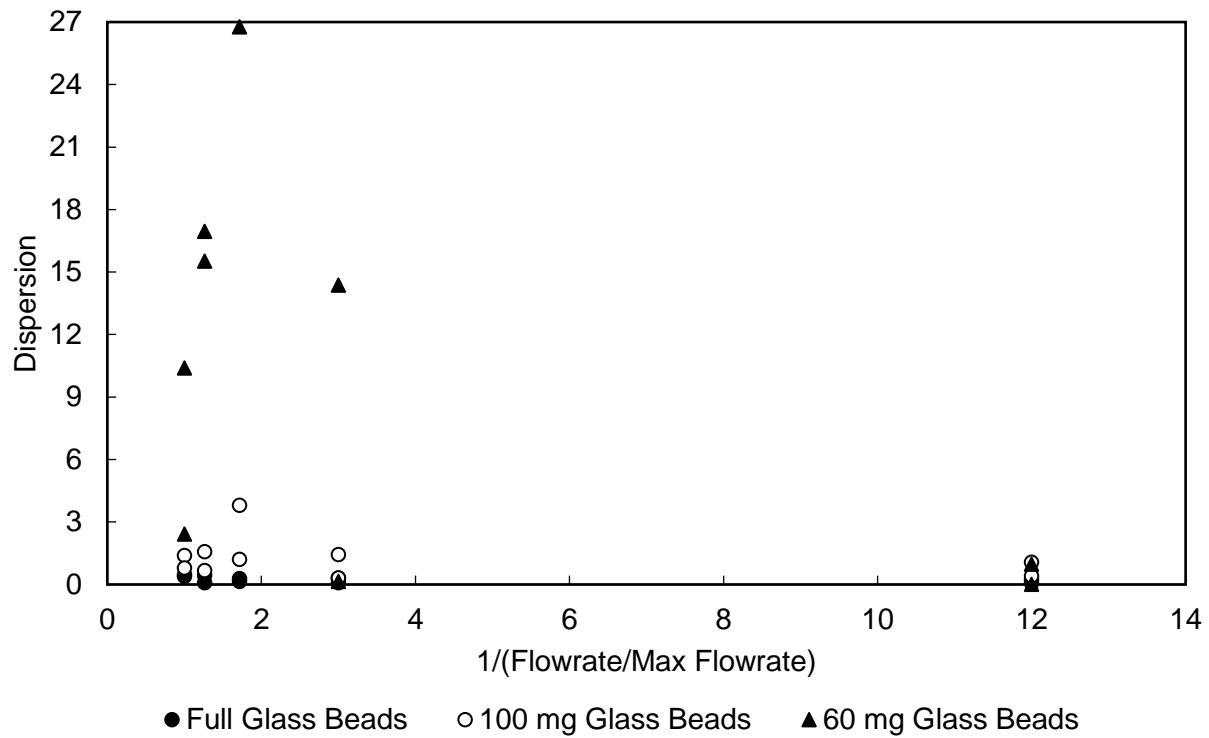


### Appendix F.3: Headspace Graphs

*Effect of headspace on residence time with glass beads*

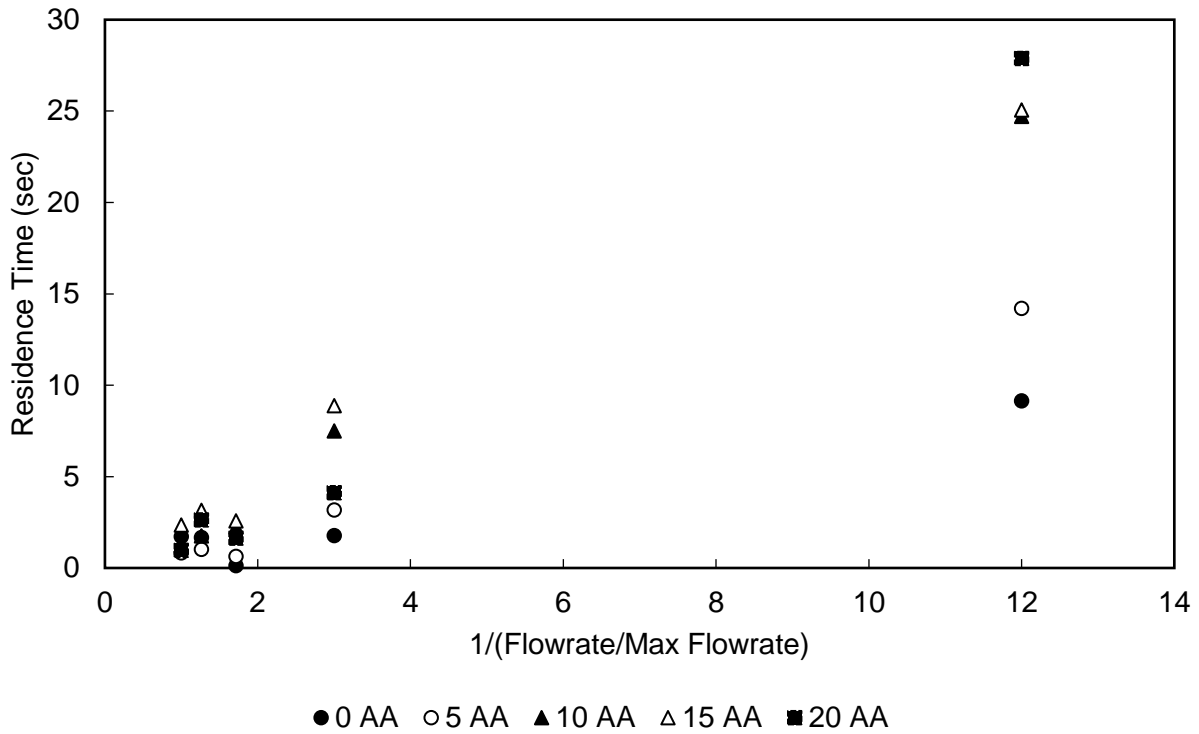


*Effect of headspace on dimensionless dispersion number with glass beads*

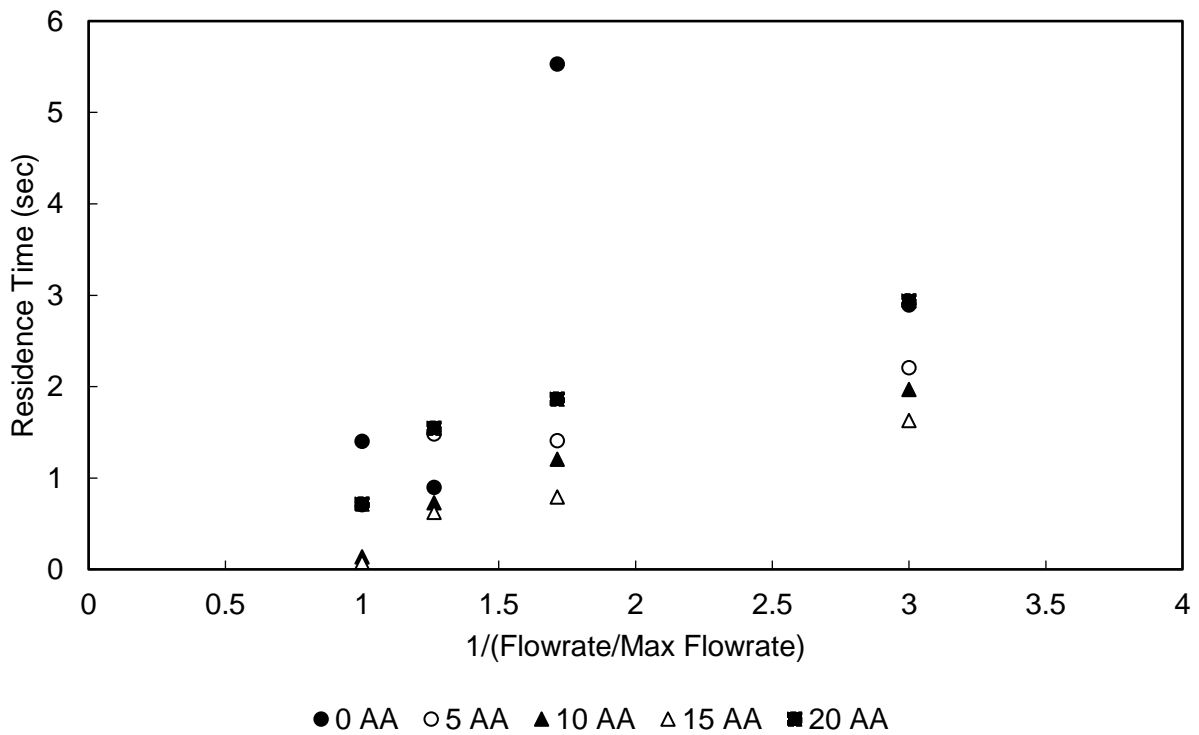


**Appendix F.4: Growing Peptide Graphs**

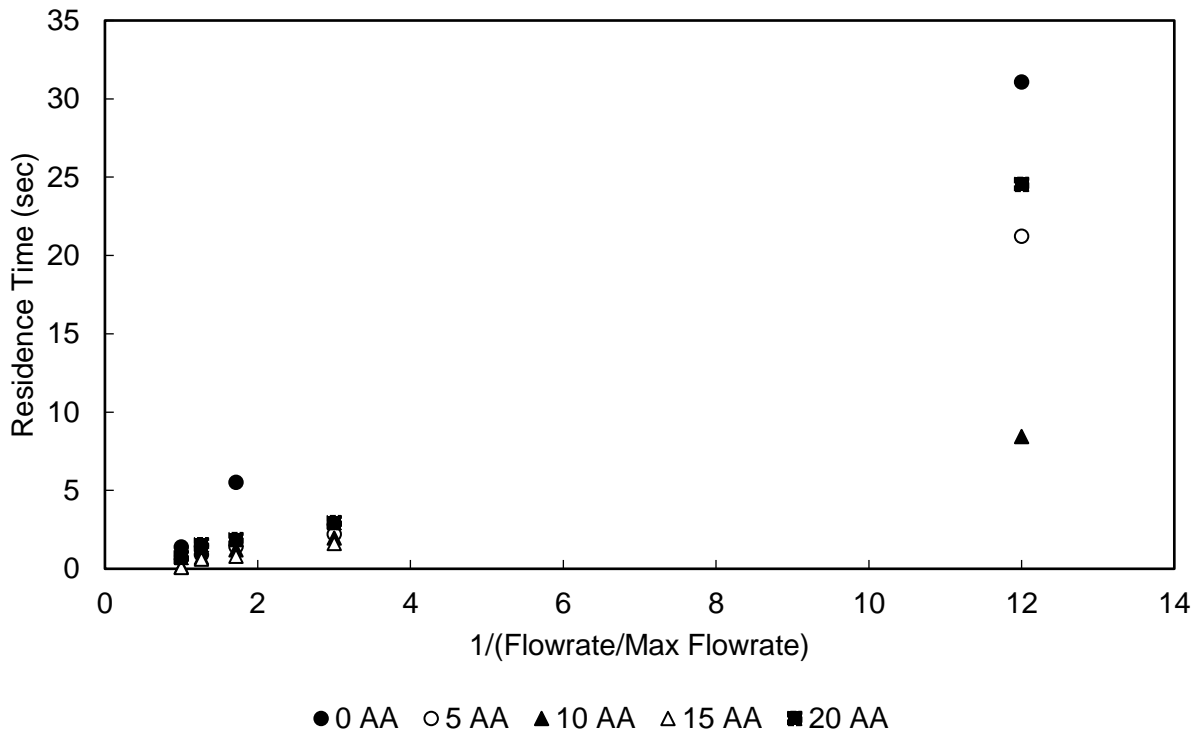
*Effect of peptide bound resin on residence time with no oscillation:*



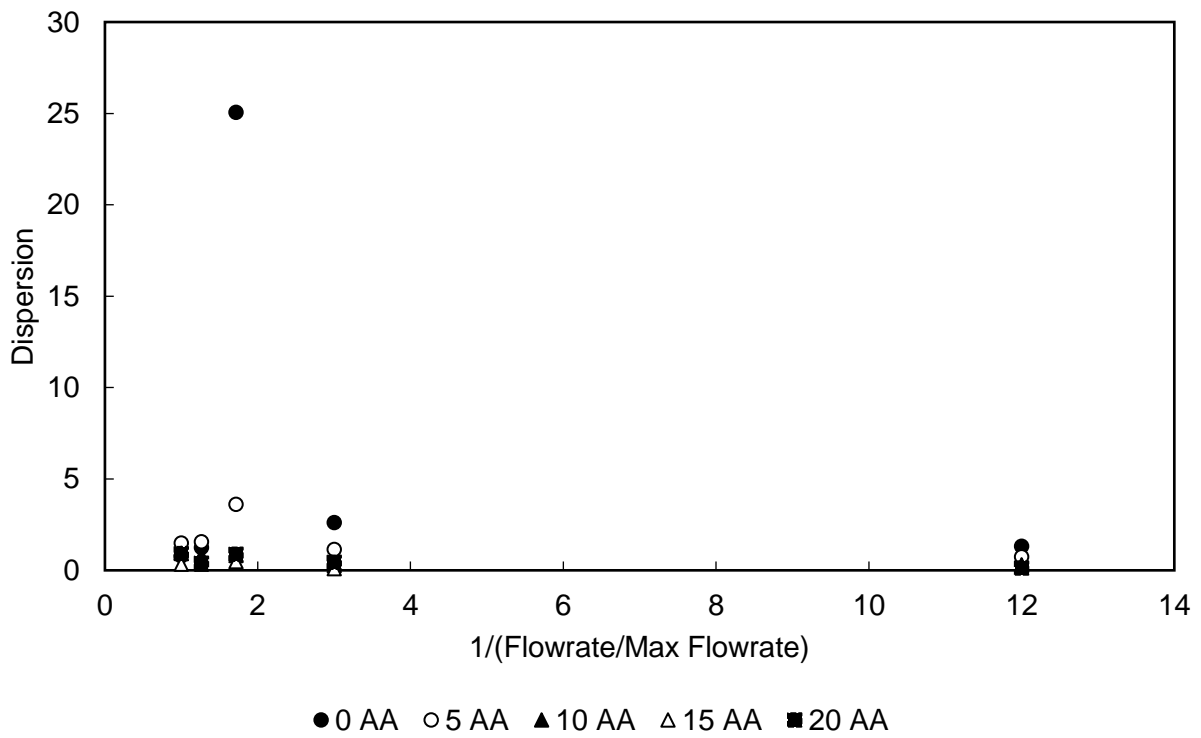
*Effect of peptide bound resin on residence time with oscillation (Flow B-E):*



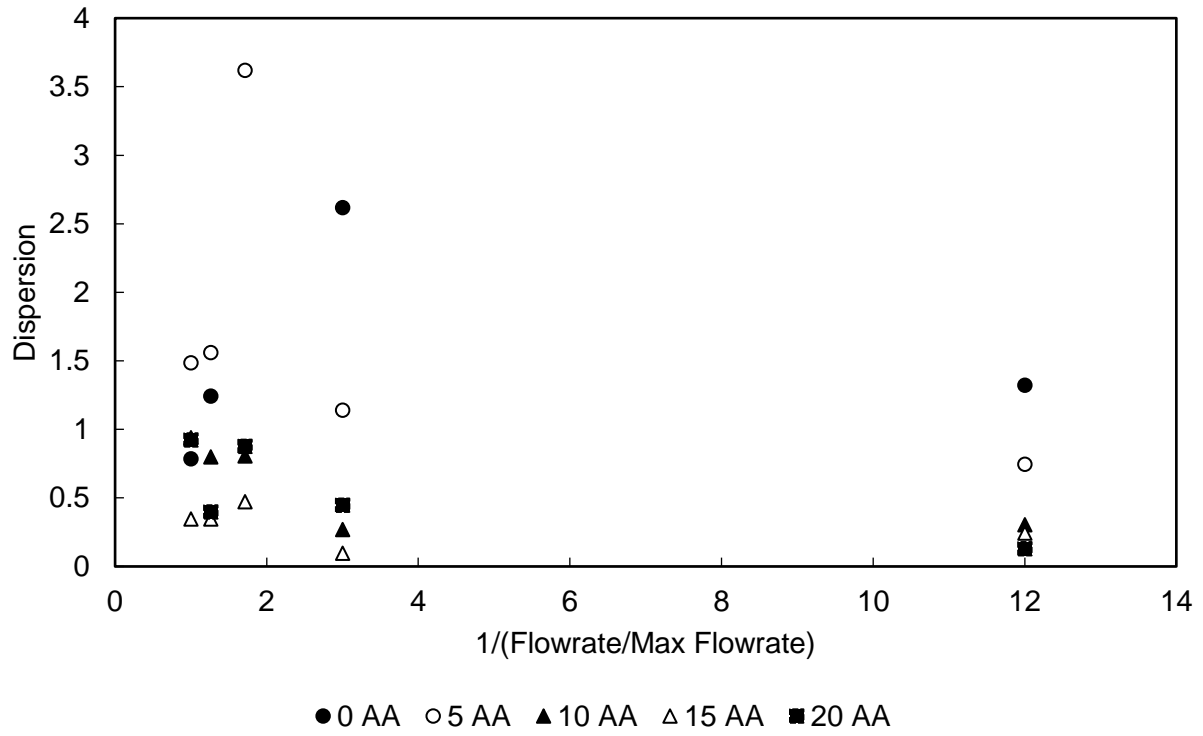
*Effect of peptide bound resin on residence time with oscillation (Flow A-E):*



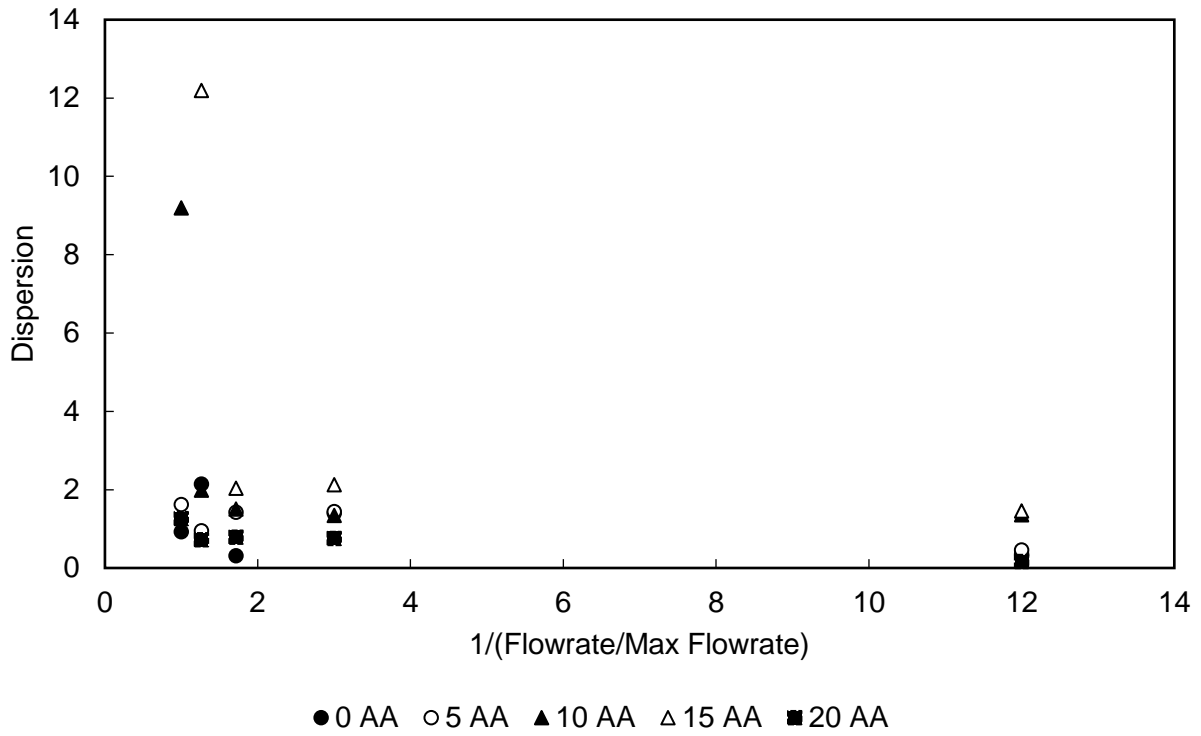
*Effect of peptide bound resin on dimensionless dispersion number with no oscillation:*



*Effect of peptide bound resin on dimensionless dispersion number with no oscillation (excluding outlier):*



*Effect of peptide bound resin on dimensionless dispersion number with oscillation:*



*Effect of peptide bound resin on dimensionless dispersion number with oscillation (excluding outliers):*

